A TIME SERIES ANALYSIS APPROACH TO TREE RING STANDARDIZATION

by

Edward Roger Cook

A Dissertation Submitted to the Faculty of the

SCHOOL OF RENEWABLE NATURAL RESOURCES

In Partial Fulfillment of the Requirements
For the Degree of

DOCTOR OF PHILOSOPHY
WITH A MAJOR IN WATERSHED MANAGEMENT

In the Graduate College

THE UNIVERSITY OF ARIZONA

1 9 8 5

THE UNIVERSITY OF ARIZONA
GRADUATE COLLEGE

As members of the Final Examination Committee, we certify that we have read the dissertation prepared by EDWARD ROGER COOK

entitled "A TIME SERIES ANALYSIS APPROACH TO TREE RING STANDARDIZATION"

and recommend that it be accepted as fulfilling the dissertation requirement for the Degree of DOCTOR OF PHILOSOPHY.

Johnson C. Ehleringer	March 5, 1985
Harold C Fritts	Date March 5, 1985
Philip M. Lowe	Date March 5, 1985
M. A. Stokes	Date March 6, 1985
Martin M. Fogel	Date March 6, 1985
Malcolm J. Zwolinski	Date March 6, 1985

Date

Final approval and acceptance of this dissertation is contingent upon the candidate's submission of the final copy of the dissertation to the Graduate College.

I hereby certify that I have read this dissertation prepared under my direction and recommend that it be accepted as fulfilling the dissertation requirement.

Malcolm J. Zwolinski	August 5, 1985
Dissertation Director	Date

STATEMENT BY AUTHOR

This dissertation has been submitted in partial fulfillment of requirements for an advanced degree at The University of Arizona and is deposited in the University Library to be made available to borrowers under rules of the Library.

Brief quotations from this dissertation are allowable without special permission, provided that accurate acknowledgement of source is made. Requests for permission for extended quotation from or reproduction of this manuscript in whole or in part may be granted by the head of the major department or the Dean of the Graduate College when in his or her judgment the proposed use of the material is in the interests of scholarship. In all other instances, however, permission must be obtained from the author.

SIGNED: Edward R. Cook

ACKNOWLEDGEMENTS

There are many people who are directly or indirectly linked to my dissertation research. Hal Fritts served as my dissertation advisor from afar and provided continual encouragement in my sometimes interminable endeavor. Mal Zwolinski helped me get through the Graduate College maze with little difficulty, for which I am especially grateful. Marv Stokes, Randy Boggess, Val LaMarche, Phil Knorr, and Marty Fogel also kindly served on my committee and reviewed my manuscript. To all, I give thanks.

Special note should be made of the encouragement and support of my wife, Michele, who probably still doesn't understand why I like tree-rings. Finally, I would like to pay special tribute to Dr. Heber C. "Doc" Donohoe who really got me started back at Trenton Junior College. He was my chief inspiration for in all that I have accomplished to date.

This research was supported by National Science Foundation Grants ATM 81-08459 and ATM 83-09491.

TABLE OF CONTENTS

TABLE OF CONTENTS--Continued

TABLE OF CONTENTS--Continued

LIST OF ILLUSTRATIONS

LIST OF ILLUSTRATIONS--Continued

LIST OF TABLES

ABSTRACT

The problem of tree-ring standardization is examined in this study from the point-of-view of standardizing closed-canopy forest ringwidth series. The problem is defined in terms of the high level of uncertainty in differentiating climatic fluctuations from those fluctuations in the ringwidths caused by competitive interactions between trees and stand disturbances.

A biological model for a tree-ring standardization method is developed through the decomposition of a theoretical ringwidth series using a linear aggregate model. By this process, it is found that one class of non-climatic variance that is frequently responsible for standardization problems could be objectively minimized in theory. This is the variance caused by endogenous stand disturbances which create fluctuations in ringwidth series that are non-synchronous or out-of-phase when viewed across trees in a stand. Since out-of-phase fluctuations cannot be logically related to the common climatic signal affecting all trees in the stand, the proposed standardization method should remove only that variance regarded as unique to individual trees and simultaneously preserve all common variance resolvable from the age trend.

A time series model based on the autoregressive process is proposed as a means of minimizing the timewise influence of endogenous disturbances in a detrended ringwidth series. Specific estimation

techniques are described for applying autoregressive modelling to the tree-ring standardization problem and for reducing the influence of disturbance-caused outliers in the mean-value function. The final chronology developed by this overall methodology is called the ARSTND chronology.

A stochastic method of detrending based on smoothing splines is tested and adopted as part of the ARSTND methodology. The theoretical signal and noise variance properties of tree-ring series are derived based on an internal additive noise model which may be autoregressive in form. Signal-to-noise ratio (SNR) properties of this general model indicate that autoregressive modelling and prewhitening of detrended ringwidth indices will result in a higher SNR if and only if autocorrelated noise is present in the series. This enables the verification of the general SNR theory and the error variance reduction property of the ARSTND methodology.

CHAPTER 1

INTRODUCTION

Annual tree-ring chronologies are being increasingly used around the world to develop long histories of climatic variations for studying climatic change. This study of past and present climate from tree rings is known as dendroclimatology (Fritts, 1976). To this end, a great deal of research has gone into developing statistical transfer functions for reconstructing past climate (Fritts et al., 1971; Stockton, 1975; Meko, 1981). Typically, the predictor variables used in these transfer functions are mean index chronologies or their orthogonal transforms. Although the transfer functions are backed by a sound body of statistical theory, the same cannot be said for the standardization procedures used to develop the mean index chronologies. The procedure of modelling and removing "non-climatic" growth trends and fluctuations is a major purpose of tree-ring standardization and is, therefore, crucial to the reliability of the resultant climatic reconstructions. Thus, it is ironic that relatively little effort has gone into developing a theoretical framework and procedures for objectively standardizing tree-ring series compared to that spent on developing transfer functions. Much of this disparity is due to the fact that most of the techniques used in dendroclimatology today were developed by the Laboratory of Tree-Ring Research in Tucson using semi-arid site tree-ring series from western North America. Such

trees often have very simple exponential or linear growth trends. Because these trends can be fit well using simple mathematical models, there was no reason to develop the standardization methodology any further.

Once dendroclimatic research left the confines of the semi-arid tree-ring sites and moved into more mesic, closed-canopy forest sites of the world, problems in tree-ring standardization quickly arose. The non-climatic growth trends could not be modelled with any consistency using simple mathematical models due to the effects of competitive interactions and sporadic disturbances on tree growth. Several procedures have been developed to accommodate these more complex non-climatic growth fluctuations (e.g. Fritts, 1976; Warren, 1980; Cook and Peters, 1981). As yet, none of them are satisfactory due to the uncertainty of removing valuable climatic information during the standardization procedure. In the following section, I will more precisely define the tree-ring standardization problem as a prelude to developing the biological and statistical models necessary to yield a satisfactory solution.

Statement of the Problem

In the semi-arid environments of western North America, trees growing at or near the upper and lower elevational limits of growth are often unaffected by stand competition and disturbances because of the wide spacing between trees. After a common short-lived increase in radial growth following germination, the growth increment curve of such open-grown trees reaches a maximum and then declines monotoni-

cally with increasing age to a relatively constant growth rate. This negative growth trend is partly related to the geometric constraint of adding an approximately equal volume of wood each year to a stem of increasing radius. Other factors contributing to this trend are declining apical dominance, increasing transport distances for food, hormones and water, and limitations on exploitable site resources for growth. The result is a growth increment curve that decays with time due to factors which are relatively independent of yearly fluctuations of climate. Because this curve is clearly associated with increasing tree age, it will be defined here as the age trend of a tree-ring series. Being non-climatic, the age trend must be approximated and removed from a tree-ring series before the series can be used to study variations of past climate. In dendrochronology, this operation of modelling and removing such non-climatic variance is known as standardization (Douglass, 1919; Fritts, 1976). Besides removing age trends, standardization reduces each ringwidth series to a series of dimensionless indices with a mean of 1.0 and a homoscedastic variance (Matalas, 1962). This allows several standardized tree-ring series from a stand to be averaged together for improving the signal-to-noise ratio of the series (DeWitt and Ames, 1978).

Once a growth curve has been estimated from the data, the standardized tree-ring indices are computed as

$$z_t = r_t/g_t \qquad 1.1$$

where z_t is the index, r_t is the observed ringwidth, and g_t is the estimated growth curve for year t. The division of r_t by g_t is meant

to stabilize the variance because the local variance of a ringwidth series is proportional to its local mean.

Theoretically, the standardization curve represents the amount of radial growth produced each year if all climatically-related growth influences in the tree's environment were held constant through time. In this sense, the standardization curve is a time series of expected values of radial growth, and the ring-width indices, or scaled variations, about the curve are the departures from expected growth due to climatic fluctuations. In the case where the expected growth series evolves through time as a simple age trend, this curve can be adequately approximated by a mathematical function of relatively simple form. When one moves from open to closed-canopy forest environments, the non-climatic increment curves of trees become more complex because of sporadic disturbances which directly or indirectly alter the growth environment of the trees. Such disturbances occur at generally unpredictable times. Growth curves which can fit monotonic age trends well are unable to account for any sudden and persistent disturbance-caused changes in growth. In this context, a <u>disturbance</u> is defined as any non-climatic event which causes an unanticipated, persistent departure in growth from the pattern expected from the age trend and climate. To differentiate a disturbance-caused growth fluctuation from the age trend, the former will be defined as a <u>disturbance pulse</u>.

In order to cope with disturbance pulses, dendrochronologists have used more flexible curve-fitting and smoothing techniques with some success. Orthogonal polynomials (Fritts, 1976) and cubic smooth-

ing splines (Cook and Peters, 1981) are two such methods which have been used for standardizing forest-interior tree-ring series. However, each of these methods suffers from a serious degree of indeterminancy in choosing the optimum degree of curve flexibility and shape. To do so exactly would require explicit knowledge of a tree's environmental history which is, of course, rarely known. If one could assume that the climatically-related departures from the growth curve were serially uncorrelated, then the solution would be a relatively trivial exercise of modelling and removing all of the persistence in the tree-ring series. But this assumption is unjustified because the climate system is known to have feedback mechanisms in the atmosphere-hydrosphere-cryosphere system which impart some stochastic predictability to many climatic time series (Mitchell, 1976). This stochastic predictability frequently takes the form of persistent departures from the mean which create many of the low-frequency fluctuations seen in temperature and precipitation series. Some other proposed sources of climatic fluctuations are solar variability (Eddy, 1976; Mitchell, Stockton, and Meko, 1979) and volcanism (Lamb, 1970; Schneider and Mass, 1975).

Because these low-frequency climatic fluctuations may be similar in form to disturbance pulses, the identification, separation and removal of only the non-climatic fluctuations presents obvious difficulties. The solution to the standardization problem requires the optimal separation of the observed low-frequency changes in radial growth into those created by climate and those created by the age

trend and disturbances, based on some objective criteria. Clearly, without any explicit knowledge of a tree's environmental history, the problem appears to be intractable because the standardization curve must "recognize" the occurrence of a disturbance and track the tree growth response to it without tracking similar fluctuations due to climate.

In defining the tree-ring standardization problem, I have emphasized the difficulty in identifying and removing disturbance pulses which distort any secular variations in the mean due to climate. This problem is rather obvious. Simply stated, we cannot preserve more information about fluctuations in the climatic mean than is allowed for by the standardization curve chosen to remove information believed to be non-climatic. Less obviously, a similar principle holds for the variance of the process. As noted earlier, standardization is meant to stabilize both the mean and variance of a tree-ring series. Since the local variance of a non-stationary ringwidth series is roughly proportional to its local mean, the procedure of dividing each ringwidth by its respective growth curve value is meant to stabilize the variance simultaneously with the mean. To what extent this is accomplished depends on how closely the curve follows the local mean of the data.

Consider for the moment the simplest standardization curve: the horizontal line through the mean of a ringwidth series. Providing that the series is stationary to begin with, this represents the expected value of the process for all years. Recalling that the

standardization curve, g_t, is a time series of expected growth values for n years, the curve constructed from the mean of the ringwidth series, z_t, is nothing more than

$$g_t = \Sigma\ r_t/n \qquad 1.2$$

for each year t. Substituting r_t for g_t in equation 1.1 and rearranging terms yields

$$z_t = nr_t/\Sigma\ r_t \qquad 1.3$$

Noting that $E[z_t] = 1.0$ for all t, the variance stabilizing properties of g_t can now be derived.

The variance of a tree-ring index series is

$$\sigma^2 = \sum_{i=1}^{n} (z_t - E[z_t])^2/n \qquad 1.4$$

where $E[z_t]$ and n are defined as before. Dropping the Σ and n which are not directly related to the local variance of r_t and substituting z_t and $E[z_t]$ with their equivalences described above, equation 1.4 can be written as

$$\sigma_t^2 = (nr_t/\Sigma r_t - 1.0)^2 \qquad 1.5$$

where σ_t^2 is the squared departure from $E[z_t]$ at year t. Expanding equation 1.5 yields

$$\sigma_t^2 = \frac{nr_t^2}{\Sigma r_t^2} - \frac{2nr_t}{\Sigma r_t} + 1.0 \qquad 1.6$$

Noting that $n/\Sigma r_t$ is the reciprocal of the mean, $\bar{x}_t$, the final form of equation 1.6 is

$$\sigma_t^2 = \frac{r_t^2}{\bar{x}_t^2} - \frac{2r_t}{\bar{x}_t} + 1.0 \qquad 1.7$$

Equation 1.7 reveals that the variance properties of z_t are determined by a quadratic relationship between r_t and the mean level of r_t used to standardize the ringwidth. Generalizing equation 1.7 to the case where g_t is a local estimate of expected growth yields

$$\sigma_t^2 = \frac{r_t^2}{g_t^2} - \frac{2r_t}{g_t} + 1.0 \qquad 1.8$$

where the $\sigma^2{}_t$ of each z_t is now locally defined by each r_t and its respective standardization curve value, g_t. Equation 1.8 avoids the stationarity condition imposed earlier on the derivation of σ_t^2 because g_t can be any stationary or non-stationary growth curve now.

The functional form of σ_t^2 can be evaluated by solving equation 1.8 for different values of g_t and r_t. Figure 1.1 shows three σ_t^2 curves. Each curve is computed for a fixed g_t to assess the change in the variance of z_t as r_t varies from its expected value. The parabolic functions are truncated and, therefore, asymmetric due to the fact that tree-rings cannot be negative.

Several interesting properties of the tree-ring indexing procedure can be deduced from these curves. The time stability of the variance in tree-ring indices is closely tied to the goodness-of-fit of the curve used to standardize the ringwidth series. The proximity of the curve to the local mean of the ringwidths defines the range within which the variance stabilizing property of indexing is symme-

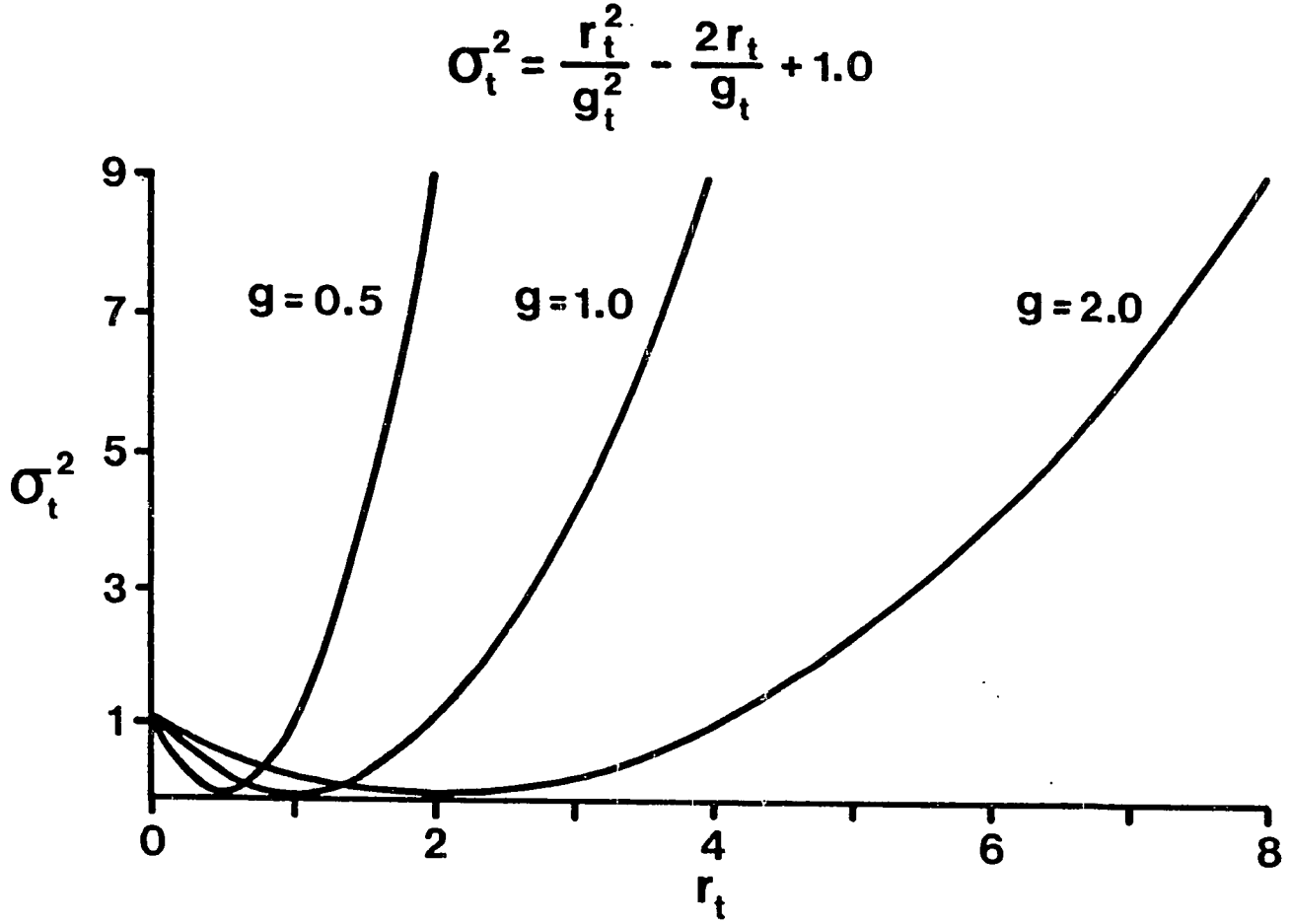

Figure 1.1. The functional form of the variance stabilizing transformation that occurs when measured tree-ring widths are transformed into dimensionless indices.

tric. For example, if the growth curve has a local value of 1.0 mm, then the variance of a tree-ring index computed from that value will be the same for ringwidths of 0.5 mm and 1.5 mm. This symmetry holds for all equal departures from the standardization curve up to $0<g_t<2g_t$. For ringwidths that exceed twice the growth curve value, the local variance can increase without limit. The consequences of these results relative to the tree-ring standardization problem are important. If the estimated growth curve follows the local mean of the ringwidth series, then the variance characteristics of the standardized series will not be seriously distorted. However, if the curve has little flexibility relative to the wanderings of the mean, then the variance of the standardized series may have secular inhomogeneities in it which are artifacts of the standardization process. This finding indicates the existence of an Uncertainty Principle in standardizing tree-ring series. Concisely stated, the preservation of long-period fluctuations of the mean may be antagonistic to the stabilization of variance in tree rings.

Previous Investigations

Having defined the tree-ring standardization problem, a critical review of the literature is necessary to show that none of the currently available methodologies offer any solution to this problem. As described earlier such a solution must, in some way, optimally and objectively separate the low-frequency changes in radial growth due to climate from those due to disturbance pulses. Fritts (1963) developed a computer program for tree-ring standardization based on the negative

exponential curve as a model for the age trend. It is expressed as

$$\hat{y} = ae^{-bx}$$

or 1.9

$$\log \hat{y} = \log a - bx$$

in linearized form. This curve proved to be quite adequate for standardizing moderate-aged conifers growing in open-canopy environments. However, equation 1.9 has the property that $\hat{y} \to 0$ as $t \to \infty$. This zero-asymtote property is not appropriate for very old conifers because the age trends of these trees frequently approached some constant level of growth, k, where k is necessarily positive. Fritts, Mosimann, and Bottorff, (1969) introduced the modified negative exponential curve

$$\hat{y} = ae^{-bx} + k \qquad 1.10$$

to account for this observed behavior in old-age conifer ringwidths. Equation 1.10 is not intrinsically linear due to the additive constant k. Because equation 1.9 is a special case of equation 1.10, the modified negative exponential curve is more flexible as an age trend model for standardizing tree-ring data from open-canopy environments. Fritts et al. (1969) note that equation 1.10 cannot model the juvenile growth period of increasing growth rate seen in many trees near the pith. They suggest deleting those rings altogether or fitting them separately with a linear regression curve of positive slope. Although more general mathematical functions exist for modelling the juvenile period simultaneously with the subsequent period of exponential decay (e.g. Yang, 1979; Warren, 1980), they have not been adequately investigated as standardization tools in dendrochronology.

When it is appropriate for the data, the modified negative exponential curve is an excellent age trend model. It is objective and biologically reasonable and is likely to preserve virtually all low-frequency climatic variance that is resolvable from the age trend. Unfortunately, there are numerous cases where equation 1.10 does not apply as an age trend model. Fritts et al. (1969) and Graybill (1979, 1982) allow for the fitting of linear regression curves if the age trend is linear or has a non-negative slope. This model is expressed as

$$\hat{y} = a + bx \qquad 1.11$$

The slope coefficient b may be constrained to be negative or zero if the a priori biological model for the age trend requires that condition. If such constraints are not placed on the model, the slope may be positive. The constrained linear age trend model is also objective, biologically reasonable, and very conservative in preserving climatic variance. The allowance for a linear model with positive slope is a pragmatic concession to violations of the biological model when it should apply on a priori grounds or when no particular model is justified. The latter condition will generally be the case in closed-canopy forest environments where competitive interactions and disturbances virtually guarantee the breakdown of any biologically-based age trend model.

Jonsson and Matern (1974) describe a method of computing tree-ring indices based on fitting a low-order polynomial (equation 1.13) to a mean-value function of log transformed ringwidths from a stand of

trees. The logarithmic transformation serves to linearize the model and stabilize the variance of the ringwidths with respect to time. Although it is not clearly stated by Jonsson and Matern (1974), this method would seem to work best for tree-ring series from even-aged stands that have similar age trends. If mixed ages are used and the age trends differ considerably in shape, the resultant logarithmic mean-value function may require a very high-order polynomial to remove these effects. The danger of removing useful climatic information may be considerable. Jonsson and Fritts compared their two standardization techniques on identical data and found a 77% agreement between final chronologies (Fritts, 1976, p. 280). The differences were attributed to within and between tree variations that were not removed by the Jonsson-Matern method. While the Jonsson-Matern method probably works well for a restricted class of tree-ring standardization problems (i.e. even-aged trees, homogeneous age trends), it lacks the necessary flexibility to deal with the more general case that includes mixed-age trees with disturbed age trends.

In related research, Kuusela and Kilkki (1963) investigated the use of exponential and power functions in modelling the growth increment percentage functions of trees. The exponential function is the same as that used by Fritts (1963). The power or hyperbolic function is expressed as

$$\hat{y} = ax^{-b}$$

or

$$\log \hat{y} = \log a - b \log x \qquad 1.12$$

in linearized form. Kuusela and Kilkki (1963) found that the power function fit the age-related growth increment percentages somewhat better than the exponential function. Hett and Loucks (1976) utilized the same two functions for modelling the age structure of balsam fir and eastern hemlock. This study is pertinent because the frequency distribution of age classes in uneven-aged forest communities often mimics the age trends seen in individual trees. Hett and Loucks (1976) also found that the power function worked better than the exponential function principally because the mortality rate of trees was not constant or linear over time. For the exponential function to work well, the mortality rate must be linear with respect to time. By analogy, this may explain why the exponential function fails with a zero asymptotic (k=0) constant for old semi-arid site conifers. The decay in growth rate is not linear with respect to time, but more nearly exponential. This causes the slope of the curve to approach zero more rapidly than can be accounted for by an exponential model. The modified negative exponential curve of Fritts et al. (1969) accounts for this circumstance by assuming that the age trend is composed of two fairly distinct periods: an early youthful period where growth rate declines linearly with age, and a later mature period of equilibrium with the environment where the level of growth is constant over time. The power function may be a useful alternative to the modified negative exponential curve in some cases.

As dendrochronology expanded into closed-canopy forest environments, it became clear that the age trend models described thus

far were inadequate for modelling and removing episodic disturbance pulses in the ringwidth series. Thus, a more data adaptive approach was deemed necessary. Fritts (1976) describes one approach to solving this problem that involves modelling the age trend and disturbance pulses collectively using orthogonal polynomials of arbitrary order. The nth order polynomial model is expressed as

$$\hat{y} = a + b_1 x + b_2 x^2 + \ldots + b_n x^n \qquad 1.13$$

The flexibility of the polynomial curve is proportional to the order with the number of inflections in the curve being equal to n-1. Because of the flexibility of polynomials and the lack of any biological model to guide the fitting, much low-frequency climatic information may be lost if a series is overfit. The obvious problem in applying the polynomial approach is determining the "correct" order fit for each ringwidth series. The order selection test used by Fritts (1976) and Graybill (1982) involves fitting a polynomial of order n to the data and computing the residual variance not accounted for by the curve. Polynomials of order n+1 and n+2 are then estimated. If either of the higher-order polynomials reduce the residual variance by a significant percent (say, 5%), then the higher order polynomial is judged superior and the testing procedure continues for two more orders. If the variance reduction test fails, the order-n polynomial is accepted as the best estimate of the standardization curve. Although this testing procedure objectively selects the poly-

nomial order once the test percentage is chosen, the percentage itself is subjective. Roughly speaking, the test percentage will guide the fitting towards a range of orders that is inversely proportional to its magnitude. Fritts (1976) used a test percentage of 5% in his example. Blasing, Duvick, and Cook (1983) found that 1% or even 0.1% produced better results for Iowa white oak. It is very unlikely that a unique percentage exists that will work well everywhere.

Another problem with polynomials is the way in which they sometimes track the general behavior of a series very well in some intervals and very poorly in others. As Rice (1969) points out, the overall behavior of a polynomial can be dominated by the behavior of the data in a small region which is quite unlike the rest of the data. In extreme cases, the inflections of a polynomial curve can, for some regions, be directly out-of-phase with the actual behavior the data. See Figure 6.5 in Fritts (1976, p. 264) for an example of this phenomenon. Thus, polynomial curves have the potential for actually exaggerating the behavior of tree-ring series in poorly-fit intervals. This is highly undesirable.

Warren (1980) introduced a generalized exponential growth function used in forestry research for modelling the age trend in tree-ring data. It is expressed as

$$\hat{y} = ax^{b}e^{-cx}$$

or 1.14

$$\log \hat{y} = \log a + b \log x - cx$$

in linearized form. The coefficients a, b and c determine the shape

of the function and allow for modelling the juvenile period of increasing radial growth seen in many trees. Because this growth function is also incapable of modelling disturbance pulses at random intervals, Warren (1980) postulated that a series of disturbance pulses could be modelled as a discrete time aggregate of generalized exponential growth functions. Given that the number of pulses is unknown at the start, Warren (1980) developed a technique that involves fitting equation 1.14 to the first N years of data and testing for the presence of another pulse by extrapolating the first estimated pulse N more years into the future. A t-test was used to decide if the extrapolated fit departs significantly from the actual data. If the null hypothesis of no departure is accepted, equation 1.14 is refitted to the enlarged time base (2N) and the next N year segment is tested against a new extrapolation. If the null hypothesis is rejected, new coefficients are estimated for the extrapolation period data, a new N year extrapolation made, and the t-test applied. The stepwise fitting and testing procedure continues until the series is exhausted. There are several problems associated with this standardization method, some of which are noted by Warren (1980). The time base N used for fitting and extrapolating is arbitrary. Warren chose N=30 years based on the results of a survey in which several persons visually examined the fits using different time bases and chose the fits that looked best. As noted by Warren, it is extremely unlikely that any one time base will work well for different species and regions. The t-test used for testing the extrapolated fit is not

appropriate unless the degrees of freedom are reduced due to the highly autocorrelated nature of most tree-ring data and the extrapolated values (Mitchell et al., 1966). Warren (1980) does not address this problem. Indeed, Box and Tiao (1975) consider the t-test to be invalid when an autocorrelated time series is being tested for the occurrence of an intervention such as a disturbance in tree-rings. While the basic standardization model of Warren (1980) is intriguing and, in some ways, conceptually appealing, the estimation procedures are subjective and statistically questionable.

Barefoot et al. (1974) applied a stochastic method of standardizing oak ringwidths using an exponentially weighted smoothing technique developed by Brown (1959) to forecast economic time series. The smoothing function consists of two components for estimating the actual ringwidth y for period i: an average, $\bar{y}_i$, and a lag correction for trend, $\tilde{y}_i$. This is expressed as

$$\hat{y}_i = \alpha\bar{y}_i + (1-\alpha)\alpha\tilde{y}_i \qquad 1.15$$

there $\hat{y}_i$ is the estimated ringwidth for period i,

$$\bar{y}_i = \alpha(y_{i-1}) + (1-\alpha)\ (\bar{y}_{i-1}) \qquad 1.16$$

and

$$\tilde{y}_i = \alpha\ (y_i - y_{i-1}) + (1-\alpha)\ /\alpha \cdot (\tilde{y}_i - 1) \qquad 1.17$$

The quantity α is a weighting factor that determines the degree of smoothing. Barefoot et al. (1974) arbitrarily selected $\alpha = 0.2$ which allows the previous 10-15 years of growth to influence the estimate of

the current righwidth. An obvious weakness of this method is the arbitrary nature of α. It is unlikely that a consistently appropriate α exists for any tree species or site type. The method also assumes that the series being smoothed is an integrated or non-stationary first-order moving average process (Box and Jenkins, 1970, p. 169). Such an assumption is questionable given the success in modelling tree-ring series as autoregressive processes (Hipel and McLeod, 1977; Meko, 1981). Thus, the method of Barefoot et al. (1974) suffers from the arbitrariness of α and an inflexible underlying model.

Bitvinskas (1974) discusses the use of moving averages for creating the smooth age trends necessary for standardization. Specifically, he describes the construction of the curve as an unweighted moving average of anywhere from 3 to 31 ringwidths for the smoothing process. This is expressed as

$$\hat{y}_j = \Sigma\, y_i/n \qquad 1.18$$

where $\hat{y}_i$ is the ith average usually centered in time in the n-ring interval used to compute the average of j ringwidths. Aside from the difficulty of selecting the "correct" number of terms to use in the moving average, this approach has an extremely bad side effect as a digital filter. It can create sinusoidal behavior in the series through what is known as the Slutky-Yule effect (Mitchell et al., 1966, p. 6). For this reason, equation 1.18 is never recommended as a filtering technique in time series analysis. The appropriate form of low-pass moving average filter is centrally weighted as

$$\hat{y}_i = \sum w_j y_j / \sum w_j \qquad 1.19$$

where the w_j are symmetric filter weights often shaped like a gaussian probability density function. See Mitchell et al. (1966) for a discussion of such centrally weighted moving averages and the construction of the appropriate weights for filtering time series. This topic is also discussed and applied to tree-ring data in Fritts (1976). A variant of the centrally weighted moving average approach to tree-ring standardization was introduced by Cook and Peters (1981). Their method utilizes a cubic smoothing spline as a low-pass filter for modelling the age trend and disturbance pulses collectively through the selection of a single smoothing parameter p. The smoothing spline represents an infinitely variable family of low-pass filters which does not require the explicit construction of filter weights as is required for equation 1.19. Thus, it is quite easy to use. However, it suffers the same problem as other filtering and smoothing techniques so far discussed. That is, the degree of filtering and smoothing is still arbitrary and often selected on a trial-and-error basis. Recent research by Blasing et al. (1983) has produced an interesting method for selecting the optimum smoothing parameter p based on the verification success of a climatic reconstruction. Since the method has been tested only on white oak from Iowa, it is too soon to tell if it will work well elsewhere.

A final problem must be noted in the use of low-pass moving average filters for constructing the standardization curve. As noted

earlier, tree-ring series often behave as autoregressive processes. Jones (1984) shows how filtering an autoregressive process can create an artificial low-frequency periodicity in the variance spectrum of the filtered series, when, in fact, none was originally present. This occurs because time series with positive autoregression have variance concentrated in the lower frequencies where the filtering occurs. By removing this low-frequency variance, an apparent spectral peak is created which is nothing more than an artifact of truncating the ascending low-frequency continuum of variance characteristic of such autoregressive processes.

Conclusions

The tree-ring standardization problem has been defined in terms of the uncertainty associated with the identification, separation and removal of disturbance pulses that mimic low-frequency fluctuations caused by climate. The mathematics of standardization has revealed that the variance stabilizing property of indexing is closely tied to the goodness-of-fit of the standardization curve. This relationship was found to be antagonistic if the standardization curve does not follow the local mean very closely. A review of the literature indicates that currently available standardization techniques lack both a theoretical model and a well-defined methodology for objectively identifying and removing non-climatic disturbance pulses from climatic fluctuations. In the next chapter, a biological model will be developed based on the stand dynamics of closed-canopy

forests. This model will offer some insights into the probable sources of non-climatic variance. Later chapters suggest and test a method for removing this variance from an ensemble of tree-ring data.

CHAPTER 2

A LINEAR AGGREGATE MODEL FOR TREE-RING SERIES

Introduction

Consider a single tree-ring series along a single radius as a linear aggregate of several subseries representing the sources of variance found in the composite series. Let this aggregated time series be expressed as

$$G = C + A + D1 + D2 + E$$

where:

G = the well-dated tree-ring widths measured along a single radius,

C = the climatically-related growth variations common to a stand of trees including the mean persistence of these variations due to physiological preconditioning and interaction of climate with site factors,

A = the age related growth trend,

D1 = the endogenous disturbance pulse originating from forces within the forest community,

D2 = the exogenous disturbance pulse originating from forces outside the forest community,

E = the series of more or less random variations representing growth influencing factors unique to each tree or radius within the tree.

The assumption of linearity and implicit independence between the subseries is a necessary oversimplification for the moment. However, the purpose of this model is not to describe exact relationships between the subseries. Rather, it allows for a discussion of certain properties of each component separately from the others as a necessary step in developing a standardization method that models the nature of the tree-ring series more adequately.

Subseries C--The Common Climate Signal

The climatically-related subseries, C, reflects certain broad-scale meteorological variables which directly or indirectly limit the growth processes of trees in a stand. These variables are assumed to be uniformly important for all trees of a given species when the site characteristics of the stand, such as hydrology, elevation, exposure and soil, are more or less homogeneous. The biology of the tree governs its capacity to respond to climate. This in turn determines the "climatic window" (Fritts, 1976, p. 238) through which climate variables create similar patterns of wide and narrow rings in different trees when matched contemporaneously. This is the phenomenon that enables cross-dating. Although cross-dating is normally associated with high-frequency change in ring width, there are also many lower-frequency variations of climate that pass through the climatic window which can also be shown to be in agreement between the trees (Fritts, 1976).

The input that produces C is assumed to involve weakly-stationary stochastic processes. That is, its mean and variance are independent of time, and the series evolves through time in a probabilistic fashion. Because of the previously mentioned feedback mechanisms affecting the climate system, the climatic signal in C will often be non-random in an autoregressive sense. This has been shown to be the case for temperature data (Jones, 1964) and Palmer drought severity indices (Katz and Skaggs, 1981), although precipitation is more frequently random (Salas et al., 1980, p. 51). When the autoregression is positive, the variance of C will be concentrated in the lower frequencies of its variance spectrum. Such series are often described as "red noise" processes (Gilman, Fuglister, and Mitchell, 1963) due to the analogy between low-freuency variance and long wave-length red light.

Frequently, the persistence observed in C will be much greater than that which can be accounted for by the persistence in climate (Matalas, 1962; Meko, 1981). This inflated persistence in the ring-width series is generally thought to come about from a variety of factors often involving the physiological preconditioning of the tree-growth system by previous environmental conditions (Fritts, 1976) and from site factors such as soil hydrology (Meko, 1981) which create lags in the tree-response system. Meko (1981) also contends that some of the excess persistence is due to residual non-climatic growth variations not removed during standardization. This contention implicitly recognizes that there must be inadequacies of current standardization methods which I have discussed in Chapter 1. Any differences between the persistence

structure of climatic variables which produce C and C, itself, can of course be adjusted for during the transfer function modelling phase of dendroclimatic reconstructions (Stockton, 1975; Fritts, Lofgren and Gordon, 1979; Meko, 1981). Meko (1981) has demonstrated how Box-Jenkins models can be used in this regard. This type of analysis occurs subsequent to standardization. Discussion of various approaches to transfer function modelling are clearly outside the current topic and will not be considered further. From a climatological point of view, the assumption of weak stationarity for the input leading to C is flawed because the climate system probably never reaches a true equilibrium state and appears to be inherently non-stationary over very long time periods. Thus, a 400-year tree-ring series could have, superimposed on its age trend, a very low-frequency climatic fluctuation on the order of several centuries long. In this case, the series would be non-stationary due to the presence of two different, but not necessarily uncorrelated, components. But in another sense, the assumption of weak stationarity is reasonable for the usual time spans under consideration. Variance spectrum analyses of climatic and proxy climatic series for the Holocene (Kutzbach and Bryson, 1975) show that such series generally have moderately "red" (ρ=0.5-0.7) spectra for time periods of 100 to 1000 years. This level of redness is well within the bounds of stationarity for a first-order autoregressive process (Box and Jenkins, 1970). Since old-growth stands of trees rarely exceed 1000 years in age, the first two moments of C may not behave differently in a statistical sense from a weakly-stationary process. Because there is strong biological basis for

expecting an age trend, virtually all tree-ring chronologies are detrended with the realization that some long-period climatic information may be lost.

Subseries A--The Age Trend

The age trend, A, was described earlier as being a monotonically non-increasing function of time which could be characterized often by a deterministic growth function of linear or exponential form. While this description holds well for trees growing in open-canopy situations, it must be generalized to allow for the occurrence of a variety of linear and curvilinear age trends of arbitrary slope sometimes found in trees from closed-canopy forests. Shade tolerant species such as eastern hemlock and red spruce may require many decades of growth to achieve a co-dominant position in the canopy. During these years of subordinate canopy position, the general trend in radial growth will often be positive as the suppressed trees grow upward into more favorable regions of the canopy. Once it becomes established in the canopy, the rate of growth may decline in the normally expected way. Since both the upward and downward trend is, again, clearly associated with increasing age, a more general age trend model should be included which may allow for linear or curvilinear trends of arbitrary slope and shape.

As noted in Chapter 1, many mathematical functions are available that seem to fit certain kinds of age trends well. For example, quadratic and power functions are reasonable alternatives to the negative exponential curve in some cases. The model for A should serve only to detrend a series and stabilize its variance to some degree. If we

define trend in mean according to Granger's (1966) definition as comprising all frequency components with wave-lengths exceeding the length of the observed time series, then linear, quadratic, exponential, and power functions are all possible models of A. They will not remove any climatic information that is resolvable from the age trend.

Subseries D1 and D2--The Endogenous and Exogenous Disturbance Pulses

The non-climatic variance accounted for by the disturbance pulses, D1 and D2, can be split into two general classes of disturbance: endogenous and exogenous (Bormann and Likens, 1979; White, 1979). Conventionally, they are differentiated by the causal mechanisms involved, i.e. forces internal to the forest community versus forces external to it, although these differences become quite blurred upon investigation (White, 1979). In the context of tree-ring standardization, another differentiating feature is pertinent: areal extent of impact. As will be described, this feature lies at the crux of the standardization method being developed here.

Like the age trend, D1 and D2 can be modelled as smooth processes. Collectively, they have been modelled deterministically using least square curve-fitting (e.g. Fritts, 1976, p. 164; Warren, 1980) and stochastically using digital filters (e.g. Bitvinskas, 1974; Cook and Peters, 1981), but the result is always a smooth, continuous curve for approximating a disturbance pulse. Superimposed upon this curve will be the higher-frequency climatic variations of C. However, because the duration of a disturbance pulse may be short compared to the length of the tree-ring series, it may be superimposed upon lower-frequency clima-

tic fluctuations as well. The shape of a disturbance pulse will also be much more variable than an age trend because a disturbance may cause growth suppression or acceleration depending on its relationship to the tree and the nature of its effect.

Endogenous disturbances are caused by factors related to characteristics of the vegetation which are independent of the environment (White, 1979). Disturbances which are often described as such in closed-canopy forest communities occur when dominant overstory trees senesce, die and topple as a natural consequence of competition, aging and stand succession. Although the senescence and death of old-age trees from internally caused factors seems biologically reasonable, it rarely occurs without the impetus of external environmental factors such as insect attack, drought and windthrow (White, 1979), hence, the difficulty in differentiating endogenous from exogenous disturbances. The removal of individual dominants creates gaps in the canopy for suppressed understory trees and adjacent codominants to grow into. These gaps also provide valuable seed beds for reproduction and regeneration. The sudden increase of available light and soil moisture may mean a dramatic increase in radial growth over several years for previously suppressed trees as they compete for dominant positions in the canopy gap. This model for structural changes in forest communities is called gap-phase reproduction by White (1979) and gap-phase replacement by Bray (1956) and Spurr and Barnes (1973, p. 344).

In the context of tree-ring standardization, truly endogenous disturbances can be expected to occur randomly in space and time in

forest communities. That is, the loss of a dominant tree in one section of a stand is not likely to be related temporally or spatially to similar losses at widely separated locations in the stand. This assumption immediately suggests that the resultant truly endogenous disturbance pulses will rarely be synchronous among distant trees in a stand except by chance alone.

Little data exists for estimating the frequency of occurrence of endogenous disturbances and the gap-sizes produced by them. However, a study of natural disturbances by treefalls in Lilley Cornett Woods (Romme and Martin, 1982) does shed some light on this matter. Lilley Cornett Woods is a 104-hectare tract of old-growth mixed mesophytic forest in eastern Kentucky. The dominant tree species are American beech (Fagus grandifolia Ehrh.) and white oak (Quercus alba L.). Over a period of eight years, 77 treefall events occurred, 66 by single trees and eleven by 2-3 trees. The major cause of treefall was ascribed to high-speed, short-duration winds. The area of each gap produced by treefall was carefully measured. The gaps ranged from $74m^2$ to $1235m^2$ in size with a mean of $374m^2$ and a median of $307n^2$ (Romme and Martin, 1982). A histogram of gap-size classes as a percent of all gaps indicates that the distribution is highly skewed. The mode lies within the $101-200m^2$ and $201-300m^2$ gap size classes which account for 46% of all gaps. A reasonable estimate of the gap size mode is $200m^2$. On the assumption that the gaps do not overlap, the radii of gap influence for the mode, median and mean are approximately 8m, 10m, and 11m, respectively. Thus, to minimize the probability of coring trees that are

affected by the same endogenous disturbance, trees separated by at least 16-22m should be cored. Only the trees tangential to a gap would be affected using this criterion.

In the 104 hectares of Lilley Cornett Woods, there are 2673-5000 potential gaps using the 200-374m^2 gap-size estimates. Allowing for an average of ten gaps/year (based on 77 tree-falls in eight years), only 0.2-0.4% of the canopy area is lost by tree-falls each year. This percent is lower than the percent of trees affected by a gap because several trees may grow around a gap perimeter. However, even if the number of affected trees is as large as 5, the percent of all trees affected by treefalls each year is still only around 1-2%. Thus, the probability of synchronous endogenous disturbance pulses in tree-ring series from Lilley Cornett Woods is quite small. This conclusion should hold for old growth stands in general where the dominant tree species are long lived and the stand is large relative to the gaps produced by treefalls.

Since the presence of D1 in the aggregate should impart more differences than similarities among a spatially broad sample of tree-ring series, an obvious approach to the standardization problem is to identify and remove only these differences. From the standpoint of minimal loss of climatic information, the identification and removal of low-frequency differences has obvious appeal because they cannot be logically related to fluctuations attributable to C. It is interesting to note that Dr. Edmund Schulman of the Laboratory of Tree-Ring Research used this concept in the pre-computer days of dendrochronology when he graphically standardized tree-ring series (B. Bannister, pers. comm.).

By plotting all of the series togther, Schulman was able to identify significant differences and modify the standardization curves to remove localized low-frequency fluctuations which did not agree among all series. The simultaneous scrutiny of tree-ring data during standardization is sometimes omitted today because of the large number of series being standardized. However, a careful examination of the fitted growth curves is advised (Fritts, 1976) and some workers do remove data that are not adequately modelled by the growth function, or they vary the growth function that is used. Often they will standardize a sample several times until the major outliers from the growth curve are identified and removed or corrected (Fritts, 1976). This is a cumbersome and sometimes burdensome process.

Exogenous disturbances are caused by environmental forces which lie external to and are independent of the vegetation (White, 1979). Unlike endogenous disturbances, these disturbances have many possible causal agents which can affect large areas of forest. Some of the important agents are fire, windstorm, ice storm, disease and insect infestation. For a complete review of exogenous disturbance agents, see White (1979). Because an exogenous disturbance can be very extensive, the resultant disturbance pulse, D2, may occur contemporaneously in virtually all affected trees in a stand. This presents obvious difficulties for standardization for these contemporaneous pulses may be impossible to distinguish from common low-frequency fluctuations of C.

The frequency of a specific exogenous disturbance will generally be inversely proportional to its magnitude and is highly dependent on

such factors as species composition, topography and geographic location (White, 1979). For example, pitch pine (Pinus rigida Mill.) and jack pine (P. banksiana Lamb.) are shade-intolerant species which require frequent fire to maintain their communities (Fowells, 1965). Thus, the frequency of fire in these communities is likely to be high. In contrast, the fire recurrence interval for northern hardwood-conifer forests in New England may be several hundred years long (Bormann and Likens, 1979). The effects of fire will greatly depend on the severity of the burn. Frequent ground fires may benefit growth of shade-intolerant species by destroying understory growth, reducing root competition for moisture and recycling nutrients trapped in forest litter. More severe fires may impair subsequent growth if some foliage is killed by heat or flames and the cambial layer is scorched. If burns are much more severe than this, the stand may be destroyed outright and the exogenous disturbance problem is moot.

Insect infestations will have variable effects of forest stands depending on the severity of injury to host species and indirect effects on non-host species (Brubaker and Greene, 1979; Wickman, 1980). Phytophagus insects reduce the photosynthetic area of host species and thus cause reductions in carbohydrate production for ring formation. Conversely, growth of non-host species in an infested stand can actually improve because host-tree defoliation reduces competition for light, water and nutrients (Wickman, 1980). Fortunately, many tree species are able to withstand light to moderate amounts of defoliation without showing a detectable reduction in radial growth in the lower trunk of the

tree (Koerber and Wickman, 1970; Brubaker and Greene, 1979). The defoliation effect is most apparent in the rings of the upper bole and branches. This is fortuitous because virtually all tree-ring specimens are taken from breast height or below on the bole. But this also suggests that defoliation effects will show up more frequently in the earlier segments of tree-ring chronologies because the crowns of trees, when younger, will be closer to the breast height region of the bole sampled by dendrochronologists.

Sampling strategies can be designed to minimize the probability of some exogenous disturbances like fire and insect infestation. Stands isolated by water or barren expanses of rock are less likely to be affected by regional fires, for example. Another approach is site redundancy whereby stands on similar but geographically separate sites in the same region are sampled with the hope that a stand disturbance peculiar to one site can be identified. Insect infestation effects may be identified by sampling host and non-host species on the same or nearby sites. These approaches do not actually solve the problem of identifying exogenous disturbance pulses during standardization. They only reduce the problems. Without any knowledge of large-scale disturbances that have affected a stand, a better solution to this problem does not seem possible.

Since the importance of D2 is extremely difficult to establish because of its dependence on such factors as the frequency and magnitude of the event, the causal agent, tree species, site topography and geographic location, it will be assumed to have a minimal contribution to

G. This assumption is valid only in the sense that, if present, D2 may be very difficult to differentiate from C during standardization and should, therefore, be regarded as a possible climatic fluctuation until proven otherwise by comparison to C in nearby sites and in different species. This is the rationale for using a number of chronologies for different species and sites in transfer function analysis (Fritts, 1976).

Subseries E--The Random Variance

The last subseries, E, is the more or less random variance in the radial tree-ring series which represents such variables as localized responses to micro-environmental factors and variations in circuit uniformity which are unrelated to the variance accounted for by C, A, D1 and D2. This variance is assumed to result from serially uncorrelated events affecting each tree which are spatially uncorrelated within the stand of trees. The standard way to reduce this random variance is through replicate sampling (Fritts, 1976). That is, a number of trees are sampled (say, 20 to 40) from a forest stand and standardized. The results are averaged together to form a mean-value function for the site.

The linear aggregate model is useful for describing the concept of the signal-to-noise ratio (SNR) in tree-ring series. For example, a semi-arid site tree-ring series will be an aggregate of C, A and E with D1 and D2 assumed to be negligible, minimized or absent. After A has been removed, the climatic SNR is the ratio of the variances of C and E. As pointed out by DeWitt and Ames (1978), this ratio will ordinarily be

considerably higher in semi-arid site chronologies than in mesic forest-interior chronologies. Given the inadequacies of current standardization techniques, it is likely that the SNR of forest-interior chronologies can be increased appreciably by improving the standardization model.

Conclusion

The linear aggregate model has identified several discrete classes of variance which can be found in a generalized ringwidth series. The two classes which have created the principal difficulties in standardizing forest interior ringwidths are the disturbance pulses, D1 and D2. The likelihood of significant non-synchroneity between endogenous disturbance pulses in a stand of trees offers a conceptual approach to optimally removing this class of non-climatic variance. That is, remove only those fluctuations that differ from tree to tree. In the next chapter, a method is developed which is based on this concept.

CHAPTER 3

A TIME SERIES MODEL FOR TREE-RING STANDARDIZATION

Introduction

The tree-ring standardization model which is developed in this chapter is based on autoregressive time series modelling and its relationship to predictive deconvolution. The model cannot be adequately understood without some familiarity with autoregressive and moving average processes. These processes and their dual properties will be described in some detail for this reason prior to discussing the operational specifics of the standardization method.

The General Time Series Model

Standardizing tree rings involves the decomposition of each radial growth increment series into two components: a non-climatically determined growth curve and a climatically determined set of scaled residuals or indices. Letting $z = C + E$ and $g = A + D1 + D2$ from the linear aggregate model in Chapter 2, this decomposition is expressed as

$$r_t = z_t \cdot g_t \qquad 3.1$$

where r_t is the growth increment series, z_t is the climatically related index series, g_t is the smooth growth increment curve. The actual procedure of indexing involves division of each r_t by each g_t which amounts to scaling the r_t into percentages of expected growth. This serves to stabilize the variance which is generally proportional to the mean in measured ring-widths.

Equivalently, equation 3.1 can be transformed to logarithms yielding the additive model

$$\log r_t = \log z_t + \log g_t \qquad 3.2$$

Since equation 3.1 and equation 3.2 are mathematically equivalent, a general linear time series model will be utilized because the usual indexing procedure, in effect, linearizes the model.

In the simple case where disturbance effects are absent (i.e. D1 and D2=0) the growth curve g_t is ordinarily modelled as a non-stationary deterministic age trend which, when removed from r_t yields a stochastic series of indices, z_t. This basic model is similar to a fundamental theorem in the decomposition of stationary time series proposed by Wold (1938). The Wold decomposition theorem states that any stationary, stopchastic process can be decomposed into two mutually uncorrelated, stationary components which are deterministic and non-deterministic. The theorem is expressed as

$$y_t = \mu_t + \nu_t \qquad 3.3$$

where y_t is the observed stochastic process, and μ_t and ν_t are the stochastic and deterministic components, respectively. The form of the Wold decomposition theorem is identical to the linearized standardization model described above. The significant difference betwen equation 3.2 and equation 3.3 is the stationarity property of ν_t because the growth curve, g_t, is likely to be non-stationary. The search for deterministic components corresponding to ν_t in individual tree-ring series (Douglass, 1919, 1929, 1936; Bryson and Dutton, 1959; LaMarche and Fritts, 1972) has always produced equivocal results. This suggests that

ν_t will rarely be a factor in modelling the stochastic properties of tree-ring series. For simplicity ν_t will be assumed equal to zero after g_t has been removed.

An important property of the stochastic component μ_t is its representation as an infinite weighted moving summation of a current and all past random shocks (Wold, 1938). Let

$$y_t = e_t + \sum_{i=1}^{\infty} \psi_i e_{t-i} \qquad 3.4$$

where μ_t is the observed stochastic series, e_t is an unobserved series of serially random shocks with a mean of zero and a variance equal to e_t^2, and the ψ_i are fixed weights. Equation 3.4 is identical to the general linear process (Box and Jenkins, 1970, p. 46) which is the basis for autoregressive and moving average stochastic modelling. Because the Wold decomposition theorem applies to all stationary stochastic processes, once the growth increment series, r_t, has its deterministic growth curve, g_t, removed the resultant z_t index series can be modelled as a stochastic process of the form in equation 3.4.

The Moving Average Time Series Model

The infinite summation in equation 3.4 is obviously unsuitable in practice. When, on statistical grounds, only the first q of the ψ-weights are non-zero, the process is called a moving average (MA) process of order q (Box and Jenkins, 1970, p. 52). To differentiate the finite order process from the infinite representation, the difference equation form of an MA(q) process is conventionally changed to

$$z_t = e_t - \sum_{i=1}^{q} \theta_i e_{t-i} \qquad 3.5$$

where the θ_i are equal to the finite set of non-zero ψ_i. Thus, moving average processes are truncated forms of the general linear process.

The moving average process represents a specific class of digital filters known as causal feedforward filters (Robinson and Treital, 1980, p. 48). The filter is causal in the sense that the current filtered output is a function of a current random shock and a weighted sum of past random shocks. The θ-weights represent the memory function or impulse response function of the filter. Additionally, this filter is physically realizable (Robinson and Treital, 1980, p. 100) because it does not need future inputs to produce the current output. The difficulty in fitting the endpoints of tree-ring series using polynomials and symmetric digital filters occurs because these filters are not purely causal and, therefore, not physically realizable. That is, each method must anticipate or guess at the behavior of the data off the ends in order to fit the ends. Thus, causal filters have a mathematical formulation that is consistent with the way tree-ring series actually evolve through time.

The feedforward property of moving average processes is expressed schematically in Figure 3.1 for the simple MA(1) process. A random shock e_t is fed into a constant box where it is multiplied by the θ-weight. The $-\theta e_t$ term then enters the time delay box where it is delayed one time unit. On exiting the time delay box, the $-\theta e_{t-1}$ term is

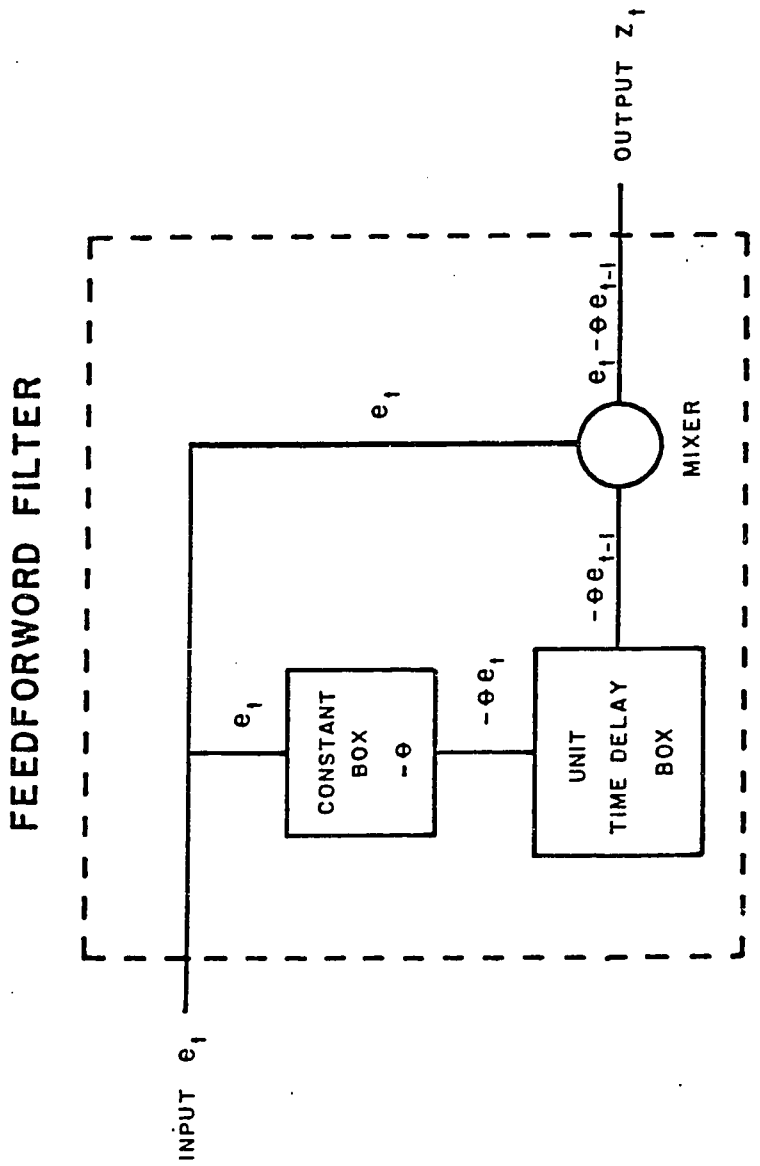

Figure 3.1. The schematic representation of a first-order causal feedforward filter.

Adapted from Robinson and Treital (1980, p. 44).

fed forward and added to a new random shock e_t to produce the output z_t. The feedforward filter schematic can be easily extended to MA(q) processes by providing q time delay boxes with delays of one to q time steps, a q θ-weights.

The Autoregressive Time Series Model

The general linear process in equation 3.4 has an alternate representation as an infinite weighted sum of all past observations and a current random shock (Box and Jenkins, 1970, p. 47). Let

$$z_t = e_t + \sum_{i=1}^{\infty} \pi_i z_{t-i} \qquad 3.6$$

where z_t is the observed process, e_t is a random shock as before, and the π_i are fixed weights related to past z_t. If $\pi_i = 0$ for all $i > p$, then the process is a finite autoregressive (AR) process of order p (Box and Jenkins, 1970, p. 51). To differentiate the finite process from the infinite process, the notation for an AR(p) process changes from equation 3.6 to

$$z_t = e_t + \sum_{i=1}^{p} \phi_i z_{t-i} \qquad 3.7$$

where $\phi_i = \pi_i$ for $i \leq p$.

The autoregressive process represents another class of digital filters known as causal feedback filters (Robinson and Treitel, 1980, p. 80). These filters are causal in the same sense as the moving average

process because only past outputs are needed along with a current input to produce the current output. For this reason, it immediately follows that autoregressive processes are also physically realizable digital filters.

The feedback property of autoregressive processes is expressed schematically in figure 3.2 for the simple AR(1) process. The current output z_t is fed into a constant box where it is multiplied by the ϕ-weight. The z_t term then enters the time delay box where it is delayed one time unit. On exiting the time delay box, the ϕz_{t-1} term is fed backwards and added to the current e_t to produce the new current output z_t. The feedback model can be easily extended to AR(p) processes by providing p time delay boxes with delays of one to p time steps, and p ϕ-weights.

The autoregressive representation of a stochastic process is especially useful for modelling the observed persistence structure of tree-ring series. Tree-ring series frequently have autocorrelation and partial autocorrelation functions which behave similarly to those functions of theoretical autoregressive processes of order p. That is, the autocorrelation function damps out with increasing lags while the partial autocorrelation function cuts off after lag p in accordance to the theoretical model (Box and Jenkins, 1970, p. 79). This behavior occurs so commonly in tree-ring series that it suggests that the physiological processes responsible for much of the observed persistence act together as feedback mechanisms to produce an autoregressive-like memory. Matalas (1962), Stockton (1971), Hipel and McLeod (1977) and Meko (1981)

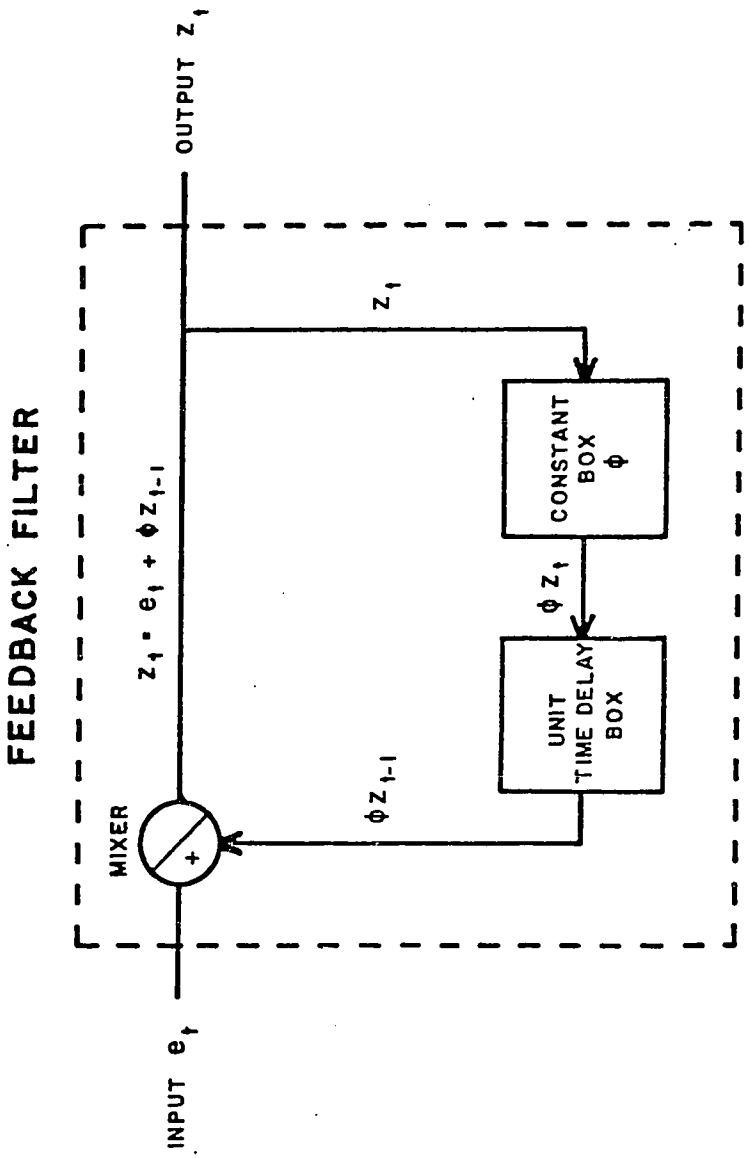

Figure 3.2. The schematic representation of a first-order feedback filter.

Adapted from Robinson and Treital (1980, p.80).

have all found that relatively low-order AR processes ($p \leq 3$) are usually sufficient to model the observed persistence structure in tree-ring chronologies from western North America. I have also applied Box-Jenkins modelling techniques to tree-ring chronologies from eastern North America and the forest-tundra ecotone of Canada and Alaska. Again, autoregressive models almost always fit the persistence structure of the data well.

The Duality Between Autoregressive and Moving Average Processes

Box and Jenkins (1970) describe in detail the duality between autoregressive and moving average processes. Specifically, any finite order AR process can be mathematically re-expressed as an infinite order MA process, and vice versa (Box and Jenkins, 1970, p. 72). This is easily illustrated for the AR(1) process:

$$z_t = \phi_1 z_{t-1} + e_t \qquad 3.8$$

By successive substitutions of z_{t-1} with its equivalence ($\phi_1 z_{t-i-1} + e_t$), the duality develops recursively as:

$$z_t = \phi_1 (\phi_1 z_{t-2} + e_{t-1}) + e_t \qquad 3.9$$

$$= \phi_1^2 z_{t-2} + \phi_1 e_{t-1} + e_t$$

$$z_t = \phi_1^2 (\phi_1 z_{t-3} + e_{t-2}) + \phi_1 e_{t-1} + e_t$$

$$= \phi_1^3 z_{t-3} + \phi_1^2 e_{t-2} + \phi_1 e_{t-1} + e_t$$

$$z_t = \phi_1^3 (\phi_1 z_{t-4} + e_{t-3}) + \phi_1^2 e_{t-2} + \phi_1 e_{t-1} + e_t$$

$$= \phi_1^4 z_{t-4} + \phi_1^3 e_{t-3} + \phi_1^2 e_{t-2} + \phi_1 e_{t-1} + e_t$$

and so on back to minus infinity to yield the MA (∞) process

$$z_t = e_t + \sum_{i=1}^{\infty} \phi_1^i e_{t-i} \qquad 3.10$$

It follows that the MA(1) process:

$$z_t = e_t - \theta_1 e_{t-1} \qquad 3.11$$

can also be expressed as an AR (∞) process:

$$z_t = e_t - \sum_{i=1}^{\infty} \theta_i^i z_{t-i} \qquad 3.12$$

by using the same recursion illustrated above.

Another means of examining their duality is by expressing AR(p) and MA(q) processes as polynomials of order p and q using the backward shift operator B (Box and Jenkins, 1970, p. 8).

Letting $B^i z_t = z_{t-i}$, the AR(1) process in equation 3.9 becomes

$$z_t = (\phi_1 B) z_t + e_t \qquad 3.13$$

or

$$(1 - \phi_1 B)\, z_t = e_t \qquad 3.14$$

and the AR(p) process in equation 3.7 becomes

$$(1 - \phi_1 B - \phi_2 B^2 - \cdots - \phi_p B^p)\, z_t = e_t \qquad 3.15$$

or more succinctly,

$$\phi(B)\, z_t = e_t \qquad 3.16$$

Likewise, the MA(q) process in equation 3.5 becomes

$$z_t = (1 - \theta_1 B - \theta_2 B^2 - \cdots - \theta_q B^q)\, e_t \qquad 3.17$$

or, in compact form

$$z_t = \theta(B)\, e_t \qquad 3.18$$

The duality now takes on a different form. That is, the AR(p) process in equation 3.16 is re-expressed as an MA(∞) process by dividing both sides of the equation by the operator $\phi(B)$. This yields

$$z = \phi(B)^{-1} e_t \qquad 3.19$$

which is mathematically equivalent to equation 3.12. Thus, when expressed as polynomials, AR and MA processes are seen to be inverse forms of each other.

The importance of these noted dualities will come clear in the next section where the basic model for predictive deconvolution (Peacock and Treital, 1969; Robinson and Treital, 1980) is described. As will be discussed, predictive deconvolution and autoregressive time series modelling are equivalent for the special case where a one-step ahead prediction is of interest. The difference lies in the application. Box and Jenkins (1970) use AR modelling for forecasting and control purposes while Robinson and Treital (1980) use it to prewhiten or deconvolve seismic traces that are contaminated by reverberations.

The Relationship Between Autoregressive Modelling and Predictive Deconvolution

The relationship between autoregressive modelling and predictive deconvolution of time series is rarely described outside of the scientific literature dealing with predictive deconvolution and autoregressive spectral estimation of geophysical data (Peacock and Treital, 1969; Freyer, Odegard and Sutton, 1975; Ulrych and Bishop, 1975; Ulrych and Clayton, 1976). In the context of standardizing tree-ring series via an

autoregressive model, this relationship is very useful towards understanding the basis of its expected performance.

Predictive deconvolution or prediction-error filtering is used extensively in geophysics to minimize the effects of echoes or reverberations in seismic traces due to the passage of sound waves through layered sediments. The desired sound reflection coefficient series which describes the structure of the layered medium is assumed to be serially uncorrelated (Peacock and Treital, 1969). In this sense, the coefficient series is equivalent to the random shock series described earlier. When an impulse of sound passes through the layers, some of the sound energy echoes backwards through the layer boundaries, creating what is known as a reverberating pulse train. The pulse train obscures the random reflection coefficient series by distributing the energy of the sound impulse at each boundary to subsequent layer boundaries. The result is the addition of stochastic predictability to the random series which degrades the resolution of the trace.

Robinson and Treital (1980) describe the pulse train as a linear aggregate of smooth sound wavelets of fixed shape that begin at the layer boundaries and propagate forward in time with diminishing energy. The energy of each wavelet depends on the strength of the reflection coefficient from which it propagates.

Wavelets have two properties which differentiate them from sample time series: a definite origin or arrival time and finite energy or transience (Robinson and Treital, 1980, p. 63). The property of origin means that the wavelet does not exist in the series prior to its

arrival, and the property of finite energy means that it decays with time and eventually disappears from the series. A wavelet can be either "short-period" or "long-period" depending on the character of the reverberations (Peacock and Treital, 1969). Short-period reverberations show up in the autocorrelation function as a waveform which damps out or decays with increasing lag. Long-period reverberations have a correlogram which maintains a strong waveform at long lags.

Robinson and Treital (1980, p. 242) express the above model mathematically as

$$x_t = b_0 e_t + b_1 e_{t-1} + \cdots = \sum_{s=0}^{\infty} b_s e_{t-s} \qquad 3.20$$

where the b_s are the coefficients of the wavelet and the e_t are the randomn shocks or reflection coefficients. Equation 3.20 is the one-sided, discrete convolution formula. Thus, the model states that the raw seismic trace x_t is created by the convolution of the wavelet b_s with the reflection coefficient series e_t. An excellent discussion of the meaning of convolution is given in Robinson and Treital (1980, p. 66). However, it is readily apparent that equation 3.20 is mathematically identical to the general linear process in equation 3.4 by letting $b_0 = 1.0$.

The goal of predictive deconvolution is to model and remove the filtering effects of the aggregated wavelets to reveal the reflection coefficient series more clearly. Since the underlying model assumes that these coefficients are serially uncorrelated, what is needed is an inverse filter which will prewhiten or deconvolve the autocorrelated sequence back to the original series of random coefficients or shocks.

This amounts to compressing the broadly distributed energy of each wavelet back to its original form as a random shock. This is accomplished by designing a prediction-error filter for which the prediction distance is unity (Peacock and Treital, 1969) or, equivalently, by fitting an autoregressive process to the data (Freyer et al., 1975). The importance of the duality between autoregressive and moving average processes now comes clear. The wavelet has been modelled as an MA(∞) process in equation 3.20. Recalling that AR and MA processes are inverse forms of one another (equations 3.18 and 3.19) and that an MA(∞) process may be parsimoniously modeled as an AR(p) process (equation 3.10), it follows that the inverse filter needed to deconvolve the autocorrelated sequence is an autoregressive process of order p. Thus, the coefficients of an AR(p) model are the coefficients of the unit-distance prediction-error filter or inverse filter of length p needed to compress each wavelet back to a random shock, the strength of each shock being proportional to the total energy of its respective wavelet.

Having noted the equivalence between autoregressive modelling and predictive deconvolution, its usefulness in minimizing the effects of non-synchronous disturbance pulses in tree-ring chronologies begins to clarify. A disturbance can be modelled as an impulse or random shock to the tree growth system because the duration of the disturbance will ordinarily be short compared to the duration of the response to the disturbance. For example, the removal of an overstory tree by windthrow occurs suddenly and is over quickly. But the gap it leaves in the canopy will influence the growth of trees in and on the perimeter of the gap

for many years. Since a disturbance has a defined arrival time and an effect on tree growth which decays asymtotically with time, the resultant disturbance pulse in the tree-ring series has the two properties of a wavelet defined earlier.

Another assumption of predictive deconvolution is that the system response to an impulse (the wavelet) is minimum-delay (Robinson and Treital, 1980, p. 241). This means that a wavelet has maximum energy shortly after the impulse arrives which subsequently decays with time. For a prediction-error filter length of $p = 1$, the filter coefficient k is said to be stable if $|k| < 1$ (Robinson and Treital, 1980, p. 82). Remembering that a unit-distance prediction-error filter is equivalent to an autoregressive model, the bounds of stability for a prediction-error filter of length $p = 1$ are identical to the stationarity requirements for a first-order autoregressive process (Box and Jenkins, 1970, p. 53). That is, for an AR(p) process where $p = 1$, the process is stationary if $|\phi| < 1$. Therefore, a tree-ring series which can be modelled as a stationary autoregressive process is approximately minimum-delay in its response to disturbance. The predictive deconvolution of tree-ring series with a disturbance pulse will result in the compression of that pulse to a random shock and a series of climatically related random shocks analogous to the reflection coefficients in seismic traces. Depending upon the severity of the disturbance, this non-climatic random shock may or may not be significantly different from the surrounding climatic random shocks. This is not a serious problem in the context of standardization because the arrival time of each disturbance is not

explicitly needed. However, the expected performance of predictive deconvolution in minimizing disturbance effects is dependent on the degree of synchrony of the disturbance arrival times through the stand of trees. If the arrival times differ from tree to tree due to localized endogenous disturbances, then the disturbance shocks will be greatly reduced or averaged-out of the mean-value function. Conversely, if the arrival times are synchronous due to large-scale exogenous disturbances, then the resultant disturbance shocks will be preserved in the mean-value function.

A caveat is necessary now in describing a tree-ring series as a minimum-delay process. While it is almost certain that a tree's physiological system will behave in a minimum-delay sense, the output of that system (the tree rings) may have long-delay properties embedded in it. How might this apparent contradiction arise? In a closed-canopy forest, a gap created by a tree-fall will allow a suppressed tree to grow upward into a codominant canopy position. This process may take several years to complete. During those years, the trend in radial growth will be positive, as available light increases, until the top of the forest canopy is reached. At this point, the tree has reached a new equilibrium state in its photosynthetic capacity. Thereafter, the trend in growth will decline to zero and subsequently go negative as expected for a normal age trend. It is apparent that the time required to reach a new equilibrium state may be much longer than is allowed for by a minimum-delay model. The forest canopy structure, itself, acts as a filter with delay properties that can prolong the response time of a tree to a

disturbance. Because the long-delay property is triggered by episodic disturbances, it is not a time-invariant characteristic of the tree-ring series. For this reason, it is embedded within the time-invariant minimum-delay model that is used to deconvolve each series. The probable effect of long-delay will be added persistence in a tree-ring series since the transience of a disturbance pulse will be "stretched out" by the forest canopy structure.

Averaging random shocks should minimize the effects of endogenous disturbances more efficiently than averaging together the original tree-ring indices. This can be appreciated by examining the transience property of some wavelets obtained from modelling tree-ring indices as autoregressive processes. The coefficients of each wavelet, which are the ψ-weights of a MA(∞) process, are obtained from the ϕ-weights of its respective AR(p) process as

$$\begin{aligned} \psi_0 &= 1.0 \\ \psi_1 &= \phi_1 \\ \psi_2 &= \phi_1\psi_1 + \phi_2 \\ &\vdots \quad \vdots \quad \vdots \\ \psi_j &= \phi_1\psi_{j-1} + \cdots + \phi_p\psi_{j-p} \end{aligned} \qquad 3.21$$

(Box and Jenkins, 1970, p. 134). Figure 3.3 illustrates some characteristic wavelets of six tree species. The wavelets all decay with time as expected, but the transience can last for many years. The oak, hemlock and pine chronologies have wavelets which die away in 10 to 20 years.

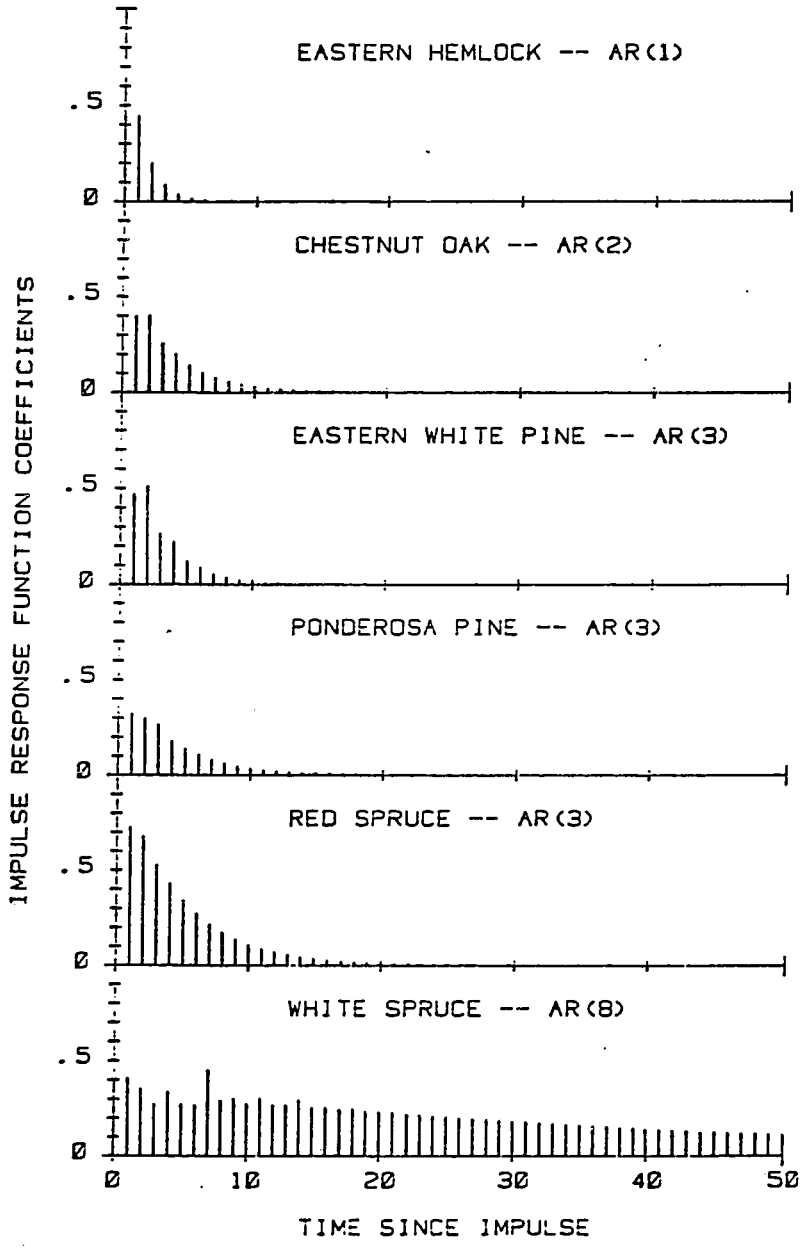

Figure 3.3. The impulse response functions or wavelets of six tree-ring chronologies.

The species and order of the autoregressive process used in computing each wavelet is seen.

The two spruce wavelets decay much more slowly, and the white spruce wavelet is still discernible after 50 years. Because the transience of a disturbance-caused wavelet may last for many years, its effect on the correlation between tree-ring series may be very strong. This will be especially so if long-delay effects are also present. If the temporal effects of disturbances can be minimized using predictive deconvolution, then the correlation between series should improve.

This property is illustrated in an ensemble of tree-ring series from eastern hemlock growing in New York. Thirty radial increment series were obtained from 15 trees. Each series was converted to indices using negative exponential or linear regression curves. Any disturbance pulse that is shorter than the length of the series in which it is found will not be removed by these standardization curves. For the common period 1842-1973, the average correlation between the indexed series was +0.30 with a standard deviation of +.07 to +0.50. After the same 30 series were deconvolved to random shocks using an AR(1) model, the average correlation rose to +0.43 with a standard deviation of +0.32 to +0.54. The change in correlation between some series can be dramatic. Before predictive deconvolution, the correlation between two indexed series from different trees was -0.43. After predictive deconvolution, the correlation rose to +0.31.

Another benefit of averaging random shocks rather than tree-ring indices is the way in which predictive deconvolution eliminates the effects of aggregating autoregressive processes when developing the mean-value function. Granger and Morris (1976) illustrate in some

detail how higher-order autoregressive-moving average (ARMA) processes may arise when aggregating simpler AR processes. For example, when two independent AR(1) processes are combined, the theoretical model of the aggregate is ARMA(2,1). Additionally, if two AR(1) processes are unequal in length, then the combined series will behave as an ARMA (2,1) process for the common interval, and as an AR(1) where no overlap occurs. This is clearly undesirable because any climatic reconstructions developed from such series would also be stochastically non-homogeneous.

Granger and Morris (1976) also show that the aggregate of k AR(1) processes will theoretically yield an ARMA(k,k-1) process. That such very high-order processes do not seem to arise by aggregating many tree-ring series into a mean-value function is probably due to "coincidental situations" (Granger and Morris, 1976) whereby several series with similar AR operators tend to cancel out each other. However, coincidental situations cannot be assumed to always ameliorate the effects of aggregating tree-ring series. Because an ensemble of tree-ring indices is almost guaranteed to have unequal length series in it, combining these series into a mean-value function may still produce a stochastically non-homogeneous composite, especially where sample depth is small or declines quickly. By averaging random shocks rather than indices, this potential problem should be minimized.

Robust Estimation of the Mean-Value Function

The standardization technique being developed here relies on the wavelet compression property of predictive deconvolution and the computation of the mean-value function of resulting random shocks to reduce or eliminate the effects of endogenous disturbances. The most critical phase of the technique, and the point at which it is most likely to break down, is in the ability of the mean-value function to "average-out" the endogenous disturbance shocks peculiar to a subset of trees in the ensemble. Under the assumption that the contemporaneous climatic shocks in the ensemble are samples from a normally distributed population, the disturbance shocks should behave as extreme values or outliers in the sample.

Chen and Box (1979b) studied several real data sets and concluded that the occurrence of outliers often results from secular inhomogeneity in the variance of the data. The probability distribution of such series could be described by a contaminated normal distribution. That is, the basic distribution is $N(\mu,\sigma^2)$ for most of the data with occasional intervals where the variance of the data suddenly increased significantly for a short time. Such behavior shows up as "long tails" in the probability distribution function of the data. Long tails can also be produced by secular inhomogeneity of the mean. Potter (1976) investigated this "shifting mean" theory as the possible explanation of the "Hurst phenomenon", an indicator of long memory that is observed in many natural time series such as streamflow.

Because no attempt is made here to insure the timewise stability of either the mean or variance in individual detrended tree-ring series, outliers produced by secular inhomogeneity are almost certain to occur. Such outliers can be viewed as existing in two dimensions: time and space. Timewise outliers exist in individual series as extreme values. These outliers may be real in a climatic sense, real in an exogenous disturbance sense, or real in an endogenous disturbance sense. For individual series viewed independently of all others in the ensemble, the three classes of outliers are likely to be indistinguishable. Only when viewed across space (or cores, if you will) can endogenous disturbance outliers be differentiated from the others. Spacewise, climatic and exogenous disturbance outliers will show up as contemporaneous across cores. Thus, while they remain outliers in a timewise sense, they will not be outliers in a spacewise sense. In contrast, endogenous disturbance outliers will not be contemporaneous across cores except by chance alone. Thus, they will act as outliers in a spacewise sense even if they are not strong outliers in a timewise sense.

As shown by Mosteller and Tukey (1977), the arithmetic mean is especially sensitive to outliers which, when present, render it an inefficient, biased estimator of location. If outliers are suspected, a robust mean should be used which discounts the influence of extreme values automatically. Mosteller and Tukey (1977, p. 205) suggest the biweight robust mean which is solved for iteratively using the arithmetic mean or median as the initial estimate.

The biweight mean is defined by Mosteller and Tukey (1977, p. 205) as

$$y^* = \Sigma\, w_i y_i / \Sigma\, w_i \qquad 3.22$$

where $w_i = [1.0 - ((y_i - y^*)/cS)^2]^2$ when $((y_i - y^*)/cS)^2 < 1.0$.

Otherwise, $w_i = 0$ when $((y_i - y^*)/cS)^2 \geq 1.0$

and S is a robust measure of variance or spread, here defined by the median absolute deviation (MAD)

$$S = \text{median}\ |y_i - y^*| \qquad 3.23$$

and c is an arbitrary constant usually between 6 and 9. Because the MAD has an expectation of 0.6754 σ for normally distributed data (Chen and Box, 1979a), any outliers exceeding 6.08 standard deviations from the uncontaminated, arithmetic mean will be completely discounted when c=9. Thus, c=9 will be used.

The variance of the biweight mean (Mosteller and Turkey, 1977, p. 208) is

$$s^2 = \frac{\Sigma' (y_i - y^*)^2 (1-u^2)^4}{[\Sigma' (1-u^2)(1-5u^2)]\,[-1+\Sigma'(1-u^2)(1-5u^2)]} \qquad 3.24$$

where: $u = (y_i - y^*)/cS$, S is the MAD, y^* is the biweight mean, and Σ' indicates summation only when $u^2 \leq 1$.

The normalized weight function corresponding to the w_i in equation 3.22 and c = 6.08 is shown in Figure 3.4. The weight function

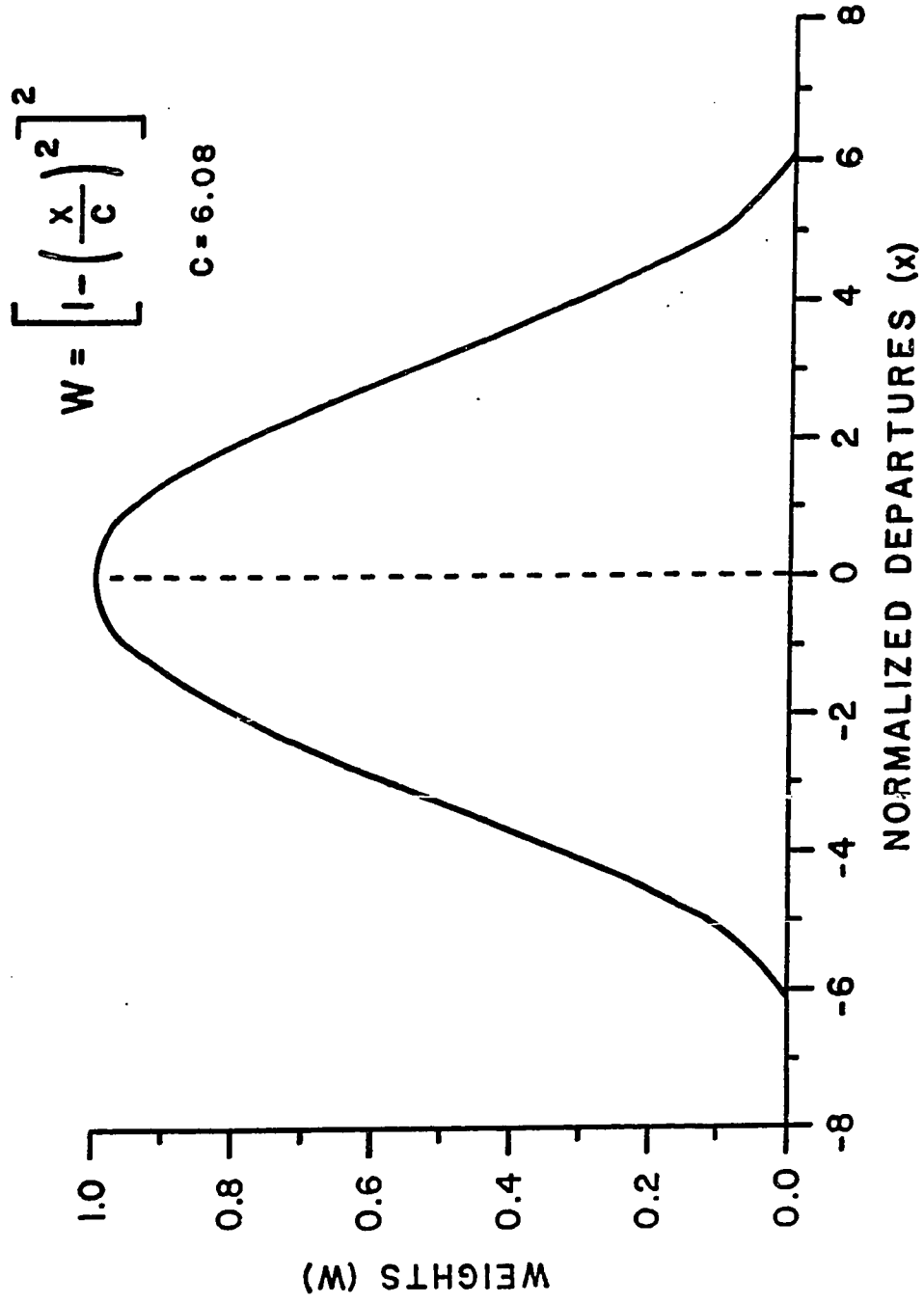

Figure 3.4. The weight function for the biweight robust mean.

behaves like a symmetric digital filter which is applied to time series for the purpose of suppressing unwanted frequencies of variance. Thus, for the normalized departure $x = 0$, $w_i = 1.0$ which maximally weights that observation. For $x = 1$, $s_i = .947$, which is a discount of about 5%; for $x = 2$, $w_i = .795$ which is a discount of about 20%; and so on. Because the weight function is symmetric, the biweight mean will produce nearly unbiased estimates of central location regardless of the presence or absence of outliers in the sample. In this sense, it is an excellent choice for automatically discounting the presence of disturbance shocks in the mean value function of tree-ring random shocks.

The penalty one incurs by using the biweight mean is a loss of estimator efficiency over the arithmetic mean when the data are normally distributed and uncontaminated by outliers. The arithmetic mean has the smallest variance among all measures of central location under the normal assumption and is, therefore, the most efficient estimator possible. This is important for the construction of confidence intervals and statistical hypothesis testing. The biweight mean is not the most efficient estimator of location under the normal assumption because the weighting procedure loses some information contained in the sample. This increases the uncertainty or variance of the estimate and results in wider confidence intervals. The efficiency of the biweight mean relative to the arithmetic mean can be expressed as a ratio of their respective variances (Mosteller and Tukey, 1977, p. 205). That is,

$$EFF = \sigma^2/\sigma_{bi}^2 \qquad 3.25$$

where σ_{bi}^2 and σ^2 are variances of the biweight and arithmetic mean,

respectively. Letting $\sigma^2 = 1.0$, the variance of the biweight mean will usually be less than 1.1. This results in a relative efficiency of more than 90% except for small sample sizes (say, $n < 10$) where it will be somewhat less. For very small sample sizes (say, $n<6$), the biweight mean can be replaced by the simpler median because not enough information exists to warrant the use of more complicated robust measures of location. The loss of efficiency (usually <10%) is a small penalty to pay for protection from the deleterious effects of outliers. When outliers are present in the tree-ring data, experience indicates that the biweight mean will be more efficient than the arithmetic mean by about 25% on the average. The overall effect will usually be a reduction in the total error variance associated with the yearly means of the mean-value function. This results in an increase in the signal-to-noise ratio of the chronology.

The biweight mean performance as a robust estimator can break down if outlier contamination is very high. Performance tests of related maximum likelihood robust estimators of location (Andrews et al., 1972) suggest that the breakdown point will be around the 40% level of contamination. That is, if more than 40% of the cores have similar endogenous disturbance outliers in any given year, the robust mean will not perform any better than the arithmetic mean. When such sample distributions are bimodal or miltimodal due to non-homogeneous growth responses across the stand, no clear region of central tendency exists for the biweight mean to iterate towards. In this case, the resultant biweight mean will converge to a Solomon-like compromise solution that

splits the modes apart. Because the arithmetic mean will not perform well here either, this condition cannot be improved upon without collecting more data or manually discarding suspected bad values.

A Pooling Procedure for Time Series Autoregression

On the assumption that the disturbance shocks have been effectively averaged out of the mean-value function, one more problem must be solved: the recovery of low-frequency climatic variance that may have been lost by removing autoregressive persistence. The non-random behavior in each z_t series, which is a composite of climatic and physiological feedback mechanisms, has been modelled as an AR(p) process. The ϕ_i, which are assumed to be time invariant, represent the memory function of the feedback filter that imparts the non-random behavior to z_t, and the e_t series reveals the time history of events or shocks that drive the system. Since the ϕ_i are related in an unknown and probably very complex way to climate, site and physiology, the safest way to reintroduce the necessary climatic persistence into e_t is to assume that all of it is related to climate in some way. What is needed is a pooled estimate of the ϕ_i which reflects the common persistence structure of the ensemble of tree-ring series. Pooling the ϕ_i should dampen out the random effects of micro-site and tree physiology differences in the stand just as robust averaging of the e_t across cores should reduce the effects of endogenous disturbances.

The solution to this problem is not trivial because the tree-ring series in the ensemble will usually be of different lengths and each series may be significantly cross-correlated with the other series

at lags other than zero. When present, the latter property is most important because it means that the persistence structure in each tree-ring series is not independent of the persistence in the other series. This precludes the naive approach to pooling the ϕ_i based on some form of simple averaging across series. The lagged interdependence between series should be expected in most tree-ring ensembles because of interactions between neighboring trees for light and soil moisture. In closed-canopy forests, canopy and root competition will assure this. In extreme open-canopy forests, these interactions should be minimal.

In order to account for the lagged interdependence beween series, multivariate autoregressive modelling (Jones, 1964) is called for. The concept of lagged interdependence can be appreciated by considering the two-variable case. Let X_t and Y_t be two auto- and cross-correlated time series. The interactions of a multivariate lag-one autoregressive model is expressed schematically as

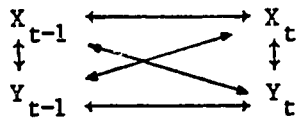

(adapted from Salas et al., 1980, p. 350).

The arrows show the way that the two series can interact. At lag-zero, the interaction of X_t and Y_t is symmetric and is described by the covariance matrix

$$\begin{bmatrix} X_t^2 & X_t Y_t \\ Y_t X_t & Y_t^2 \end{bmatrix}$$

where X_t^2 and Y_t^2 are variances of X_t and Y_t, and X_tY_t are covariances between X_t and Y_t. The lag-one interaction of X_t and Y_t is <u>not</u> symmetric however because X_t lags Y_t and Y_t lags X_t which yields different values unless $X_t = Y_t$. The lag-one matrix is

$$\begin{bmatrix} X_tX_{t-1} & X_tY_{t-1} \\ Y_tX_{t-1} & Y_tY_{t-1} \end{bmatrix}$$

where X_tX_{t-1} and Y_tY_{t-1} are lag-one autocovariances, and X_tY_{t-1} and Y_tX_{t-1} are lag-one cross-covariances. Clearly, if the off-diagonal terms are non-zero, pooling terms along the principal diagonals (the naive approach) will yield incorrect estimates.

An elegant solution to the pooling problem, which takes into account the off-diagonal terms, was recommended by R.H. Jones (pers. comm., 1982). Instead of computing lag-covariance matrices as described above, the lag-product sum matrices are computed. The lag-product sums are equal to n times the lag-covariances where n is the number of terms in each sum. If all of the series are equal in length, the matrices computed either way will yield identical results. However, when the series are unequal in length (which is usually the case for tree-ring series), each lag-product sum will be proportional to n, the number of common observations for each pair of tree-ring series.

The lag product sums $\Gamma^{(k)}$ are m by m matrices computed as

$$\Gamma^{(k)} = \sum_{i=k+1}^{n} X_iX_{i-k} \qquad 3.26$$

where X_i is the matrix of m properly aligned time series with their means removed and k is the order of the lag matrix. Because the m series will usually be of different lengths, n equals the maximum length of the composite time series in the ensemble. For those series that are less than length n, zeroes can be appended to the ends to pad out the matrix. The zeroes ensure that each lag-product sum will only reflect the number of non-zero products in each sum. Beginning with k=0, the $\Gamma^{(k)}$ are computed for an arbitrarily large number of lags because the order of pooled autoregression is unknown. All that matters is that k is greater than the order p likely to be encountered. Lag-product sums computed out to 10 lags (k = 11) have been sufficient for all tree-ring ensembles tested to data. Other results of modelling tree-ring series as ARMA processes (Hipel and McLeod, 1977; Meko, 1981) support this choice of k.

Once the $\Gamma^{(k)}$ are computed, the pooling is accomplished by summing the elements in each matrix into a grand sum $\bar{\Gamma}^{(k)}$

$$\bar{\Gamma}(k) = \sum_{i=1}^{m} \sum_{j=1}^{m} \bar{\Gamma}(k) \qquad 3.27$$

where $\bar{\Gamma}^{(k)}$ is now a vector of length k. The k terms in $\bar{\Gamma}^{(k)}$ provide the pooled lag-product sums needed for solving the Yule-Walker estimates of the autoregressive coefficients. One can also obtain pooled autocorrelations $\bar{R}^{(k)}$ as

$$\bar{R}(k) = \bar{\Gamma}(k)/\bar{\Gamma}(0) \qquad 3.28$$

for all k.

This pooling procedure is analogous to a weighted regression analysis wherein each variable is weighted by the reciprocal of its variance (Steele and Torrey, 1960, p. 180). Because variables with large variances are weighted less than those with smaller variances, the resultant regression coefficients will be more precise. The variance of autocorrelations is approximately equal to 1/n (Box and Jenkins, 1970, p. 35). Using lag-product sums automatically weights each sum by n, the reciprocal of the normalized variance of that sum. This procedure should produce more precise pooled estimates of ensemble lag-structure. Additionally, by including the off-diagonal elements in the $\bar{\Gamma}(k)$, the lag covariance between series is automatically compensated for in the pooled estimate.

The Yule-Walker estimates of autoregressive coefficients are described in detail in Box and Jenkins (1970). The coefficients up to order p require the solution of

$$[a_1 \cdots a_p] = \Gamma_1 \cdots \Gamma_p \begin{bmatrix} \overline{\Gamma_0} & \Gamma_1 & \cdots \Gamma_{p-1} \\ \Gamma_1 & \Gamma_0 & \cdots \Gamma_{p-2} \\ \vdots & \vdots & \vdots \\ \underline{\Gamma_{-(p-1)}} & \Gamma_{-(p-2)} & \cdots \underline{\Gamma_0} \end{bmatrix}^{-1} \qquad 3.29$$

where the a_i are the autoregressive coefficients. Although there is a small sample bias towards zero associated with these estimates, for any reasonable length series (say, n=100), the bias is negligible. The coefficients can be solved stepwise in successively increasing order from p = 1 to p = k-1 using the computationally efficient Levinson-

Durbin recursion (Levinson, 1947; Durbin, 1960). Using the notation of Jones (1982), the recursion begins by estimating the first-order autoregressive coefficient

$$a_1^{(1)} = \Gamma_1/\Gamma_0 \qquad 3.30$$

and the residual sum-of-squares

$$S_1 = \Gamma_0 - a_1^{(1)}\Gamma_1 \qquad 3.31$$

where the Γ_i are lag-product sums as before. If the process is first-order, a_1 equals the first-order autocorrelation coefficient. The general step proceeds from p = 2 to k-1 calculating the pth order partial autocorrelation coefficient

$$a_p^{(p)} = [\Gamma_p - \sum_{j=1}^{p-1} a_j^{(p-1)}\Gamma_{p-j}] \; / \; S_{p-1} \qquad 3.32$$

for j = 1, 2,....,p-1, and

$$a_j^{(p)} = a_j^{(p-1)} - a_p^{(p)}a_{p-j}^{(p-1)}$$

and

$$S_p = (1 - [a_p^{(p)}]^2) \; S_{p-1} \qquad 3.33$$

completing the recursion.

Since the order of autoregression is unknown at the start, a test must be applied to determine the value of p beyond which any higher-order coefficients are not significantly different from zero. In the next section, such a test is described.

Selecting the Order of Autoregression

Several criteria are available for selecting the order of an autoregression (e.g. Akaike, 1974; Schwarz, 1978; Hannan and Quinn, 1979). The Akaike Information Criterion (AIC) (Akaike, 1974) is a widely used criterion for selecting time series models and will be used here. It is defined as

$$AIC = n \ln (RSS) + 2p \qquad 3.34$$

where n is the number of time series observations and RSS is the sum-of-squares of the residuals after fitting an order p autoregression to the series. The right-hand term of equation 3.34 is a penalty function associated with the number of parameters in the model. If the mean is subtracted from the data prior to fitting, p must be increased by one. The correct order autoregression is selected as the one which yields the minimum AIC. This represents the point at which additional coefficients do not reduce RSS enough to offset an increase in the penalty function.

Ideally, the AIC decreases monotonically with increasing order to a single minimum and then increases monotonically thereafter. Unfortunately, this is not always the case, and two or more minima (or dips) in the AIC trace may occur. This happens when the time series being fitted has a large partial autocorrelation coefficient that is preceded by one or more small partial autocorrelation coefficicients. When competing minima occur, the principle of parsimony usually prevails and the simpler model is chosen (Jones, 1982). Another reason for accepting the simpler model is the finding of Shibata (1976) that the AIC is not a consistent statistic. That is, the minimum AIC does not

converge to the true order of autoregression as n increases to infinity. This lack of consistency results in an occasional overestimation of the true order, based on simulation experiments (Hannan and Quinn, 1979). Strongly consistent estimators have been formulated (Schwarz, 1978; Hannan and Quinn, 1979), but at the expense of lower power in identifying the true order of autoregression when the magnitude of the coefficients and/or the number of observations is small. Based on the principle of parsimony and the properties of the AIC noted above, the order of autoregression will be chosen using a first-minimum AIC selection criterion.

It should be pointed out that the first-minimum AIC search will not necessarily yield the best model for explaining the complete stochastic behavior in the tree-ring series. Important long-lag persistence may be missed. For example, an AR(2) model selected by the first-minimum search would miss a large partial autocorrelation coefficient at lag-5 which could have climatic significance. However, the purpose of this modelling is not to develop a high-resolution spectrum, which can be obtained by allowing the AR order to increase. At this stage, it is only necessary to characterize the short-lag persistence structure which describes the minimum delay properties of the tree's physiological system. Because the tree growth response to climate and disturbance will be approximately minimum delay, most of the information needed to deconvolve the series will be contained in the short lags. Long-lag persistence, which is more likely to arise from long-term climatic fluctuations, will not be affected by the deconvolution and will be preserved

in the random shocks. In this context, "random" must be qualified to mean only the short-lag behavior of the shock series.

The first-minimum AIC criterion can be applied for fitting autoregressions to the individual series and the pooled data. This would seem to be the optimum approach because each series can "speak for itself" in selecting the best model for deconvolution. Operationally, some problems can arise from this approach however. The order selected by the AIC can vary considerably between series due to random fluctuations of each partial autocorrelation function and the length of each series being tested. The power of the AIC is proportional to the length of the series being fitted. This being the case, shorter series will tend to be underfitted relative to longer series in the ensemble.

The pooled AR order selected by the AIC represents an estimate of common persistence structure due to species and site specific characteristics. Because all data are used in estimating the pooled AR order, this estimate should be more robust than that derived from any one series. To ensure that each tree-ring series is deconvolved in a way that is consistent with the others, the AR order fit to each series will be constrained to equal that of the pooled order. This approach ensures that the pooled autoregression added to the mean-value function of random shocks at the last stage of chronology development will always be of the same order removed from each series.

The Composite Site Chronology

The last step in developing the site tree-ring chronology is the addition of the pooled autoregression to the robust mean-value function

of random shocks. This final chronology has the form

$$z_t = e_t + \sum_{i=1}^{p} \phi_i z_{t-i} + \delta \qquad 3.35$$

where z_t is the composite growth index for year t, e_t is the robust mean random shock, ϕ_i is the autoregressive coefficient of the pooled AR(p) process, and δ is a constant related to the AR process and its mean level. The δ is needed because all tree-ring index series have a mean of 1.0, but the e_t have a mean of zero. This constant is related to the ϕ_i as

$$\delta = 1.0 - \sum_{i=1}^{p} \phi_i \qquad 3.36$$

for the case where E[z] = 1.0.

In examining equation 3.35, an obvious problem is the lack of z_{t-i} values to start the recursion. A number (=p) of starting values are needed to produce the first p tree-ring indices after which the recursion proceeds on its own. If no information is available for selecting the starting values, the unconditional expected value of the process can be used. If the unconditional mean is used, the first few values of z_t will be biased towards 1.0. The transient effect of the starting values is proportional to the wavelet of the AR(p) process being generated and the order p. The wavelets in Figure 3.3 indicate that this effect will usually disappear after 20-30 years in most series.

Another way of generating starting values is to use the tree-ring indices of the longest series that were lost when that series was fit as an AR process. For example, if the longest series begins in 1600 and is modelled as an AR(5) process, then the indices lost through fitting (1600-1604) can be used as starting values for the e_t which begin in 1605. If several series begin in the interval 1600-1604, then a mean-value function of starting values is possible. Using actual tree-ring indices for starting values seems preferable to the unconditional mean because these indices provide some information about what actually occurred even though that information may not be very accurate due to small sample size. The key assumption is that these start-up indices are not seriously biased.

Operationally, the issue of starting value transience will not be a problem in many cases. Tree-ring chronologies are frequently several decades longer than the useful length for dendroclimatic studies due to sample size decline. If these early decades are not used in subsequent analyses, then the choice of starting values will not measurably affect the results.

Conclusion

The biological and statistical models developed in Chapter 2 and here provide a theoretical framework for a new tree-ring standardization method. Because this method is based on the autoregressive time series model, it will be given the acronyn ARSTND (for AutoRegressive STaNDardization). The ARSTND method is performed in the following series of

steps after the tree-ring data for a site have been well-dated and measured.

1. Detrend and index each individual ring-width series with a curve that is "stiff" relative to the shorter-term fluctuations seen in the series. Consider the "trend-in-mean" concept as a useful criterion for determining the minimal stiffness that is acceptable.

2. Estimate the pooled autoregression model of the ensemble of tree-ring index series. Use the first-minimum AIC to select the order of the model. Save the AR coefficients of this model for later addition to the residual mean-value function.

3. Model each tree-ring index series as a constrained order AR process equal to that of the pooled AR model, but compute the coefficients from the individual series. These coefficients may differ considerably from those of the pooled process.

4. Prewhiten or deconvolve the individual series using the AR coefficients estimated from the constrained fitting procedure and save the resultant ensemble of white-noise residuals or random shocks.

5. Compute the mean-value function of residuals using the biweight robust mean or the median if the sample size is small (say, less than six). By this procedure, any anomalous disturbance effects will be automatically discounted in the mean-value function.

6. Using the coefficients of pooled autoregression, add lost persistence back into the residual mean-value function to create the final ARSTND chronology.

CHAPTER 4

A DATA ADAPTIVE METHOD FOR DETRENDING RINGWIDTHS PRIOR TO AUTOREGRESSIVE MODELLING

Introduction

The detrending curves used to standardize individual series prior to autoregressive modelling are designed to remove the non-stationary variance due to age-related trends and fluctuations. In theory, this should be a simple procedure since any least squares simple regression curve will remove the linear trend in the data. Unfortunately, tree-ring data from forest interior sites rarely have purely linear age trends. The true trends may be somewhat exponential or parabolic in shape. More commonly, the trends look like compound or piecewise functions of all three kinds of curves. Such complex trends are very difficult to estimate with mathematical models as pointed out in chapter 1. As a result, the data may be fitted very well in some intervals and very poorly in others.

Recently, H.C. Fritts and R.L. Holmes (pers. comm.) reported that the variance spectrum of an ARSTND chronology is sensitive to the initial detrending procedure. They found this sensitivity to be most apparent in the lowest frequencies of the spectrum where the variance is affected most strongly by detrending. Specifically, they found inflated variance in this spectral region when the detrending curves were poor approximations of the underlying age trends. This inflation probably occurred as a result of residual non-stationary age trends in the indi-

vidual detrended series. They were not adequately minimized in the mean-value function due, most probably, to coincidental agreement of residual age trends among series. This problem should be most acute in the poorly replicated sections of a chronology where the powers of robust mean estimation and the Law of Large Numbers are weakest. Because the method of detrending will, to some degree, dictate the final low-frequency properties of the ARSTND chronology, it is necessary that a method be found which will satisfactorily remove complex age trends and yet preserve as much low-frequency climatic variance is possible. Such a method, based on smoothing splines, will now be described.

A Data Adaptive Method of Detrending Based on Smoothing Splines

Due to the inhomogeneous character of many age trends seen in forest-interior tree-ring series, a data adaptive, stochastic method of detrending based on smoothing splines will be investigated. The formulation of this detrending method is based on the "trend in mean" concept of Granger (1966). "Trend in mean" refers to all variance in a time series with wavelengths longer than the length of the series. The lowest frequency harmonic that may be resolved from the trend in a series is equal to 1/N where N is the series length. This corresponds to a cycle with a period equal to the series length and is the fundamental frequency of the series (Jenkins and Watts, 1968, p. 19). Variations at frequencies lower than 1/N may appear as a trend because the cycle is incomplete. This provides a well defined resolution limit on the recovery of low-frequency climatic variance given the almost ubiquitous presence of age-related trends in the ringwidth data. Thus, based on the

"trend in mean" concept, detrending should not remove variance resolvable from the trend.

The 1/N limit provides an objective guideline for using the cubic smoothing spline (Cook and Peters, 1981) to detrend and index a ringwidth series prior to autoregressive modelling. The spline should remove virtually all variance at frequencies lower than 1/N and, at the same time, leave higher frequency variance unaffected. Due to the shape of the spline frequency response function (Cook and Peters, 1981), this cannot be done exactly as phrased. In fact, some higher-frequency variance will always be lost. Using equations 2 and 3 in Cook and Peters (1981) and a hypothetical series 100 years long, a smoothing spline with a 50% frequency response at frequency 1/100 (the 1/N criterion) will reduce the amplitude of a harmonic at frequency 1/75 by about 24%. The equivalent variance reductions, obtained by squaring the amplitude responses, are 25% and 5.8% for frequencies 1/100 and 1/75, respectively. Thus, 5.8% of the variance is lost at a period of 75 years which violates the "trend in mean" concept to a small degree. Unfortunately, the reduction of variance at a period of 100 years is only 25% which may be insufficient. This has probably caused the inflated low-frequency variance noted by Fritts and Holmes in experimenting with splines using a 1/N 50% frequency response criterion. Given the shape of the spline frequency response functions, an acceptable 50% cut-off criterion probably lies somewhere between 1/N and 2/N. Splines in this range should remove most of the variance associated with age-rela-

ted trends and, yet, preserve most of the shorter term variance that may be related to climate.

Using an ensemble of disturbed eastern hemlock ringwidth series from eastern New York, four chronologies will be developed using four percentages of N in the range 1/N - 2/N: 100%N, 75%N, 67%N and 50%N. In addition, a chronology will be created using a combination of linear regression and negative exponential detrending curves, and a double-detrending (D-D) method conceived by R.L. Holmes (pers. comm.). The D-D method first fits a negative exponential curve or linear regression line to a series to remove any trend attributable to either of these models. The tree-ring indices resulting from the initial detrending are then filtered with a smoothing spline to remove residual stochastic trends. The spline 50% frequency cutoff is 100%N if the series is detrended initially with a negative exponential curve. Otherwise, a 67%N cutoff is used. The D-D method is based on the premise that the overall age trend can be decomposed into a deterministic trend and a residual stochastic trend not fit by the deterministic model. Fritts and Holmes (pers. comm.) report that the D-D method reduced the inflated low-frequency variance they observed in earlier detrending experiments.

The effect of the detrending method will be evaluated by comparing the spectra of the resultant ARSTND chronologies and the theoretical spectra of the AR processes obtained from the ARSTND procedure. Each theoretical spectrum will be, in effect, the null continuum of the underlying process because of the low-order selection tendency of the first-minimum AIC criterion described in chapter 3. The actual spectrum

will vary about the continuum depending on the frequency distribution of variance. However, if the AR model is correct and the detrending procedure is reasonable, than the general shape of the actual spectrum should be similar to that of the null spectrum. The AR coefficients used to compute the null spectra will be estimated from the actual ARSTND chronologies instead of the pooled AR coefficients. This is necessary because the coefficients of the chronologies will always differ slightly from their respective pooled values due to random effects in the residual mean-value function.

The results of these detrending experiments are given in table 4.1. In every case, a pooled AR(1) model was selected. The pooled coefficients are very similar, ranging from 0.451 for the 100%N case to 0.412 for the 50%N case. The average variance explained by autoregression in the individual series ($\bar{R}^2$) shows the effects of differing detrending much more strongly. The $\bar{R}^2$ ranges from 41.4% for the exponential-straight line (E-S) case to 26.9% for the 50%N case. Given the strong similarities of the AR coefficients, the $\bar{R}^2$ statistics are reflecting the removal of long-period non-synchronous age trends from the data as the detrending curves become more flexible. If this were not the case (i.e. the age trends were synchronous), the AR coefficients would show progressive deflation from the E-S to 50%N splines as more common low-frequency variance was removed from the data. This non-synchronicity property is also supported by the signal-to-noise ratio (SNR) comparisons in table 4.1. The SNR's were computed from the average correlations between series following Wigley, Briffa, and Jones,

Table 4.1 Autoregressive modelling and signal-to-noise ratio results for an eastern hemlock ensemble using different detrending options.

E-S = exponential and straight line detrending; D-D = double detrending; %N = spline detrending using a 50% frequency response cutoff equal to a percentage of each series length; integer values (i.e. 200, 100, ...) are fixed 50% frequency response cutoffs applied to all series; $\bar{R}^2$= average variance explained by the AR(p) model; $\bar{r}$ = average correlation between series (1841-1973 period); SNR = signal-to-noise ratio computed from $\bar{r}$.

	DETRENDING OPTIONS					
	E-S	D-D	100%N	75%N	67%N	50%N
AR(p)	1	1	1	1	1	1
ϕ_1	.445	.443	.451	.443	.436	.412
$\bar{R}^2$	41.1	34.6	37.9	32.7	31.1	26.9
$\bar{r}$	.293	.347	.336	.367	.376	.399
SNR	6.21	7.98	7.60	8.71	9.04	9.97

	DETRENDING OPTIONS				
	200	150	100	50	25
AR(p)	1	1	1	1	1
ϕ_1	.448	.436	.398	.313	.215
$\bar{R}^2$	34.5	30.7	24.6	14.3	5.3
$\bar{r}$	.353	.377	.413	.449	.434
SNR	8.18	9.09	10.56	12.20	11.50

(1984). The SNR increases by about 60% as the flexibility of the curves increase. This would not be the case if the splines were only removing synchronous or common fluctuations from all the series. The SNR results seem to support the 50%N spline as the best detrending choice. As will be shown by spectral analyses and additional spline experiments, this simplistic choice based on maximum SNR is not advisable.

The variance spectra of the ARSTND chronologies based on the detrending methods just described are shown in fig. 4.1. Each spectrum was computed from 28 lags of the autocorrelation function which is about 12% of the series length. Only the estimates for periods of 8 years or longer are shown because all of the spectra are virtually identical at shorter wavelengths. Superimposed on each spectrum is the theoretical null continuum and its 95% confidence limit (Mitchell et al., 1966). The E-S, D-D, 75%N and 67%N spectra are all extremely similar to each other. The E-S spectrum shows slightly more variance at infinite period which may be reflecting the inflated variance phenomenon noted by Fritts and Holmes. However, each of these spectra follows the shape of the null continuum very well. There is no indication of variance loss or distortion in the low-frequency band as a result of D-D, 75%N or 67%N detrending. This indicates that the "trend in mean" concept is being conserved even though the splines are removing some higher frequency variance. This behavior is probably due to relatively little variance removal near the fundamental frequency coupled with a general lack of coherence between series around that frequency band.

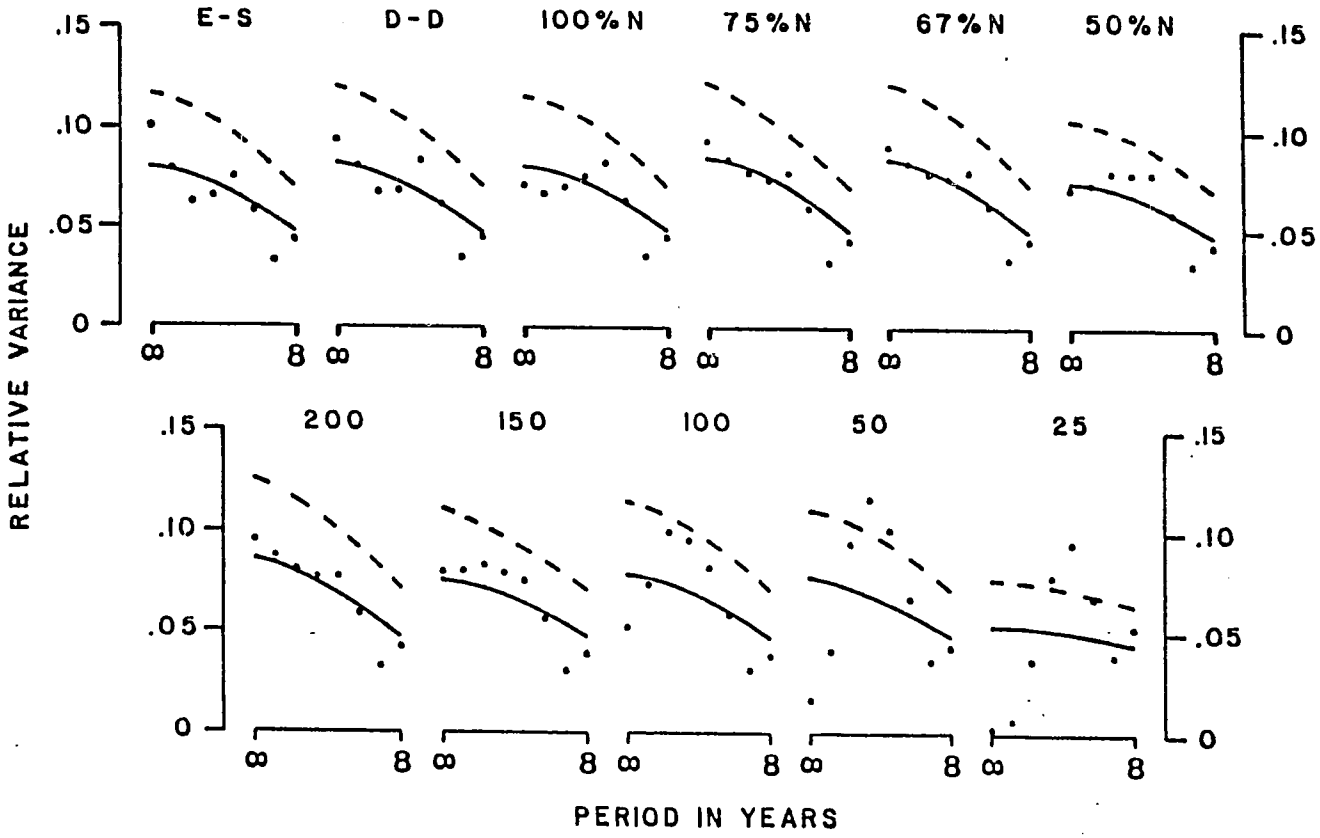

Figure 4.1. Variance spectra of an eastern hemlock chronology based on different detrending options. The dots are actual spectral estimates. The null continuum (solid line) and its 95% confidence level (dash line) are shown. E-S = exponential-straight line detrending; D-D = double detrending; _%N = spline detrending using a 50% frequency response cutoff equal to a percentage of each series length; 200, 100, ... are fixed 50% frequency response cutoffs applied to all series. Periods shorter than 8 years are not shown.

The 100%N and 50%N spectra show some peculiar differences from the others. The former has less low-frequency variance than the tighter splined series which seems contradictory. It is likely that this was caused by poor curve fits that left in strongly out-of-phase residual age trends. These trends could dominate and cancel out common long-period fluctuations and, thus, reduce the low-frequency power. Similarly, the 50%N spectrum shows a loss of low-frequency variance and some increase in the middle frequencies. In this case, the distortion in the spectrum is probably being caused by the excessive removal of low-frequency variance as described by Jones (1984) and in chapter 3. Based on these analyses, the D-D, 67%N and 75%N spline detrending methods appear to be superior.

As mentioned earlier, selecting a detrending method based on maximum SNR is not advisable. This judgment was supported by the spectral analyses just discussed. To examine the correctness of this judgment further, the hemlock ensemble was detrended with splines of increasing flexibility to examine the SNR properties and spectra of the resultant ARSTND chronologies. In this experiment, the splines were chosen to remove 50% of the amplitude in every series at periods of 200, 150, 100, 50, and 25 years. The tighter curve fits clearly violate the "trend in mean" concept because many of the hemlock series are over 200 years long. Examining the effects of these tighter curve fits is instructive because they have been advocated and used in the literature. Cook and Peters (1981) and Blasing et al. (1983) have used splines in the 50% frequency response cutoff range of 30 to 100 years. And,

Briffa, Jones and Wigley (1983) used a Gaussian low-pass filter with a 50% variance (or about 70% amplitude) cutoff at 30 years to standardize British Isles oak chronologies for climate studies.

Table 4.1 shows the results of these detrending choices. As before, a pooled AR(1) model was selected in every case. This time, however, the AR coefficients show progressive decay from 0.448 to 0.215 as the spline flexibility increases. At the same time, the SNR shows an increase of about 49%. Given the fact that each case is still modelled as an AR(1) process, this null continuum model will again be used in examining the spectra.

The spectra are plotted as before in fig. 4.1. The 200-year spline spectra is extremely similar to the 67%N and 75%N spectra. This is due to the prevelence of 200-300 year long series which make the 200-year spline detrending nearly equivalent to 67%N-75%N detrending. The 150-year spline spectrum shows the same characteristics as the 50%N spectrum. After that, the spectra show a very rapid decay of low-frequency variance in violation of the underlying AR null continuum. The result is the development of statistically significant peaks in the 50-year and 25-year spectra which are artifacts of the spline detrending. This illusion is caused by the way in which the higher frequencies contribute more relative variance to the spectrum after low-frequency variance is removed. This is precisely the phenomenon described by Jones (1984) when an autoregressive process is filtered by a high-pass moving average filter. Clearly, a spline detrending approach predicated

on a maximum SNR criterion would lead to an extremely distorted variance spectrum and the possible creation of spurious low-frequency peaks.

There seems to be little difference between the D-D, 75% and 67%N detrending methods based on their respective spectra. To test this conclusion, the D-D, 75%N and 67%N detrending methods were applied to a different ensemble of 26 Jeffrey pine (Pinus jeffreyi) cores from the San Pedro Martir Mountains in Mexico. The chronology from this data set is the one in which Fritts and Holmes found excessive low-frequency variance due to inadequate detrending. In addition, a baseline chronology was created using the E-S detrending method. A chronology based on 100%N detrending could not be developed because the spline growth curve went negative. The theoretical null continua of the E-S, D-D and 67%N chronologies are based on the AR(3) model estimated from each series using the first-minimum AIC criterion. The continuum of the 75%N chronology is based on an AR(2) model estimated in identical fashion. These spectra with their 95% confidence limits are shown in Figure 4.2.

The E-S, 75%N and 67%N spectra all show inflated low-frequency variance that exceeds the 95% confidence limit. The inflation in the E-S case is caused by poor curve fits in 14 of the 26 cores which had been identified *a priori* by R.L. Holmes as needing polynomial or spline detrending. In contrast, the variance inflation in the 67%N and 75%N cases is caused by poor fitting in the steeply exponential juvenile growth periods of the 12 cores requiring the negative exponential curve option (R.L. Holmes, pers. comm.). The D-D method, which is a hybrid of the E-S and %N methods, has produced a chronology without the inflated

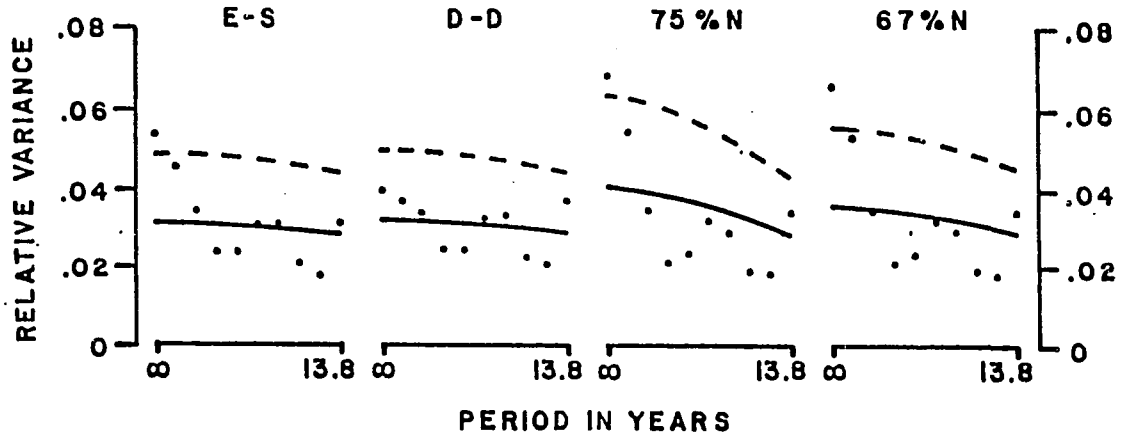

Figure 4.2. Variance spectra of the San Petro Martir Jeffrey pine chronology based on different detrending options.

The dots are actual spectral estimates. The null continuum (solid line) and its 95% confidence level (dash line) are shown. The null continuum models are AR(2) and AR(3) processes. E-S = exponential-straight line detrending; D-D = double detrending; _%N = spline detrending using a 50% frequency cutoff equal to a percentage of each series length. Periods shorter than 13.8 years are not shown.

low-frequency variance seen in the other spectra. At the same time, it has conserved low-frequency variance in accordance with the theoretical null spectrum. The hybrid nature of double detrending makes it a general and robust detrending method for the ARSTND methodology.

Discussion

Age-trend removal using the double detrending method is a good compromise between the desire to preserve as much low-frequency variance as possible and the need to minimize the effects of age-related, non-climatic variance. The initial use of negative exponential and linear regression curves removes the deterministic portion of the age trends. The residual stochastic age trends are removed with splines that conserve the "trend in mean" concept.

The %N criterion used in the spline fitting makes the double detrending method easily applicable to tree-ring series of general length. This is a highly desirable quality. A drawback of the %N criterion is the way in which shorter series will have less resolvable long-period variance compared to longer series. This problem is implicit when detrending any ensemble containing variable length series. On this basis, it is desirable that the minimum length in a tree-ring ensemble be a large fraction of the maximum or useful length of the final chronology. In this way, very little long-term variance in common to all series will be lost within the resolution limits of spectral analysis. As a result, the spectrum may be more easily fit by a theoretical null continuum which will fascilitate the construction of fiducial limits for hypothesis testing purposes. More importantly, any climatic

inferences or reconstructions made from these chronologies will not be seriously biased because of the detrending method.

CHAPTER 5

THE THEORETICAL SIGNAL AND NOISE PROPERTIES OF THE ARSTND METHODOLOGY

Introduction

The double detrending method described in chapter 4 will remove most of the non-stationary variance due to deterministic and stochastic age-trends without seriously distorting the low-frequency variance characteristics of the ARSTND chronology. The remaining signal and noise variance with periods shorter than the series length will now be modelled based on the probable characteristics of the signal and noise, and on the likely way in which the two variances are associated. In so doing, the theoretical signal-to-noise ratio and minimum error variance properties of the ARSTND methodology will be derived.

The General Configuration of the Signal and Noise Variances in Detrended Tree-Ring Series

There are basically two signal and noise configuration that can be postulated for the detrended tree-ring series. One is the classic signal plus noise model

$$Z_t = S_t + N_t \qquad 5.1$$

where S_t is the signal or variance in common among all series, and N_t is the noise or variance that is unique to each series. Although S_t and N_t are often assumed to be serially uncorrelated, the autocorrelated nature of tree-ring indices allows for both S_t and N_t to be autocorrelated as

$$Z_t = \sum_{i=1}^{p} \hat{\phi}_i \, s_{t-i} + S_t + \sum_{j=1}^{q} \tilde{\phi}_j \, N_{t-j} + n_t \qquad 5.2$$

where S_t is now an AR(p) process and N_t is an AR(q) process. Although the S_t and N_t models could be easily generalized to include mixed autoregressive-moving average processes, only the AR description will be examined because this is the time series model on which the ARSTND methodology is based.

The signal and noise configurations of eqs. 5.1 and 5.2 assume that the noise evolves from sources that are independent of the signal in the observed process, Z_t. This is equivalent to saying that the noise in tree-rings is added by a process that is either separate from or external to the tree's physiological processes that are responsible for encoding the signal in the ringwidths. It is difficult to defend the proposition that the noise evolves from a separate or compartmentalized set of processes within the physiological system. The observed differences between series are more likely to arise from differential rates of the same processes that create the common persistence in the signal. However, there is a source of noise that is added after, or is external to, the formation of the ringwidths. This is the variance arising from the accuracy and precision of the ringwidth measurements. This noise will be referred to as <u>external additive noise</u>. Its likely contribution to the total noise varince in a tree-ring series will be considered later.

An alternate model for autocorrelated signal and noise variance is one in which the noise evolves in direct association with the signal, namely

$$Z_t = \sum_{i=1}^{p} \hat{\phi}_i Z_{t-i} + (s_t + n_t) \qquad 5.3$$

In this model, both the serially random signal, s_t, and noise, n_t, become autocorrelated via a common AR operator, $\hat{\phi}_i$, which, in this case, represents the tree's physiological system that produces the ringwidths. The important difference between this model and eq. 5.2 is the way in which the noise is an integral or internal part of the autoregressive representation of the tree-ring series. For this reason, eq. 5.3 will be referred to as the internal additive noise model. Note that the internal and external noise models differ only when autoregression is present. Otherwise, each model reduces to eq. 5.1 where S_t and N_t are serially uncorrelated. Eq. 5.3 can be generalized further by letting the noise be separately autocorrelated as in eq. 5.2, namely

$$Z_t = \sum_{i=1}^{p} \hat{\phi}_i Z_{t-i} + (s_t + \sum_{j=1}^{p} \tilde{\phi}_j N_{t-j} + n_t) \qquad 5.4$$

This model still maintains the internal character of the noise, but now allows it to contribute additional autocorrelation to the observed series, Z_t.

Eq. 5.4 has particular relevance to the ARSTND methodology. It states that a tree-ring series can be decomposed into a signal, s_t, and persistence, $\hat{\phi}_i Z_{t-i}$, which are common to all series in the ensemble. In

addition, each series can be decomposed into a noise component, n_t, and persistence, $\tilde{\phi}_j N_{t-j}$ which are only associated with that series. The $\hat{\phi}_i$ can be thought of as representing the persistence due to macro-environmental influences and genetically predisposed physiological processes of the tree species. In contrast, the $\tilde{\phi}_j$ arise from the persistent departures from expected growth due to local environmental influences such as endogenous disturbances.

A hybrid noise model incorporating both internal and external additive noise is clearly possible. However, before considering this added complexity, the relative contributions of internal and external noise to the total noise variance will be estimated. As will be shown, the external noise estimate is small enough to ignore for all practical purposes.

The Estimated Contributions of External and Internal Additive Noise

In tree-ring research, external additive noise comes from two sources: the precision of the machine used to measure the ringwidths and the accuracy of the person who makes the measurements. The precision of most currently available measuring machines is ± 0.01 mm. The measurement accuracy is more difficult to estimate because it is based on the experience and care of the measurement technician, and on the degree of circuit uniformity and ring boundary definition of the tree-rings. Fritts (1976, p. 250) considered the issue of measurement accuracy by having several experts measure identical 20-year sequences from arid-site conifers and temperate-forest white oaks. Frequency histograms of the sum-of-squared departures between the replicates (Fritts,

1976, p. 251) were developed as guides for assessing measurement accuracy. The mode of the histogram for arid-site conifers is approximately 0.02. This corresponds to a most frequent accuracy of ± 0.03 mm which yields an additive noise variance of 0.0011. For the temperate-forest oaks, the mode is about 0.10 which represents an accuracy of ± 0.7 mm and an additive noise variance of 0.0053. Measuring machine precision is embedded in these estimates.

The percent contribution of this noise variance depends on the variance of the tree-ring series being measured. Results of Fritts and Shatz (1975) indicate that many arid-site chronologies will have variances of about 0.14. Using this value, the external additive noise variance is only 0.8% of the total variance. Mesic-site tree-ring chronologies are likely to have variances of about 0.06 based on results of DeWitt and Ames (1978). Using this value, the external additive noise represents about 8.8% of the total variance. These estimates are undoubtedly high, however, because the variances of individual detrended series will be higher than that of the mean-value function. For this reason, external additive noise in individual mesic-site tree-ring series will probably be less than 5% of the total variance.

The contribution of external additive noise to the total noise variance in an ensemble can be estimated from the SNR study of DeWitt and Ames (1978). Using an average fractional common variance estimate of 29%, the average total noise variance for mesic-site tree-ring chronologies is 71%. Then using a 5% estimate for external additive noise, this noise component accounts for only 7% of the total error variance.

Thus, internal additive noise with its average contribution of 93% must dominate the SNR of a tree-ring chronology. For simplicity, external noise will be assumed non-existent and eqs. 5.3 and 5.4 will be used exclusively in the SNR derivations presented next.

Theoretical Signal-to-Noise Ratio Properties of Tree-Ring Data

Using the signal and noise configurations of eqs. 5.3 and 5.4, the signal-to-noise ratio (SNR) properties of tree-ring data will be derived now. These derivations will be somewhat different from those of Wigley et al. (1984) because the effect of autocorrelation on the SNR will be considered. Wigley et al. (1984) implicitly assumed that the signal and noise were serially uncorrelated.

Among others, one unbiased estimate of SNR from Wigley et al. (1984) is

$$SNR = N\,\hat{a} \,/\, (1-\hat{a}) \qquad 5.5$$

where $\hat{a}$ is an unbiased estimate of fractional common variance such as the average correlation between trees and N is the number of trees in the ensemble. The formula for SNR on which the derivations for autocorrelted noise will be based is

$$\overline{SNR} = \bar{\sigma}_s^2 / \bar{\sigma}_n^2 \qquad 5.6$$

where $\bar{\sigma}_s^2$ and $\bar{\sigma}_n^2$ are the variances of the serially random signal and noise, respectively. $\overline{SNR}$ expressed in eq. 5.6 is a biased estimator of the sample signal-to-noise ratio because it does not take into account the contribution of noise variance to the estimate of the signal vari-

ance. The bias is not important here, however, because this analysis is a purely relative comparison of SNR's in the presence and absence of autocorrelated noise. The results presented here can be applied to the unbiased estimates of SNR derived by Wigley et al. (1984).

The basic time series model for autocorrelated signal and noise will be the autoregressive process. In order to derive the various SNR's, the variances with and without autocorrelation are necessary. For the serially random case, the unbiased estimate of population variance for series e_t is

$$\sigma_e^2 = \sum_{i=1}^{n} (e_t - \bar{e})^2 \; / \; (n - 1) \qquad 5.7$$

which is standard to any elementary statistics books. For the case where the series in question is autoregressive, the variance estimate of an AR(p) process is

$$\sigma_z^2 = \frac{\sigma_e^2}{1 - \phi_1\rho_1 - \phi_2\rho_2 - \ldots - \phi_p\rho_p} \qquad 5.8$$

(Box and Jenkins, 1970, p. 56) where σ_e^2 is the variance of the serially random shocks or residuals from eq. 5.7 and the ϕ_i and ρ_i are autoregressive and autocorrelation coefficients of the order p process. For the simple AR(1) process, eq. 5.8 reduces to

$$\sigma_z^2 = \frac{\sigma_e^2}{1 - \phi_1^2} \qquad 5.9$$

(Box and Jenkins, 1970, p. 58). The stationarity condition of the AR(1) process requires that ϕ_1 must lie between $\pm$ 1.0. Thus, $\phi_1^2 < 1.0$ and, consequently, $\sigma_z^2 > \sigma_e^2$. This variance inflation property of autoregression is a crucial concept in understanding the effect of autocorrelated noise on the SNR.

The following SNR derivations will be based on an AR(1) model when the signal and noise are autocorrelated. As will be clearly evident, the results can be easily extended to the general AR(p) model. The general formulation of the AR(1) model used in the derivations is, from eq. 5.4,

$$Z_t = \hat{\phi}_1 Z_{t-1} + (s_t + \tilde{\phi}_1 N_{t-1} + n_t) \qquad 5.10$$

where Z_t is one observed autocorrelated series of an ensemble, $\hat{\phi}_1$ is the autoregression coefficient common to the ensemble or the system that the ensemble represents, s_t is the serially random common signal, $\tilde{\phi}_1$ is the autoregression unique to the noise, N_t is the autocorrelated noise, and n_t is the serially random noise. The model assumes that s_t and n_t are uncorrelated within each Z_t and that all n_t series are mutually uncorrelated within the ensemble.

The SNR's for two cases will now be derived: 1) the common autocorrelation-random noise case; and 2) the common autocorrelation-autocorrelated noise case.

The Common Autocorrelation-Random Noise Case

The time series model for this case derives from eq. 5.3 and simplifies from eq. 5.10 to

$$Z_t = \hat{\phi}_1 Z_{t-1} + (s_t + n_t) \qquad 5.11$$

by noting that $\tilde{\phi}_1 = 0.0$. Hence, the serially random signal, s_t, is contaminated with serially random noise, n_t. The observed process, z_t, is autocorrelated through $\hat{\phi}_1$, which like s_t, is common to an ensemble of Z_t. Using eq. 5.9 and the additivity property of variances, the variance of Z_t is

$$\sigma_z^2 = \frac{\bar{\sigma}_s^2 + \bar{\sigma}_n^2}{1 - \hat{\phi}_1^2} \qquad 5.12$$

or

$$\bar{\sigma}_z^2 = \frac{\bar{\sigma}_s^2}{1 - \hat{\phi}_1^2} + \frac{\bar{\sigma}_n^2}{1 - \hat{\phi}_1^2} \qquad 5.13$$

The SNR for the case where no autocorrelation exists has been defined previously as

$$\overline{SNR} = \bar{\sigma}_s^2/\bar{\sigma}_n^2$$

We now define the SNR for the common autocorrelation case as

$$\hat{SNR} = \hat{\sigma}_s^2/\hat{\sigma}_n^2 \qquad 5.14$$

where $\hat{\sigma}_s^2$ and $\hat{\sigma}_n^2$ are the signal and noise variances after the addition of common autocorrelation. In this case, from eq. 5.13

$$\hat{\sigma}_n^2 = \frac{\bar{\sigma}_s^2}{1 - \hat{\phi}_1^2} \qquad 5.15$$

and

$$\hat{\sigma}_n^2 = \frac{\bar{\sigma}_n^2}{1 - \hat{\phi}_1^2} \qquad 5.16$$

Substituting the right-hand side of equs. 5.15 and 5.16 into eq. 5.14 yields

$$\hat{SNR} = \frac{\bar{\sigma}_s^2/(1-\hat{\phi}_1^2)}{\bar{\sigma}_n^2/(1-\hat{\phi}_1^2)} \qquad 5.17$$

or

$$\hat{SNR} = \bar{\sigma}_s^2/\bar{\sigma}_n^2 \equiv \overline{SNR} \qquad 5.18$$

from eq. 5.6. Thus, autocorrelation common to both the signal and noise has no effect on the signal-to-noise ratio of an ensemble. In this case, there would be no advantage in using autoregressive modelling to develop a tree-ring chronology when the noise is random within and between trees.

The Common Autocorrelation-Autocorrelated Noise Case

This case is based on the full model described by eq. 5.10. That is,

$$Z_t = \hat{\phi}_1 Z_{t-1} + (s_t + \tilde{\phi}_1 N_{t-1} + n_t)$$

where all terms are defined as before. This model represents the general noise case where there are non-synchronous (i.e. non-climatic) growth fluctuations in the detrended tree-ring indices.

To derive the SNR for autocorrelated noise, first define this SNR as

$$\tilde{SNR} = \hat{\sigma}_s^2 / \hat{\sigma}_n^2 \qquad 5.19$$

where $\hat{\sigma}_s^2$ and $\hat{\sigma}_n^2$ are autocorrelated signal and noise variances, respectively. The $\hat{\sigma}_s^2$ can be expressed (via eq. 5.15) as

$$\hat{\sigma}_s^2 = \frac{\bar{\sigma}_s^2}{1 - \hat{\phi}_1^2} \qquad 5.20$$

The $\hat{\sigma}_n^2$ is a little more complicated to express because of the contributions of both $\hat{\phi}_1$ amd $\tilde{\phi}_1$. First define the variance of the autocorrelated noise, N_t, as

$$\tilde{\phi}_n^2 = \frac{\bar{\sigma}_n^2}{1 - \tilde{\phi}_1^2} \qquad 5.21$$

where $\bar{\sigma}_n^2$ is the serially random noise variance. Now define the total noise variance after the addition of common autoregression to both s_t and N_t as

$$\hat{\sigma}_n^2 = \frac{\tilde{\sigma}_n^2}{1 - \hat{\phi}_n^2} \qquad 5.22$$

or, using eq. 5.21

$$\hat{\sigma}_n^2 = \frac{\bar{\sigma}_n^2 / (1-\tilde{\phi}_1^2)}{1 - \hat{\phi}_1^2} \qquad 5.23$$

This leads to

$$\hat{\sigma}_n^2 = \frac{\bar{\sigma}_n^2}{(1-\hat{\phi}_1^2)\ (1-\tilde{\phi}_1^2)} \qquad 5.24$$

Using results of eq. 5.20 and 5.24, the SNR in eq. 5.19 becomes

$$\tilde{SNR} = \frac{\bar{\sigma}_s^2/(1-\hat{\phi}_1^2)}{\bar{\sigma}_n^2/(1-\hat{\phi}_1^2)(1-\tilde{\phi}_1^2)} \qquad 5.25$$

or

$$\tilde{SNR} = \frac{\bar{\sigma}_s^2(1-\tilde{\phi}_1^2)}{\bar{\sigma}_n^2} \qquad 5.26$$

Because $(1-\tilde{\phi}_1^2)$ is always less than 1.0, the SNR of an ensemble contaminated with autocorrelated noise will always be less than the SNR of an ensemble containing serially random noise. That is, $\tilde{SNR} < \hat{SNR}$.

The effect of autoregressive modeling and prewhitening on the SNR will now be examined for the autocorrelated noise case. We begin by defining the SNR of the serially random mean-value function obtained by prewhitening the individual series as

$$\ddot{SNR} = \ddot{\sigma}_s^2/\ddot{\sigma}_n^2 \qquad 5.27$$

This SNR differs notationally from $\overline{SNR}$ (eq. 5.6) because $\ddot{\sigma}_s^2$ and $\ddot{\sigma}_n^2$ are unlikely to equal $\bar{\sigma}_s^2$ and $\bar{\sigma}_n^2$ even though each SNR is based on serially random data from the same ensemble. The variance in the estimates of autoregression used to prewhiten each series will ensure that $\ddot{SNR} \neq \overline{SNR}$. However, if the AR coefficient estimates are unbiased, then $E[\ddot{SNR}] = \overline{SNR}$. This suggests that reasonable estimates of $\ddot{\sigma}_s^2$ and $\ddot{\sigma}_n^2$ should be available from $\bar{\sigma}_s^2$ and $\bar{\sigma}_n^2$ via eqs. 5.20 and 5.24. Thus,

$$\ddot{\sigma}_s^2 = \hat{\sigma}_s^2 \, (1-\hat{\phi}^2_1) \qquad 5.28$$

and

$$\ddot{\sigma}_n^2 = \hat{\sigma}_n^2 \, (1-\hat{\phi}^2_1) \, (1-\tilde{\phi}_1^2) \qquad 5.29$$

Substituting the right-hand sides of eqs. 5.28 and 5.29 into eq. 5.27 yields

$$\ddot{SNR} = \frac{\sigma_s^2 \, (1-\hat{\phi}_1^2)}{\tilde{\sigma}_n^2 \, (1-\hat{\phi}_1^2) \, (1-\tilde{\phi}_1^2)} \qquad 5.30$$

or, from eqs. 5.20 and 5.21

$$\ddot{SNR} = \frac{\bar{\sigma}_s^2}{\tilde{\sigma}_n^2 \, (1-\tilde{\phi}_1^2)} \qquad 5.31$$

Again, nothing that $(1-\tilde{\phi}^2_1)$ is always less than 1.0, the variance of the

autocorrelated noise will always be less after prewhitening. Thus, $\ddot{SNR} > \tilde{SNR}$.

Eq. 5.31 shows that $\ddot{SNR}$ is an estimate of signal-to-noise in the residual mean-value function which is one-half of the final ARSTND chronology. However, it is clear now that this is also the SNR of the ARSTND chronology obtained after adding pooled autoregression to the residual mean-value function. This follows from the common autocorrelation-random noise SNR derivation which showed that common persistence added to both the signal and noise has no effect on the signal-to-noise ratio. Thus, the error variance reduction property of autoregressive modelling which was hypothesized in chapter 3 has been derived in theory.

Eq. 5.30 suggests the need for estimating both $\hat{\phi}_1$ and $\tilde{\phi}_1$ in order to optimally prewhiten the series. Unfortunately, neither coefficient is known at the start. However, $\hat{\phi}_1$ can be estimated using the pooled autoregression procedure described in chapter 3. Given this estimate of pooled or common ensemble persistence, the prewhitening procedure could occur in two different ways.

The first way, suggested by eq. 5.30, is a two-stage procedure whereby each Z_t series is first prewhitened using the pooled AR coefficient $\hat{\phi}_1$. This would yield (from eq. 5.10)

$$Z_t = s_t + \tilde{\phi}_1 N_{t-1} + n_t \qquad 5.32$$

Then, each Z_t would be modelled and prewhitened again by estimating $\tilde{\phi}_1$ uniquely for each series to yield

$$Z_t = s_t + n_t \qquad 5.33$$

It is also possible to obtain a direct estimate of the endogenous disturbance pulse(s) within each series by noting that the expected value of the serially random signal, s_t, in the presence of serially and spatially random noise, n_t, is the mean-value function, $\hat{s}_t$. Since $E[s_t] = \hat{s}_t$, we can estimate the endogenous disturbance pulses by subtracting $\hat{s}_t$ from each Z_t, after prewhitening with $\tilde{\phi}_1$, which yields an estimate of $\hat{n}_t$ as

$$\hat{n}_t = (s_t + n_t) - \hat{s}_t \qquad 5.34$$

Then, given the estimated noise series, $\hat{n}_t$, the disturbance pulse can be estimated as

$$\widehat{\tilde{\phi}_1 N_{t-1}} = (s_t + \tilde{\phi}_1 N_{t-1} + n_t) - \hat{s}_t - \hat{n}_t \qquad 5.35$$

Eqs. 5.34 and 5.35 provide explicit estimates of the random variance and disturbance shocks in $\hat{n}_t$ and the tree-ring response to the $\hat{n}_t$ in $\widehat{\tilde{\phi}_1 N_{t-1}}$. These estimates would be very useful in stand dynamics studies because the interference of the common environmental signal has been eliminated.

The solution for $\hat{n}_t$ and $\widehat{\tilde{\phi}_1 N_{t-1}}$ also highlights the fundamental difference between the ARSTND methodology and the more traditional flexible curve-fitting procedures. The latter explicitly estimates $\widehat{\tilde{\phi}_1 N_{t-1}}$ in each tree-ring series as a smooth flexible curve without any clearly objective method for differentiating the signal, s_t, from the noise, n_t. In contrast, the ARSTND methodology produces a robust, minimum variance estimate of the common signal among series without the need to explicitly estimate $\widehat{\tilde{\phi}_1 N_{t-1}}$ at all.

The alternate method of prewhitening each Z_t series is to estimate $\hat{\phi}_1$ and $\tilde{\phi}_1$ together as a composite estimate of common and unique persistance in Z_t. This is the procedure advocated in chapter 3 under the constraint that the AR-order fit to each Z_t must equal that of the pooled autoregression model. Since the best estimate of $\hat{\phi}_1$ is the pooled estimate, the constraint implicitly assumes that the noise model has the same order as the signal model. This is a reasonable assumption given the fact that the autocorrelation structure in the signal and noise will be dominated by persistence due to tree physiology in most cases (Matalas, 1962; Meko, 1981). Thus the same system and, hence, the same model should be imparting persistence to the signal and the noise.

The principal advantage of estimating individual series autoregression as a composite of signal and noise persistence is computational efficiency. The AR modelling is only done once for each series instead of twice in the two-stage procedure. Unless stand dynamics information is of interest, this more efficient method is suggested.

Discussion

A plausible model for the configuration of signal and noise in detrended tree-ring series has been constructed. Based upon this model and the variance formula of an autoregressive process, the theoretical SNR properties of the ARSTND methodology have been derived. For the case where the noise variance is serially random, the SNR of a tree-ring chronology cannot be improved by AR modelling and prewhitening of the individual series. However, for the case where the noise is autocorrelated, AR modelling and prewhitening should increase the SNR through the reduction of noise variance that was previously inflated by autoregression. In this sense, the ARSTND methodology is likely to produce a chronology with minimum error variance.

The SNR of the final ARSTND chronology was also shown to be the same as that of the residual mean-value function prior to the addition of pooled autoregression. This SNR and its estimate of fractional common variance can be compared to the same statistics estimated from the detrended indices prior to prewhitening. In addition, actual estimates of error variance in both chronologies can be calculated and compared. These comparisons will provide objective tests of the theoretical SNR property of the ARSTND methodology.

CHAPTER 6

VERIFICATION TESTS AND PERFORMANCE PROPERTIES OF THE ARSTND METHODOLOGY

Introduction

The theoretical signal and noise models for tree-ring series derived in chapter 5 indicate that autoregressive modelling should be useful in reducing error variance when it is autocorrelated. Verification of this proof is crucial before it can be accepted as true and before the ARSTND methodology can become an accepted method of standardizing tree-ring series. In order to do this, an empirical estimate of the level of autocorrelated noise in a tree-ring ensemble will be proposed. This estimate will then be correlated with an empirical estimate of error variance reduction due to autoregressive modelling in an attempt to verify the theory.

In addition, the performance characteristics of the biweight robust mean will be examined in computing the chronology mean-value function. This is the second stage of the ARSTND methodoloby which is intended to reduce the effects of disturbance-related outliers in the mean-value function.

Empirical Estimates of Autocorrelated Noise and the Reduction of Error Variance Due to Autoregressive Modelling

The fractional variance due to pooled or common autoregression can be estiamted from the variance formula of an autoregressive process of order p, viz.

$$\sigma_z^2 = \frac{\sigma_e^2}{1 - \phi_1 p_1 - \phi_2 \rho_2 - \ldots - \phi \rho_p} \qquad 6.1$$

In this case, σ_z^2 is the pooled variance of the observed ensemble, σ_e^2 is the pooled variance of the unobserved white noise of the ensemble, and ϕ_i and ρ_i are the pooled autoregression and autocorrelation coefficients, respectively. From eq. 6.1, it is easy to show that the fractional variance due to pooled autoregression is

$$\hat{R}^2 = \sum_{i=1}^{p} \phi_i \rho_i \qquad 6.2$$

The average fractional variance due to all sources of autoregression ($\bar{R}^2$) in the individual series is simply

$$\bar{R}^2 = \sum_{i=1}^{p} R^2{}_i / N \qquad 6.3$$

where R_i^2 is the fractional variance due to autoregression in series i and N is the number of series in the ensemble. From eqs. 6.2 and 6.3, the proposed measure of autocorrelated noise is, simply, the

difference between $\bar{R}^2$ and $\hat{R}^2$. That is,

$$\Delta R^2 = \bar{R}^2 - \hat{R}^2 \qquad 6.4$$

If the noise is serially random, $\hat{R}^2 = \bar{R}^2$ and, hence, $\Delta R^2 = 0$. If the noise is autocorrelated, $\bar{R}^2 > \hat{R}^2$ and, hence, $\Delta R^2 > 0$.

According to the theoretical signal and noise properties of tree-ring data derived in chapter 5, autoregressive modelling will reduce the error variance in the mean-value function if and only if autocorrelated noise is present, i.e. $\Delta R^2 > 0$. Having formulated an estimate of the level of autocorrelated noise in an ensemble, an estimate of error variance reduction is now needed. This estimate will be based on the change in fractional common variance before and after the autoregressive modelling. Specifically, let this change be defined as

$$\Delta\bar{r} = \bar{r}_r - \bar{r}_s \qquad 6.5$$

where $\bar{r}_s$ and $\bar{r}_r$ are the estimates of fractional common variance before and after autoregressive modelling of the previously detrended and indexed ensemble of radial increment series. The estimate of each $\bar{r}$ is the average correlation between trees following Wigley et al. (1984). If $\bar{r}_r > \bar{r}_s$ after prewhitening, then some reduction in error variance may be attributed to autoregressive modelling since all other

variables have been held constant. This leads to the verification test that ΔR^2 and $\Delta \bar{r}$ must be positively correlated if the theory in chapter 5 is correct.

The Verification Data and Test Results

The verification test was made utilizing estimates of $\bar{r}_s$ and $\bar{r}_r$ from 66 tree-ring ensembles comprising four tree genera: Tsuga, Quercus, Picea and Pinus. The ring-width series of each emsemble were double-detrended and indexed, in the manner described in chapter 4, prior to the autoregressive modelling. The estimates of $\hat{R}^2$, $\bar{R}^2$, and, therefore, ΔR^2 were derived from the total length of each series in the ensemble. This means that variable record-length tree-ring series were used in these estimates. In contrast, $\bar{r}_s$, $\bar{r}_r$ and, hence, $\Delta \bar{r}$ were derived from the period of record in common among all series which is shorter in length than many of the individual series. This means that the time windows utilized in estimating ΔR^2 and $\Delta \bar{r}$ for an ensemble are not identical. To minimize the error variance in the estimates of ΔR^2 and $\Delta \bar{r}$ which may be attributable to the different time windows, the length of the common period used in estimating $\Delta \bar{r}$ averages over 200 years. This is almost always a large fraction of each series' length. Because each genus could represent a different population of ΔR^2 and $\Delta \bar{r}$ values (in both a statistical sampling and biological sense), the data were stratified by genus into four independent groups. This resulted in a sample size of 26 for Tsuga, 14 for

Quercus, 13 for Picea, and 13 for Pinus. The null hypothesis being tested in each case is: There is no positive linear dependence between ΔR^2 and $\Delta\bar{r}$. To test this null hypothesis, linear regression and correlation will be used. Because the theory being tested indicates that autoregressive modelling will cause an increase in fractional common variance when autocorrelated noise is present, the predictor variable will be ΔR^2 and the predictand $\Delta\bar{r}$.

Table 6.1 contains the means, standard deviations and standard errors of ΔR^2 and $\Delta\bar{r}$ for each genus along with the intermediate statistics used to estimate them. The average ΔR^2 is 0.097 for Pinus, 0.125 for Picea, 0.139 for Quercus, and 0.157 for Tsuga. This is the ranking from lowest to highest in terms of absolute levels of autocorrelated noise. Each ΔR^2 value can be interpreted as the fractional variance component due to autoregression within individual series that is unique to those series. In contrast, each $\hat{R}^2$ value can be interpreted as the fractional variance component due to autoregression between series that is common to all series. Thus, the decomposition of $\bar{R}^2$ into ΔR^2 and $\hat{R}^2$ can be interpreted much like the component variances in a one-way analysis of variance. Although ΔR^2 is the principal statistic of interest here as it relates to $\Delta\bar{r}$, its percent contribution to $\bar{R}^2$ (denoted as $\%\Delta\bar{R}^2$) reveals the relative level of out-of-phase persistence between series within each ensemble. $\%\Delta\bar{R}^2$ is analogous to the percent variance components reported by Fritts (1976,

Table 6.1. The mean statistics of autoregressive modelling and its effect on fractional common variance.

A total of 66 tree-ring ensembles have been stratified by genus into four groups. The sample sizes are 26 for Tsuga, 14 for Quercus, 13 for Picea, and 13 for Pinus.

A. Tsuga	$\hat{R}^2$	$\bar{R}^2$	ΔR^2	$\%\Delta\bar{R}^2$	$\bar{r}_s$	$\bar{r}_r$	$\Delta\bar{r}$	$\%\Delta\bar{r}_s$
Mean	.332	.493	.161	32.7	.304	.420	.116	38.1
Stand. Deviation	.108	.081	.065	13.8	.075	.056	.054	27.4
Stand. Error	.021	.016	.013	2.7	.015	.011	.011	5.4
B. Quercus								
Mean	.205	.344	.139	40.4	.276	.336	.059	21.8
Stand. Deviation	.099	.075	.044	17.3	.060	.075	.032	11.1
Stand. Error	.026	.020	.012	3.4	.016	.020	.009	2.9
C. Picea								
Mean	.393	.518	.125	24.1	.279	.356	.076	27.2
Stand. Deviation	.154	.061	.104	22.8	.071	.077	.086	33.6
Stand. Error	.043	.017	.029	6.3	.020	.021	.024	9.3
D. Pinus								
Mean	.311	.407	.096	23.6	.338	.389	.051	15.1
Stand. Deviation	.149	.123	.056	15.7	.101	.086	.049	12.6
Stand. Error	.041	.034	.015	4.4	.028	.024	.014	3.5

$\hat{R}^2$ = fractional variance due to pooled or common autoregression.
$\bar{R}^2$ = total fractional variance due to all sources of autoregression.
$\Delta R^2 = \bar{R}^2 - \hat{R}^2$ = fractional variance due to autocorrelated noise.
$\%\Delta\bar{R}^2 = (\Delta R^2/\bar{R}^2) \cdot 100$ = percentage of total fractional variance due to autoregression that is accounted by autocorrelated noise.
$\bar{r}_s$ = fractional common variance among all series before autoregressive modelling.
$\bar{r}_r$ = fractional common variance among all series after autoregressive modelling.
$\Delta\bar{r} = \bar{r}_r - \bar{r}_s$ = the change in fractional common variance due to autoregressive modelling.
$\%\Delta\bar{r}_s = (\Delta\bar{r}/\bar{r}_s) \cdot 100$ = percentage increase in fractional common variance due to autoregressive modelling.

p. 282) in his analysis of variance results. From table 6.1, the $\%\Delta\bar{R}^2$ values of the four genera are 23.6% for Pinus, 24.1% for Picea, 32.7% for Tsuga, and 40.4% for Quercus. The ranking of Quercus and Tsuga is reversed when autocorrelated noise is viewed in terms of relative contribution to total autoregression. These statistics indicate that individual tree-ring series, even after double-detrending, can have a substantial level of residual non-synchronous tree-ring variance that needs to be minimized.

The average change in fractional common variance after autoregressive modelling ($\Delta\bar{r}$) is 0.051 for Pinus, 0.059 for Quercus, 0.076 for Picea, and 0.116 for Tsuga. These values may also be interpreted as the average increase in fractional common variance due to the noise reduction property of autoregressive modelling. The mean $\Delta\bar{r}$ values appear to be rather modest until they are examined as percentage increases in fractional common variance, $\%\Delta\bar{r}_s$, compared to $\bar{r}_s$. When this is done, the percentabe improvement in fractional common variance is 15.1% for Pinus, 21.8% for Quercus, 27.2% for Picea, and 38.1% for Tsuga. In both the $\Delta\bar{r}$ and $\%\Delta\bar{r}_s$ statistics, Picea and Tsuga appear to show the greatest benefit of autoregressive modelling.

Prior to the correlation and regression tests, an equality of means test was performed for each group of ΔR^2 and $\Delta\bar{r}$ means using a t-test (Sokol and Rolf, 1981, p. 243). The results are shown in table 6.2. Tsuga has a significantly greater average ΔR^2 when compared to

Table 6.2. The equality of means tests of ΔR^2 and $\Delta \bar{r}$ stratified by genus.

A t-test is used which utilizes the pooled variance of all 66 samples in the estimate of the standard error of the difference between each pair of means. As a result, each t-test has 62 degrees of freedom and the critical t-statistic for rejection of the null hypothesis at the 95% confidence level of 2.00. The significantly different pairs of means are denoted by asterisks.

A. Equality of Means Tests For ΔR^2

t-tests

	Tsuga	Quercus	Picea	Pinus
Tsuga	--	0.78	1.35	2.54*
Quercus	--	--	0.52	1.57
Picea	--	--	--	1.03
Pinus	--	--	--	--

B. Equality of Means Tests for $\Delta \bar{r}$

t-tests

	Tsuga	Quercus	Picea	Pinus
Tsuga	--	3.07*	2.07*	2.57*
Quercus	--	--	0.82	0.34
Picea	--	--	--	0.31
Pinus	--	--	--	--

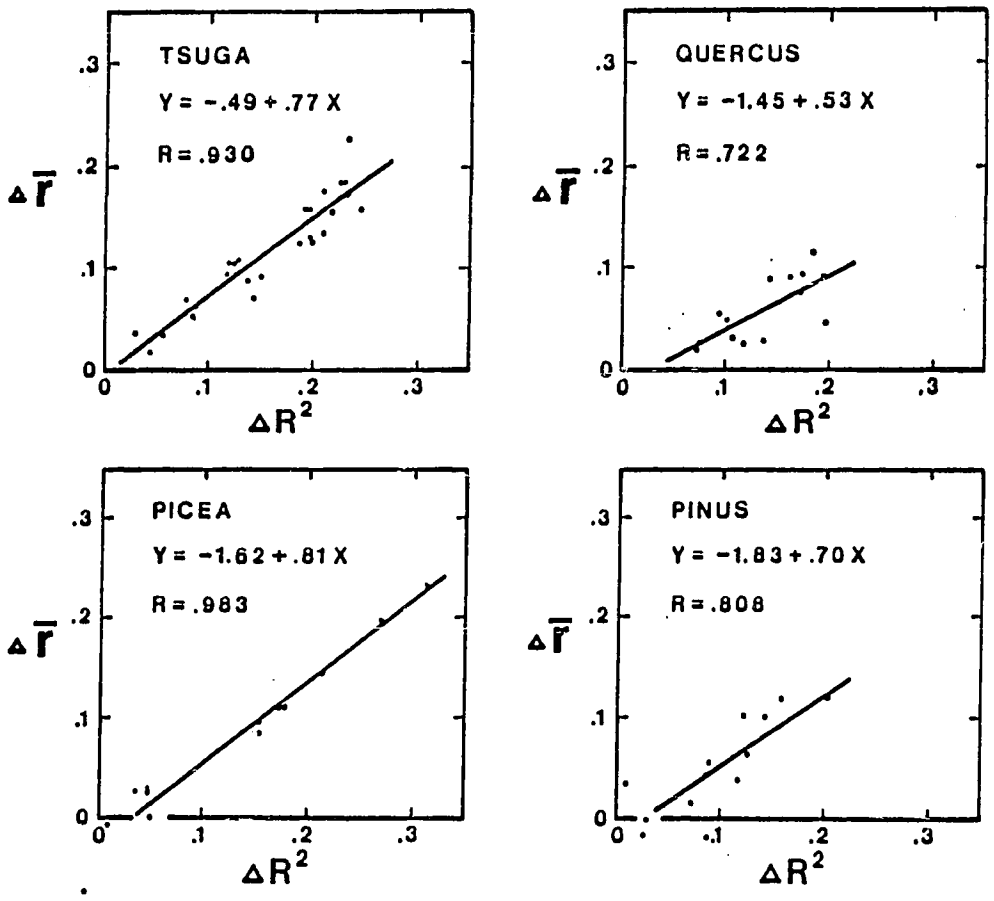

Figure 6.1. The linear regressions and correlations of ΔR^2 versus $\Delta \bar{r}$ for four tree genera.

Each regression is statistically significant at the 99% confidence level.

Pinus and a significantly greater average $\Delta\bar{r}$ compared to all other genera. These results suggest the potential for genus-related differences in the levels of autocorrelated noise and the resultant change in fractional common variance due to autoregressive modelling. However, caution is required in interpreting any apparent genus-level differences in ΔR^2 and $\Delta\bar{r}$ because of the limited sample sizes.

The linear regressions and correlations of ΔR^2 versus $\Delta\bar{r}$ were computed next for each genus. Fig. 6.1 shows the four scatter plots with fitted curves. Each genus shows a statistically significant correlation between ΔR^2 and $\Delta\bar{r}$ that exceeds the 99% confidence level. These results clearly verify the theoretical signal and noise models of chapter 5 and the efficacy of autoregressive modelling in reducing noise variance when it is autocorrelated. Tsuga and Picea show the strongest relationship between ΔR^2 and $\Delta\bar{r}$ and the greatest range in each statistic. The high ($\Delta R^2 > .20$) levels of autocorrelated noise seen in some Tsuga and Picea ensembles are conspicuously rare or absent in Quercus and Pinus. This may reflect higher competition levels in some of the Tsuga and Picea stands. The range of response to competition and disturbance may also be greater in shade-tolerant species compared to those with moderate to low shade tolerance. A test of the equality of the four regression curves was performed (Sokol and Rolf, 1981, p. 499) to see if the slopes were homogeneous. No statistically significant differences were found.

This analysis indicates that the rate of change of $\Delta\bar{r}$ with respect to ΔR^2 appears not to be genus dependent.

One consistent feature that seems to contradict theory is the occurrence of negative y-intercepts in every case. Theoretically, one should expect $\Delta\bar{r}=0$ when $\Delta R^2=0$ because this is the point where the noise is perfectly random. The negative y-intercepts imply that a small, but real, loss in fractional common variance may occur due to autoregressive modelling when the level of autocorrelated noise is very low. However, the 95% confidence intervals for the y-intercepts include the origin for all but Picea. Thus, the problem could be dismissed as a chance phenomenon of statistical sampling. An alternative explanation is that the loss of common variance is due to the removal of the smoothing effect produced by positive autoregression. Chen and Box (1979b) show that smoothing due to positive autoregression has a normalizing effect on the probability distribution of time series. This could artificially enhance the estimate of the common signal by diminishing minor differences between series. This phenomenon is equivalent to the degrees-of-freedom problem noted by Mitchell et al. (1966) in statistical hypothesis testing when data are autocorrelated. The lack of serial independence creates an environment for inflated estimates of association between series. In this sense, the estimate of $\bar{r}$ based on the prewhitened data should be preferred in computing the signal-to-noise ratio instead of $\bar{r}$ esti-

mated from the original autocorrelated series. Thus, it is probable that any decrease in $\bar{r}$ after prewhitening can be attributed to the removal of smoothing due to autoregression.

Discussion

An empirical estimate of the relative level of autocorrelated noise in a tree-ring ensemble was proposed in order to test the theoretical signal and noise properties derived in chapter 5. This statistic, ΔR^2, was correlated with the change in fractional common variance after autoregressive modelling ($\Delta\bar{r}$) for each of 66 tree-ring ensembles stratified into four genera. The results show that the theory is valid. That is, autoregressive modelling will reduce the error variance in a mean-value function when autocorrelated noise is present in the original series. The average increase in fractional common variance appears to be somewhat genus dependent with Tsuga showing a significantly greater gain over Quercus, Picea and Pinus. Better replication for Quercus, Picea, and Pinus will more clearly define the level of genus-related differences.

Empirical Properties of the Biweight Robust Mean

The biweight robust mean is used in the second stage of the ARSTND methodology after autoregressive modelling has reduced the error variance associated with non-synchronous disturbance pulses. It is intended to discount the effects of outliers in computing the mean-

value function of prewhitened indices in an effort to minimize the error associated with non-synchronous disturbances. This form of error reduction differs from the autoregressive modelling procedure in that it minimizes error across space or between trees for any given year rather than through time for any given series.

Three properties of the robust mean will be examined to assess its performance: (1) The percentage of means which are improved by robust estimation. The criterion for improvement is a smaller standard error of the mean using the biweight mean compared to that of the arithmetic mean. As described in chapter 3, this measure of performance is indicative of some level of outlier contamination in the sample. (2) The average change in error variance using robust estimation. The measure of error variance change (Δs^2) is

$$\Delta s^2 = (s_a^2 - s_r^2) \; / \; s_a^2 \qquad 6.6$$

where s_a^2 is the variance of the arithmetic mean and s_r^2 is the variance of the robust mean. When Δs^2 is positive, $s_r^2 < s_a^2$ and a percent reduction in error variance equal to Δs^2 has occurred. Conversely, when Δs^2 is negative, $s_r^2 > s_a^2$ and a percent increase in error variance equal to $|\Delta s^2|$ has occurred. The positive and negative Δs^2 are summed separately over the number of improved and unimproved means, respectively, to produce average estimates of error variance reduction and

increase due to robust estimation. (3) The net change in chronology error variance due to robust estimation. This is simply the average of the positive and negative Δs^2 for the chronology.

These statistics have been obtained in the course of computing the residual mean-value functions for the same set of 66 tree-ring ensembles used in the previous section. As before, the statistics have been stratified by genus to see if any genus-level differences exist in the performance of the robust mean. Table 6.3 shows the means and standard deviations of the percentage of improved mean (%IMP), the percent reduction in error variance (%RED), the percent increase in error variance (%INC), and the net percent reduction in error variance (NET). Also shown are the equality-of-means test results using the same t-test as in the previous section.

The %IMP statistics indicate that 40% to 50% of the means can be improved on the average by using robust estimation when examined across all genera. These are rather large percentages considering that each ensemble has been collected from a geographically limited site with reasonably "homogeneous" physical characteristics. This is indicative of the very high noise level in individual tree-ring series from closed-canopy forests. The equality-of-means tests reveal an interesting stratification of the %IMP. Tsuga and Picea each have significantly greater mean %IMP's compared to Quercus and Pinus. An obvious correlate for explaining this effect is the level of competi-

Table 6.3. The biweight robust mean statistics stratified by genus.

The equality of means among genera is tested for each performance statistic of the robust mean. Each t-test has 62 degrees of freedom, as before. Those t-values exceeding the critical t-value at the 95% confidence (t=2.00) are denoted by asterisks.

Percent Improved Means (%IMP)

	Tsuga	Quercus	Picea	Pinus
Mean	49.99	41.00	49.19	41.86
Stand. Deviation	6.62	7.25	9.96	6.64
Standard Error	1.30	1.94	2.76	1.84

t-tests

Tsuga	--	3.61*	0.31	3.18
Quercus	--	--	2.83*	0.30
Picea	--	--	--	2.49*
Pinus	--	--	--	--

Percent Reduced Error Variance (%RED)

	Tsuga	Quercus	Picea	Pinus
Mean	22.83	22.14	24.03	20.28
Stand. Deviation	3.79	4.09	3.80	2.72
Standard Error	0.74	1.09	1.05	0.76

t-tests

Tsuga	--	0.55	0.99	2.04*
Quercus	--	--	1.34	1.29
Picea	--	--	--	2.65
Pinus	--	--	--	--

Table 6.3. (cont.)

Percent Increased Error Variance (%INC)

	Tsuga	Quercus	Picea	Pinus
Mean	7.34	7.86	7.45	7.92
Stand. Deviation	0.70	1.10	1.39	0.90
Standard Error	0.14	0.29	0.39	0.25

t-tests

Tsuga	--	1.58	0.33	1.72
Quercus	--	--	1.07	0.16
Picea	--	--	--	1.21
Pinus	--	--	--	--

Net Reduced Error Variance (NET)

	Tsuga	Quercus	Picea	Pinus
Mean	7.63	4.61	8.04	4.22
Stand. Deviation	3.50	3.16	3.07	2.49
Standard Error	0.69	0.85	0.85	0.69

t-tests

Tsuga	--	2.87*	0.38	3.17*
Quercus	--	--	2.81*	0.32
Picea	--	--	--	3.07*
Pinus	--	--	--	--

tion tolerance and, by extension, the level of competition itself. Tsuga and Picea are extremely shade tolerant wheras Quercus and Pinus only possess moderate to low shade tolerance.

The %RED statistics indicate that the error variance of the improved means is reduced by 20% to 24% on the average across all genera. The equality of means tests indicate that Picea has a significantly greater average %RED compared to Pinus. All other means are statistically the same. There is no clear stratification of genera by competition tolerance in this particular case.

The %INC statistics indicate that the error variance increase caused by robust estimation, when none is necessary, averages 7.6% across all genera. This penalty is quite small compared to the gain due to %RED using robust estimation. No statistically significant differences in mean %INC were found between genera.

The net effect of robust estimation on the level of error variance in the mean-value function is shown in the NET statistics. The average NET ranges from 4.22% to 8.04% reduction in error variance. The equality of means tests show the same stratification by competition tolerance as the %IMP means. This is not surprising since the NET statistics reflect the average information contained in the other statistics.

Discussion

The performance results of the biweight robust mean indicate

that there is a substantial amount of outlier contamination in tree-ring ensembles from closed-canopy forests. This is probably due to the high level of competition between trees and the occurrence of episodic endogenous disturbances. The percentage of years in which outlier contamination occurs appears to be stratified along competition tolerance lines. The corollary agent which could produce this stratification is competition level or intensity. For this hypothesis to be true, the average level of competitition in Tsuga and Picea stands would have to be significantly greater than in Quercus and Pinus stands. Testing this hypothesis is difficult because the level of competition today, as measured by some competition index, may not be the same as it was in the past for the sampled trees. However, some insights may be gained by correlating such indices against the robust mean results if one assumes a uniform competition level in the past.

Conclusions

The theoretical error variance reduction property of autoregressive modelling has been verified for a suite of 66 tree-ring ensembles representing four tree genera. The technique appears to work more efficiently for Tsuga than for Picea, Quercus or Pinus. The reality of this genus-level difference cannot be firmly established until additional samples of the latter three genera are available.

The biweight robust mean was shown to be very useful in

reducing the effects of outliers in the mean-value function. The level of outlier contamination, as reflected in the number of improved means, can be substantial. This number may be related to some aspect of competition tolerance and/or intensity based on the significant differences between the Tsuga-Picea and Quercus-Pinus groups. Again, more samples are needed to substantiate these differences.

The net result of the ARSTND methodology is a two-stage reduction of error variance in the mean-value function. This is accomplished by methods which are totally independent in design and application. The fractional common variance and resultant signal-to-noise ratio calculated from the average correlation between trees only reflects the effects of autoregressive modelling. These estimates do not include the additional reduction in error variance due to robust estimation which will increase the total fractional common variance above that estimated by the average correlation between trees alone. Until a robust estimate of fractional common variance is derived based on concepts related to the biweight robust mean, the signal-to-noise ratios of ARSTND chronologies computed from the fractional common variance between trees will be biased conservatively downward from their true levels.

CHAPTER 7

COMPARISON OF ARSTND WITH ACCEPTED STANDARDIZING METHODS

Introduction

The theoretical and empirical results in chapters 5 and 6 revealed some important properties of ARSTND that support its use as a standardization method. To further bolster the validity of the ARSTND methodology, actual tree-ring data will be standardized and compared using accepted methods (e.g. Fritts, 1976; Graybill, 1982) and ARSTND.

This detailed comparison will be made using two tree-ring ensembles that are inferred to be free of disturbance pulses. This inference is based on the way in which each ensemble can be standardized satisfactorily using simple linear and exponential growth curves to model the observed age trends. ARSTND is not likely to offer any demonstrable improvements when the age trends can be modelled as simple, monotonic growth functions. Thus, the ARSTND chronology and the chronology developed by standard methods (Graybill, 1982) should be statistically identical. The latter chronology will be referred to as the standard (STNDRD) chronology in all subsequent discussions.

The two tree-ring ensembles come from different tree species growing in radically different geographic areas and environments: semi-arid site ponderosa pine in New Mexico and lake-site bald cypress in Arkansas. The different species and environments produced tree-

ring ensembles with very different time series characteristics. Thus, each test case will provide new and independent information about the properties of the ARSTND methodology.

Ditch Canyon Ponderosa Pine

The ring-width measurements of 24 increment cores from Ditch Canyon, New Mexico, ponderosa pine (Pinus ponderosa Laws.) will be examined first. These data were obtained from Dr. William J. Robinson of the Laboratory of Tree-Ring Research at the University of Arizona. The Ditch Canyon site is a classic open-canopy, semi-arid tree-ring site. The final chronology, which is published in Drew et al. (1976), has excellent statistical characteristics for dendroclimatic analyses based on the results of Fritts and Shatz (1975). Most importantly, the age trends of the individual cores are, in general, nicely modelled by negative exponential curves. Thus, this data set has minimal problems regarding tree-ring standardization. Each ring-width series was standardized using a curve-fit option that first tries to model the age trend as a modified negative exponential curve. If the non-linear estimation procedure failed to converge or the data had a non-negative slope, a linear regression line of either positive or negative slope was fit to the series. This procedure resulted in 15 cores being standardized with negative exponential curves, 8 with regressions of negative slope, and 1 with regression of positive slope. This last series (I.D. #012082) does not conform to the biological model of open-growth trees which predicts that the age trend should be negative. Although it could be deleted from the

ensemble for this reason, it will be left in since it was used in the chronology published in Drew et al. (1976).

At this stage, the STNDRD site chronology was computed as the mean-value function of the standardized ring-widths or indices using the biweight robust mean. This was done because the ARSTND methodology relies on the robust mean to censor outliers in the random shocks. If the arithmetic mean were used in computing the STNDRD chronology, any differences between that series and the ARSTND chronology could be related only to the different methods of computing the mean-value function rather than those differences in the ARSTND methodology relating to the autoregressive modelling. To evaluate the performance of the biweighting procedure, each robust mean was compared to the corresponding arithmetic mean following the methods in chapter 6.

The results of the biweighting procedure are given in table 7.1. For the STNDRD chronology, the percentage of improved means (%IMP) was 37% with an average percent error reduction (%RED) of 25.7%. The remaining unimproved means have an average percent error increase (%INC) of 8.6%. The net reduction in error variance (NET) is 3.6%. The %IMP and NET statistics are less than the averages for Pinus in Chapter 6. This is consistent with the belief that these open-grown trees should be less affected by competition and disturbances than closed-canopy trees. The resultant robust STNDRD chronology covers the years 1555-1971.

The next step in the ARSTND methodology is the selection of

Table 7.1. The chronology statistics for the standard (STNDRD) and ARSTND chronologies of the Ditch Canyon Ponderosa Pine test case.

	ROBUST STATISTICS				CHRONOLOGY STATISTICS				
	%IMP	%RED	%INC	NET	m.s.	s.d.	r1	g1	g2
STNDRD	37.0	25.7	8.6	3.6	.365	.393	.496	.029	3.05
ARSTND	32.1	22.5	9.4	3.8	.352	.379	.456	.136	3.25

	ARMA-MODELLING				COMMON INTERVAL ANALYSIS	
	AR(p)	ϕ_1	ϕ_2	ϕ_3	$\bar{r}$	SNR
STNDRD	3	.363	.199	.081	.629	18.6
ARSTND	3	.345	.179	.078	.610	17.2

%IMP = percentage of means improved by robust estimation
%RED = percent reduction in error variance of the improved means
%INC = percent increase in error variance of those means not improved by robust estimation
NET = net percent reduction in error variance for all means
m.s. = mean sensitivity
s.d. = standard deviation
r1 = first-order autocorrelation coefficient
g1 = coefficient of skewness
g2 = coefficient of kurtosis
AR(p) = autoregressive process of order p
ϕ_i = the coefficients of autoregression
$\bar{r}$ = average correlation between trees
SNR = signal-to-noise ratio

the pooled AR order and computation of the pooled coefficients. As described in Chapter 3, this is accomplished through the construction of lag-product sum matrices for lags t=0 to t=10. The importance of this pooling approach is the way in which the off-diagonal terms serve as measures of covariance between the series at lags other than zero. If the series covary in common at these lags, then the terms in the upper and lower triangles will have the same sign as those in the principal diagonal. This means that each tree is encoding common environmental information via a common set of physiological processes. Clearly, this is exactly what we hope to find because it should provide the cleanest dendroclimatic signal to analyze. A roughly equal number of positive and negative terms in the off-diagonal elements would indicate that either some trees are encoding environmental information differently from other trees or they are encoding different information. The components responsible for these differences may be site heterogeneity, random variability in each tree's physiological system and endogenous disturbances. Because of the large number of terms in each lag-product sum matrix, a parsimonious representation of each matrix is needed. The sign test (Siegel, 1956) is a simple non-parametric method which provides a significance test for this test of homogeneity. Each lag-product sum was coded as plus, minus or zero within each matrix depending on its departure from the expected value of zero for random numbers. The number of pluses and minuses were summed separately and each sum was scaled to a percentage of the total number of pluses and minuses. The percentages can be

plotted as a function of lag and tested for significance. The number used to compute the 95% significance levels is equal to number of series used to compute the lag-produce sum matrices. This represents the number of samples (N) that is contributing "independent" information to the sign test, not the N^2 terms in each lag matrix. The null hypothesis states that there is no common positive or negative covariance within the particular lag matrix. If the number of pluses or minuses exceed the number expected by chance alone at the 95% level, the null hypothesis is rejected. The results of this analysis for Ditch Canyon ponderosa pine is shown in Figure 7.1a. Each vertical line has a range totaling 100% which includes the %+ (upper limit) and %- (lower limit) values. The lag-product sum matrices have significant positive covariance out to lag 5 after which random effects dominate the remaining multivariate persistence structure. The lag-product sums were then pooled as described in Chapter 3. Using the Levinson-Durbin recursion and the first-minimum AIC search criterion (see Figure 7.1d), a pooled AR(3) order was selected as the common persistence operator among all the trees. The pooled AR coefficients are: ϕ_1=0.320, ϕ_2=0.193 and ϕ_3=0.109. The fractional variance due to pooled autoregression ($\hat{R}^2$) is .324. The pooled autocorrelation function (ACF) and partial autocorrelation function (PACF) obtained from this analysis are illustrated in Figures 7.1b and 7.1c. The ACF coefficients are computed as described in Chapter 3 while the PACF coefficients are produced as an intermediate result of the recursion. The pooled ACF damps out and drops below the approximate 95% confi-

dence limits after lag 6. This agrees well with the pooled sign tests. The PACF cuts off after lag 3 in accordance with the theoretical behavior of an AR(3) process. The absolute (but second) minimum AIC occurs at lag 7. The source of this 7th order minimum is apparent in the PACF where a significant lag is indicated. The AR coefficients for the selected order are illustrated in Figure 7.1e. The positive signs of all three coefficients indicate the persistence in the tree rings is a linear aggregate of mixed exponentials produced by the convolution of the wavelet of the AR(3) process with the series of random shocks. That wavelet is illustrated in Figure 7.1f. It requires about 15 years to dampen out.

Having estimated the pooled AR order, the 24 core index series were modelled as AR(3) processes and prewhitened to produce residual series. Although the AR order was estimated from the pooled data, the AR coefficients were estimated separately from the properties of each series. The maximum entropy method (Ulrych and Bishop, 1975) was used to estimate the coefficients. The average fractional variance explained by total autoregression ($\bar{R}^2$) was 0.305. From $\hat{R}^{-2}$ and $\bar{R}^2$, the level of autocorrelated noise (ΔR^2) is -.019. Thus, there is no evidence of autocorrelated noise in the ensemble and, hence, no out-of-phase fluctuations in the individual series. In each case, the residual autocorrelation function (RACF) was examined for randomness using the modified portmanteau statistic (Ljung and Box, 1977). The number of lags examined by this procedure was 25. As noted in Chapter 3, constraining each series to be modelled as a pooled AR order may

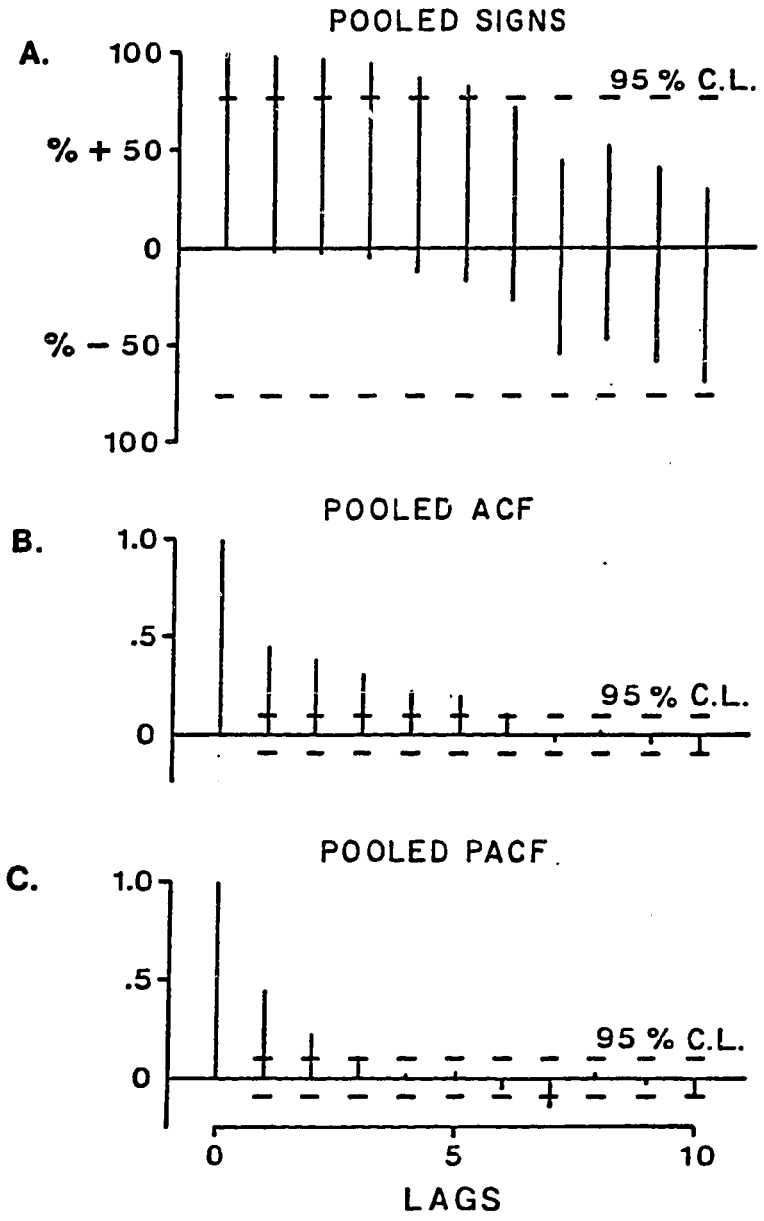

Figure 7.1. The pooled signs (A), pooled autocorrelation function (B), pooled partial autocorrelation function (C), AIC trace (D), pooled autoregressvie coefficients (E), and wavelet or impulse response function of the pooled autoregressive coefficients (F) for the Ditch Canyon ponderosa pine tree-ring ensemble.

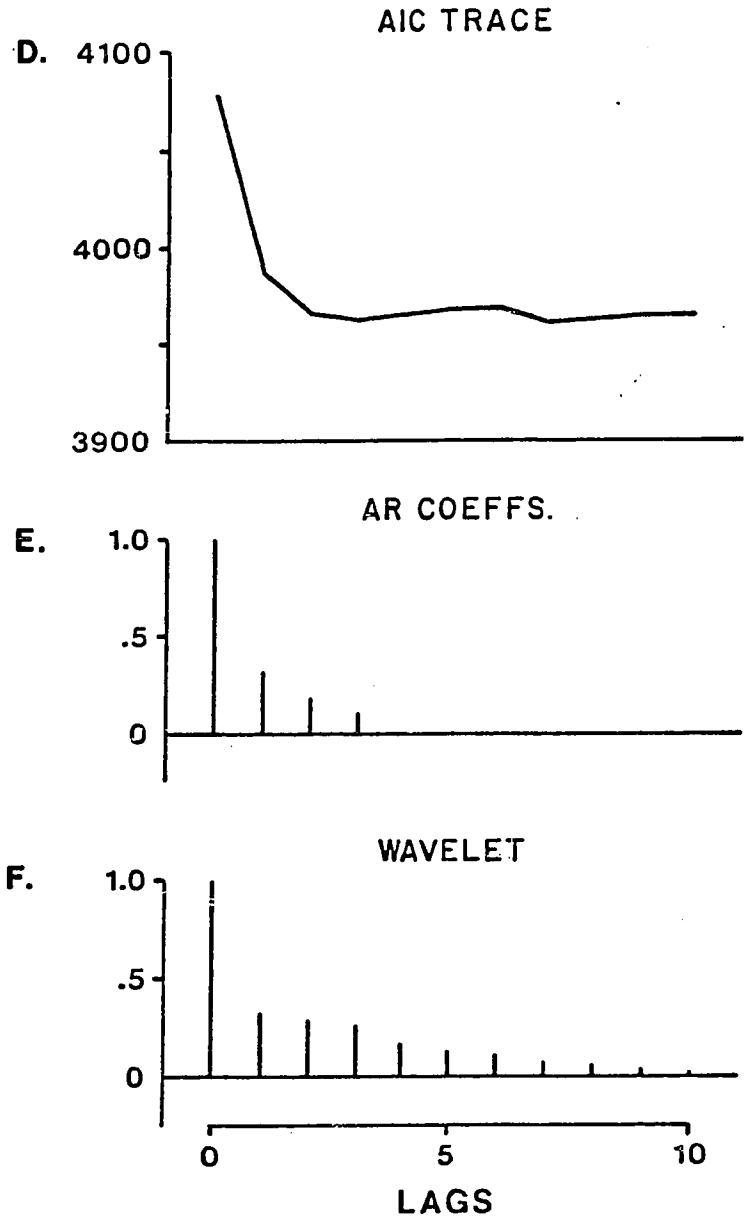

Figure 7.1. (cont.)

result in some residual series having non-random RACF's because of unremoved longer lag persistence. In this instance, all 24 series passed the portmanteau test for randomness at the 95% level. This is another indication of the excellent stochastic homogeneity in the Ditch Canyon tree-ring ensemble.

The robust mean-value function of residuals was computed next. The %IMP, %RED, %INC, and NET statistics in Table 7.1 are quite similar to those of the standard chronology robust mean-value function computed earlier (also in Table 7.1). Due to the autoregressive modelling, the first three values of every series were lost. Hence, the residual mean-value function begins in 1558 instead of 1555.

The RACF of the residual mean-value function passed the portmanteau test for randomness (p=0.637). The standard errors of the RACF were also computed using the impulse response function weights of the pooled AR process (Box and Pierce, 1970). This extremely sensitive test suggested lag-1 non-randomness in the RACF. The lag-1 r of 0.029 has a 2 standard error limit of 0.011. Although statistically significant, the lag-1 persistence is very small and probably not operationally significant. An AR modelling of the residual series using the minimum AIC failed to identify any autoregression in the series, which supports the latter contention. On this basis, the residual mean-value function was accepted as a serially random process.

The pooled autoregression was added back in at this point as described in Chapter 3 (equations 3.36 and 3.37). The starting values

were obtained from the standard chronology for the years 1555-1557. Because these starting values are real data, the resulting ARSTND chronology incorporates them and, therefore, is equal in length to the STNDRD chronology.

Mean sensitivity (m.s.), standard deviation (s.d.) and lag-1 autocorrelation (r1) are frequently used to judge the probable dendroclimatic value of tree-ring chronologies (e.g. Fritts and Shatz, 1975). Therefore, the first comparison of the STNDRD and ARSTND chronologies will use these statistics. From Table 7.1, these statistics are: m.s.= 0.365 and 0.352, s.d. = 0.393 and 0.379, and r1 = 0.496 and 0.456, respectively, for the STNDRD and ARSTND chronologies. Very little difference is seen between the two series using these statistics. The higher moments are also preserved nicely. The coefficients of skew and kurtosis (Table 7.1) are 0.029 and 0.136, and 3.051 and 3.253, respectively. None of these summary statistics reveal any differences between the STNDRD and ARSTND chronologies.

Cross-spectral analysis (Jenkins and Watts, 1968) will be used next to compare the frequency domain properties of the STNDRD and ARSTND chronologies. The spectra used for this purpose are the coherency, gain and phase spectra. The coherency spectrum is the frequency domain analogue of the squared correlation coefficient. That is, it measures the percent variance agreement between two series as a function of frequency. The ideal is a coherency spectrum of 1.0 for all wavelengths. This indicates that the two series behave identically in a relative sense although their variances may not be equal.

The gain and phase spectra are useful in characterizing the linear filter that transforms an input series into a new output series. In the sense used here, the input series is the STNDRD chronology, the linear filter is the ARSTND methodology and the output series is the ARSTND chronology. The gain spectrum will reveal how well the filter passes variance as a function of frequency. If the ARSTND methodology is unbiased, the resulting gain will be near 1.0 everywhere. This means that the technique has recovered 100% of the variance in the chronology at all wavelengths. The phase spectrum will reveal if the output series leads or lags the input series due to the filtering operation. Again, for the ARSTND methodology to be unbiased, the phase angle between the input and output series should be near zero everywhere.

In this and all subsequent spectral analyses, the spectra will be computed from the autocovariance functions of the series. The number of lags will be 25% of the total observations in every case. This means that the equivalent degrees of freedom (EDF) and, hence, the variance of the spectral estimates will be constant for the three test cases. Using the Hamming window, each spectral estimate has 10 degrees of freedom. The drawback to the constrained lag approach is the way in which the spectra of longer series will be resolved better than shorter series because more lags are available. However, it is more important here to maintain a constant EDF so that the results of the test cases are comparable.

The spectra were computed using 104 lags of the autocovariance

functions. The coherency, gain and phase spectra of the STNDRD and ARSTND Ditch Canyon chronologies are shown in Figure 7.2. The coherency spectrum shows an extremely high percentage agreement across all frequencies. Except for the first coherency estimate corresponding to infinite period, all estimates exceed the 99% significance level (coherency = 0.83). There is a small drop in coherency around the 3.5 year period (harmonics 58-59). This is close to the AR order for prewhitening. Since the AR process is a finite-order approximation of an infinite-order general linear process, this may be a truncation effect of the model. Overall, the coherency spectrum does not reveal any significant difference in the ARSTND chronology.

The gain spectrum indicates that the ARSTND series has the same variance characteristics as the standard chronology. Most of the gain estimates fall between 0.90 and 1.10. Two estimates fall outside the 95% limits which is about the expectation by chance alone. There is a tendency for the gain to stay below 1.0 in the lowest frequencies. This is due to small differences in the level of autoregression between the series. These differences will be described and discussed in more detail later. At this stage, it need only be remembered that autoregressive processes such as these are "red noise" processes (Gilman et al., 1963). As such, any differences in the coefficients will be most readily seen in the low-frequency or "red" end of the spectrum. The phase spectrum also verifies that the ARSTND chronology is unbiased. Only one estimate exceeds the 95% limits.

The cross-spectral analyses have not revealed any significant

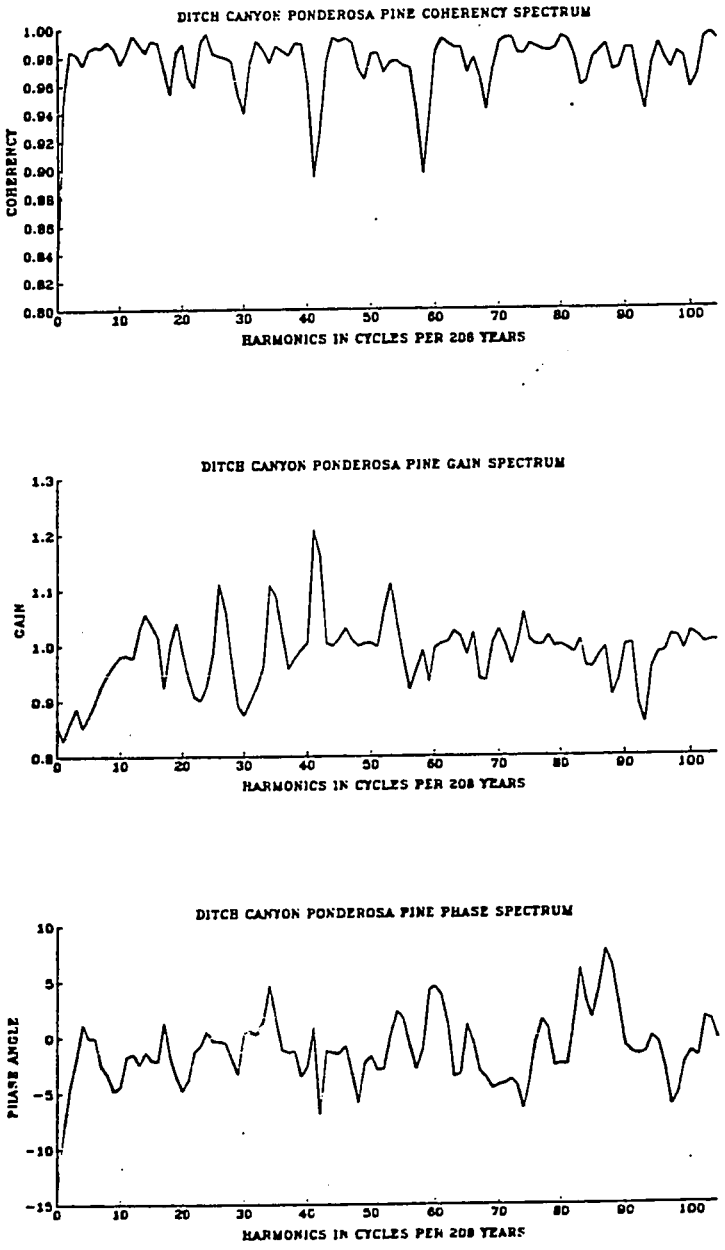

Figure 7.2. The coherency (A), gain (B), and phase (C) spectra for the Ditch Canyon ponderosa pine STNDRD chronology versus the ARSTND chronology.

Each spectrum is computed from the auto- and cross-covariance functions of 104 lags. Each spectral estimate has 10 degrees of freedom.

differences between the STNDRD and ARSTND chronologies. Another method of comparison will be to compare the time domain stochastic structures of the two series. This will be done by fitting each series as an ARMA (p,q) process for all possible orders up to p=3 and q=3. The minimum AIC will be used to select the best model. The stochastic properties of the ARSTND chronology have not been constrained in any way to be like those of the standard chronology. Thus, this test could reveal some differences between the two series both in the order of the stochastic model and the estimated ARMA coefficients. Ideally, no significant differences will be found. Using the minimum AIC criterion, the STNDRD chronology was fit best as an AR(3) process. The AR coefficients are $\phi_1 = 0.363$, $\phi_2 = 0.199$ and $\phi_3 = 0.081$. The ARSTND chronology was also fit best as an AR(3) process which, of course, agrees with the pooled model. These estimated coefficients are: $\phi_1 = 0.345$, $\phi_2 = 0.179$ and $\phi_3 = 0.078$. It can be seen again that the two chronologies agree very well in both the order of the selected model and the model coefficients. The only difference seems to be slightly smaller coefficients for the ARSTND model.

The two chronologies are plotted together for visual comparison in Figure 7.3. The two series agree exceptionally well. The greatest disparity is in the earliest portion of the record where the replicaiton is poorest. This result was anticipated because it is the interval where the mean-value function has little or no statistical precision. The differences are probably due to variability in the persistence structure of individual series and the pooled estimates.

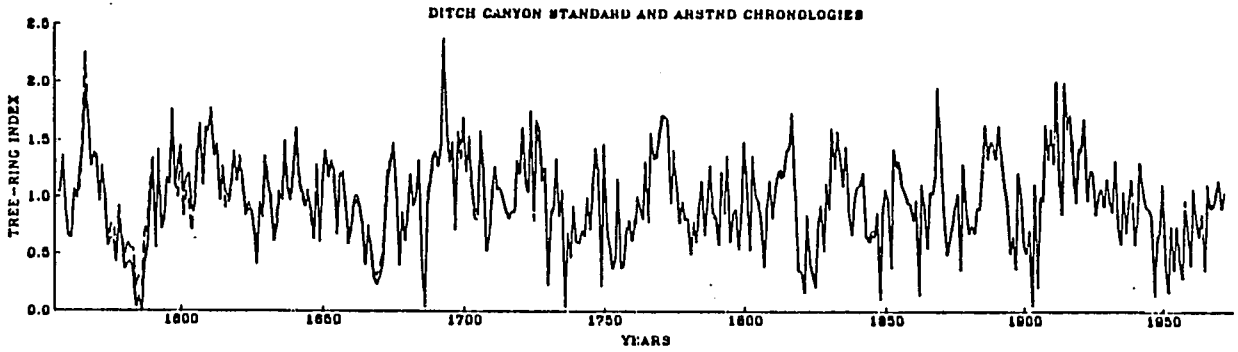

Figure 7.3. The Ditch Canyon ponderosa pine standard (STNDRD) and ARSTND chronologies.

The STNDRD chronology is the solid line plot and the ARSTND chronology is the dashed line plot.

These differences should be expected to surface where replication is poor, in this case only 1 to 3 cores for the 1555-1609 period. A particularly inter-esting phenomenon shows up for the years 1583, 1584 and 1585 where the replication is only 3 cores based on two trees. In the STNDRD chronology, the mean indices are 0.044, 0.147 and 0.000 compared to 0.229, 0.333 and 0.231 for the ARSTND chronology. These are rather large differences, especially for the 1585 growth year which resulted from a locally absent ring in all three cores. The ARSTND estimates indicate that the input environmental signal (as reflected in the residual mean-value function) and the physiological persistence (as reflected in the pooled autoregression coefficients) are insufficient to explain the observed indices in the STNDRD chronology. Sampling variability due to the very small sample depth in this sequence of means may be largely responsible for these differences since no similar departures exist in the better replicated portion of the chronolgies. However, there is some indication that the ARSTND chronology underestimates persistent extremes compared to the standard chronology. Consider the following intervals for the STNDRD and ARSTND chronologies. For the 1663-1670 period, the interval means are 0.468 and 0.516, respectively. For the 1818-1824 period, the means are 0.381 and 0.424. For the 1884-1892 period, the means are 1.422 and 1.492. In every case, the ARSTND chronology underestimates the magnitude of persistent extremes. This would be undesirable if it represents a loss of climatic information. More likely, the observed differences in persistent extremes are due to small differences in the

level of autoregression in each series. As described in Chapter 5, the variance of autoregressive process is proportional to the variance of the random shocks and the level of autoregression in the process (equation 5.8). This means that the slightly larger AR coefficients of the STNDRD chronology (Table 7.1) will produce a chronology with more variance than the ARSTND chronology given the same set of random shocks. The variances of the STNDRD and ARSTND chronologies are 0.155 and 0.144, respectively. The former is about 7.6% greater than the latter. The difference in the variance that can be attributed to the coefficients can be estimated from the variances of the random shocks obtained by fitting the two chronologies as AR(3) processes. The variance of the STNDRD and ARSTND random shocks are 0.110 and 0.109, respectively. The former is now only 0.9% greater than the latter. Re-examining the four periods of extremes using the zero-mean random shocks of the STNDRD and ARSTND chronologies, the results are as follows. For the 1663-1670 period, the means are -0.284 and -0.269, respectively. For the 1818-1824 period, the means are -0.358 and -0.354. And, for the 1884-1892 period, the means are 0.238 and 0.239. The differences between the means are now much smaller than before and, for the third interval, reversed. These results indicate that the ARSTND methodology has not resulted in any appreciable loss of climatic variance with regard to persistent extremes.

The signal-to-noise ratio (SNR) properties of the Ditch Canyon ensemble will now be examined based on the SNR derivations described in Chapter 5. This analysis is done on a time period that includes as

many cores as possible from the ensemble. For the Ditch Canyon ensemble, 22 of 24 series from eleven trees covering 1868-1971 were used. Each SNR will be estimated from the average correlation between trees following Wigley et al. (1984). As shown in chapter 5, the SNR for the ARSTND chronology is the same as that of the mean-value function of prewhitened indices or residuals. The SNR of the STNDRD chronology is based in the detrended indices prior to autoregression modelling.

In table 7.1, fractional common variance as measured by the average correlation ($\bar{r}$) and SNR of the STNDRD chronology are 0.629 and 18.6, respectively. The corresponding figures for the ARSTND chronology are 0.610 and 17.2. The difference in fractional common variance ($\Delta\bar{r}$) is -.019. There is virtually no difference between the chronologies in terms of average correlation and SNR. The near-zero $\Delta\bar{r}$ agrees with the ΔR^2 in support of Chapter 5 theory.

Discussion

The Ditch Canyon standardization comparisons indicate that the ARSTND methodology can produce a site chronology that is virtually indistinguishable from one produced by accepted methods when the accepted method works well. Thus, while little is gained through the increased computational burden of autoregressive modelling, this burden does not result in a loss of chronology fidelity.

Hemstead County Bald Cypress

The second data set used to test the ARSTND methodology was provided by David W. Stahle of the University of Arkansas. It is the

ring-width measurements from 29 increment cores of bald cypress (Taxodium distichum [L.] Rich.) growing in a lake in Hemstead County, Arkansas. Stahle et al. (1982) reported that every increment core series could be standardized well using negative exponential curves and regressions of negative slopes. In May 1982, I visited this site with Stahle and found that it is an undisturbed stand of widely spaced cypress growing in shallow water. This finding, coupled with the classic age trend behavior observed in the ring-width series, makes the Hemstead County site an excellent test case using ARSTND. In addition, it is radically different from the Ditch Canyon site in terms of species and site characteristics which enhances its value for study.

As was done with the Ditch Canyon ensemble, each cypress ring-width series was standardized by trying the modified negative exponential curve first. If that option failed, a linear regression curve was fit to the series. Of the 29 series, 25 were standardized with negative exponential curves and four with negative slope regression curves. These standardization curves agree with Stahle's treatment of the data. The standard chronology mean-value function was then computed using the robust mean as before. The results of biweighting procedure are given in table 7.2. For the total period with a minimum replication of six cores, the %IMP is 42% and the %RED is 22.7%. The remaining unimproved means have a %INC of 7.4%. The NET effect is a 4.2% error reduction using the robust mean. The STNDRD chronology covers the 1766-1980 interval.

Table 7.2. The chronology statistics for the standard (STNDRD) and ARSTND1, and ARSTND2 chronologies of the Hemstead County Baldcypress test case.

	ROBUST STATISTICS				CHRONOLOGY STATISTICS				
	%IMP	%RED	%INC	NET	m.s.	s.d.	r1	g1	g2
STNDRD	42.0	22.7	7.4	4.2	.437	.370	.096	.485	3.26
ARSTND1	44.0	24.2	7.4	5.9	.467	.370	-.083	.447	3.21
ARSTND2	--	--	--	--	.428	.370	.099	.520	3.32

	ARMA-MODELLING				COMMON INTERVAL ANALYSIS	
	MA(q)	θ_1	θ_2	θ_3	$\bar{r}$	SNR
STNDRD	3	-.055	-.373	-.116	.401	12.0
ARSTND1	3	-.077	-.434	-.038	.447	14.5
ARSTND2	3	-.061	-.421	-.101	--	--

%IMP = percentage of means improved by robust estimation
%RED = percent reduction in error variance of the improved means
%INC = percent increase in error variance of those means not improved by robust estimation
NET = net percent reduction in error variance for all means
m.s. = mean sensitivity
s.d. = standard deviation
r1 = first-order autocorrelation coefficient
g1 = coefficient of skewness
g2 = coefficient of kurtosis
MA(q) = moving average process of order q
θ_i = the moving average coefficients
$\bar{r}$ = average correlation between trees
SNR = signal-to-noise ratio

The pooled autoregression was estimated from the lag product sum matrices. Figure 7.4a shows the percent agreement by sign for each lag matrix. The matrices show significant homogeneity with positive signs for lags t=0 and t=2, and negative signs for t=8. The subsequent AR fitting procedure selected an AR(2) model using the first-minimum AIC search. The pooled AR coefficients are: ϕ_1 = 0.070 and ϕ_2 = 0.351. The fractional variance due to pooled autregression ($\hat{R}^2$) is .138. The pooled ACF and PACF obtained from the analysis are illustrated in Figure 7.4b and 7.4c. The AIC trace (Figure 7.4d) shows an absolute minimum at lag 8 which also shows up as significant in the pooled signs, ACF and PACF. However, the first minimum AIC order selection will be used here given the properties of the AIC statistic noted in chapter 3. The AR coefficients and their equivalence in wavelet form are also shown in Figure 7.4. The wavelet behaves in a damped sawtooth-like fashion due to the difference in the AR coefficients. It effectively diminishes to zero after lag 8.

All 29 series were prewhitened as AR(2) processes. The average fractional variance due to all sources of autoregression ($\bar{R}_2^2$) is 0.191. From $\hat{R}^2$ and $\bar{R}^2$, the level of autocorrelated noise (ΔR^2) is estimated to be 0.053. This indicates that a very small amount of autocorrelated noise is in the data which probably has little operational significance in selecting and fitting standardization curves. The residual series were tested for randomness using the portmanteau test as before. This time, the test failed to pass four of the 29 series for randomness at the 95% level. The failed series

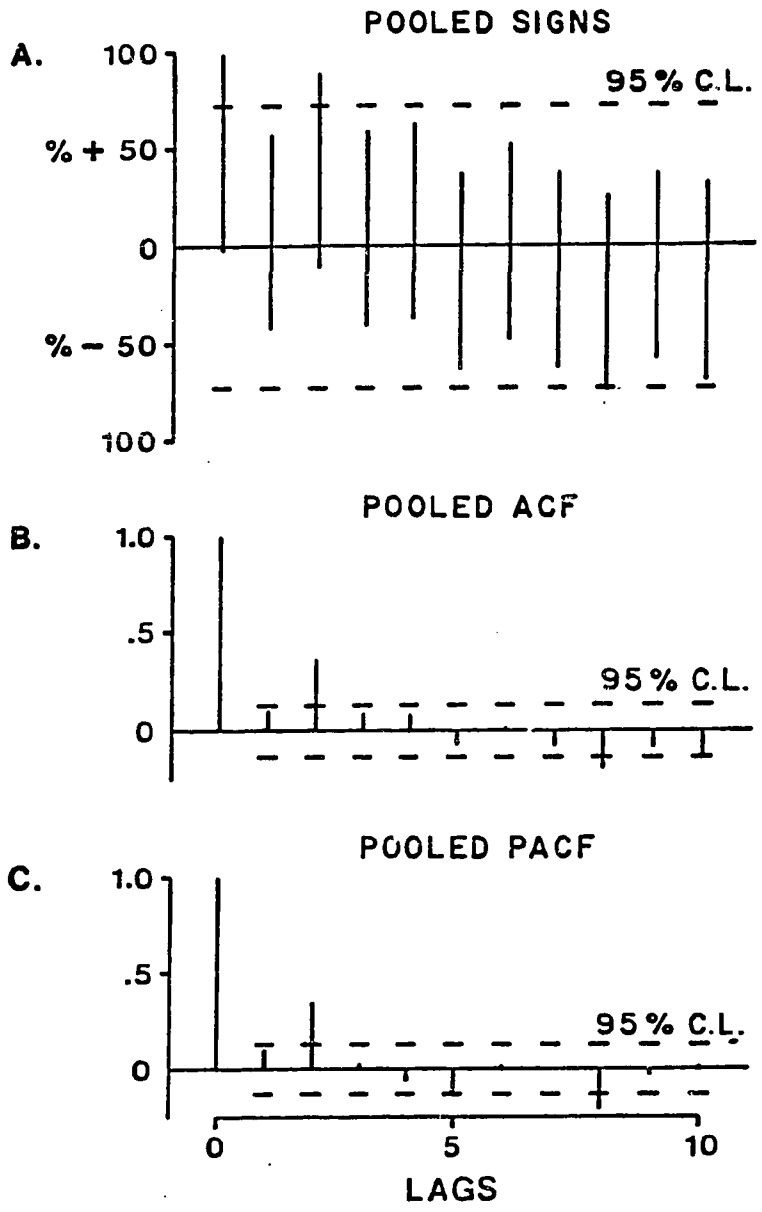

Figure 7.4. The pooled signs (A), pooled autocorrelation function (B), pooled partial autocorrelation function (C), AIC trace (D), pooled autoregressive coefficients (E), and wavelet or impulse response function of the pooled autoregressive coefficients (F) for the Hemstead County bald cypress tree-ring ensemble.

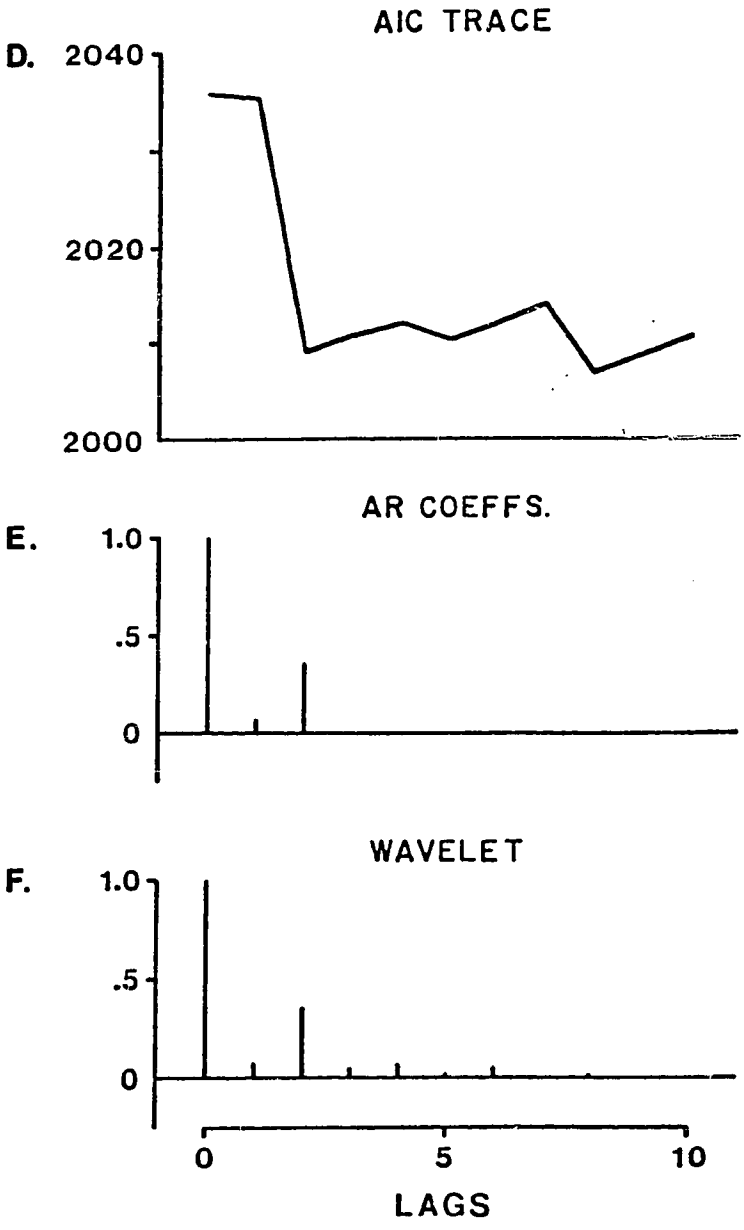

Figure 7.4. (cont.)

were not the ones standardized by linear regression curves. Longer-lag persistence associated with the 8th-order term in the pooled estimates may be partly responsible for this problem along with random effects in the autocorrelation functions. As discussed in Chapter 3, this problem was anticipated because of the constrained nature of the fitting procedure. No additional modelling was perfomed on these series in order to maintain an order of prewhitening consistent with the pooled estimate.

The robust mean-value function of residuals was computed next. The biweighting procedure results are shown in Table 7.2. The %RED is 24.2% for the 44% %IMP means. In contrast, the %IMP is 7.4% for the remaining 56% unimproved means. The NET effect is a 5.9% reduction in error variance. The results are very close to those of the STNDRD chronology (also in Table 7.2). Although most of the individual series appeared to be serially random, the residual mean-value function contained significant short-lag persistence. This was revealed through a significant ($p=.037$) portmanteau statistic and a surprisingly large lag-1 autocorrelation coefficient of -0.135. Using the wavelet form of the pooled AR order (Figure 7.4f) to compute the standard errors of the RACF (Box and Pierce, 1970), this coefficient is almost six standard errors from the expected value of zero. This was quite unexpected because the average first-order coefficient of the individual series was only 0.0002 with 16 being positive and 13 being negative. The range of values is 0.082 to 0.075. Thus, the lag-1 coefficient of the RACF even exceeds the range of the single

series coefficients.

Several possible causes for this anomalous lag-1 persistence were hypothesized and tested. The mean residual series was recomputed using the arithmetic mean instead of the robust mean to see if the lag-1 persistence could be an artifact of the biweighting procedure. The lag-1 coefficient obtained from the arithmetic mean series was -0.143 which is marginally more negative than the robust mean coefficient. Thus, the biweighting procedure is not the source of the lag-1 residual persistence.

Another cause of the lag-1 persistence could be the constrained fitting procedure imposed on the individual series. This was examined by independently applying the first-minimum AIC search to each series. In this case, each series is modelled as an AR process without the constraint that the fitted order is the same as the pooled order. Thus, each series model may differ from the others. This resulted in 22 AR(2) selections and seven AR(3) selections. The ACF of the residual mean-value function developed from this fitting procedure was essentially identical to the constrained model ACF. The lag-1 coefficient was -0.138 which is extremely close to the constrained run result. The series were then refit as AR(8) processes in accordance with the absolute minimum AIC choice. The ACF for the residual mean-value function from this extended model was, again, very similar to the others. In fact, the lag-1 coefficient equalled -0.158 which is slightly more negative than the simpler models. The cause of the residual persistence does not appear to be related to the con-

strained AR fitting procedure. In fact, the method appears to be rather robust in this regard.

Another possible cause for the lag-1 persistence is the inadequacy of the autoregressive model to precisely explain the stochastic properties of each series. This admits the possibility that MA or mixed ARMA processes may be more appropriate stochastic models in some cases. To test this hypothesis, the bald cypress STNDRD chronology was modelled as an ARMA (p,q) process for all possible orders up to ARMA (3,3). The minimum AIC criterion was used to select the best model. The STNDRD chronology is being used here to estimate the "true" stochastic model of the individual series in much the same way as the AR pooling procedure estimates the common persistence structure of the ensemble. By this procedure, an MA(3) process was selected with several mixed models in close competition. Out of the 15 models tested by this procedure, the AR(2) model used for prewhitening ranked as the sixth best. This finding suggested that the residual persistence may be due to model inadequady which does not show up strongly until the residual mean-value function is computed. The AR(2) model falls above the median in goodness-of-fit which indicates that it is a reasonable model, but not the very best.

To see if, in fact, a misspecified model was responsible for the residual persistence, the bald cypress indexed cores were remodelled as MA(3) processes. Again, the lag-1 RACF coefficient was strongly negative, equalling -0.148. The individual series were then remodelled as MA(8) processes in accordance to the absolute minimum

AIC obtained by applying the AIC search for all MA models out to order 10. The lag-1 coefficient equalled -0.148 for this model which is identical to the MA(3) results. It is clear from these tests that the significant negative lag-1 persistence is not an artifact of model misspecification. In fact, none of the tests have resulted in any reduction of the lag-1 coefficients below that produced by the constrained AR(2) model.

Although the above testing failed to identify the source of residual persistence, the MA modelling identified a highly desirable property of the ARSTND methodology. The method seems to be robust not only with respect to the order of AR process used for prewhitening, but also in the case of model misspecification. This means that reasonable results should be expected over a broad range of ARMA models even though ARSTND is based on the autoregressive time series model. The reason for this result is related to the mathematical duality of AR and MA processes described in Chapter 3. Box and Pierce (1970) show that the random shocks of an ARMA (p,q) process can be closely approximated by an AR (p+q) process. The closeness of the approximation can be appreciated by comparing the coefficients of AR(3) and MA(3) processes fitted to the bald cypress standard chronology. Recall that an MA(3) model is probably the correct one for this time series. The "correct" MA(3) coefficients are: $\theta_1 = -0.055$, $\theta_2 = -0.3675$ and $\theta_3 = -0.1134$. The "approximate" AR(3) coefficients are: $\phi_1 = 0.0557$, $\phi_2 = 0.3037$ and $\phi_3 = 0.0351$. The similarity in the magnitudes of the coefficients indicates that either model will pro-

duce similar random shocks, in agreement with Box and Pierce (1970). The pooled AR coefficients also agree well with the first two coefficients of the MA(3) process. This indicates that the pooled AR coefficients are reasonable approximations of the common stochastic behavior in the ensemble even when the correct model is moving average.

Having eliminated the biweighting procedure and the stochastic model choice as causes of the lag-1 residual persistence, the ensemble of tree-ring residuals were examined for multivarate persistence using the AR pooling procedure. The sign tests of the lag-product sum matrices revealed significant negative lag-1 persistence in the ensemble in agreement with the residual mean-value function. This means that the serially random individual series were not multivariately random due to lag-covariance between the ensemble pairs. Thus, the residual persistence appears to be a statistical artifact of the univariate AR fitting procedure which is totally "blind" to any stochastic structure between series. The order of the residual multivariate dependence obtained from the pooled AR modelling is AR(1). The pooled AR coefficient is -0.157 which is slightly larger than the lag-1 coefficient of the residual mean-value function.

Because the lag-1 residual persistence has been identified as an artifact of the univariate modelling procedure, the removal of this effect is justified. This is most easily accomplished by modelling the residual mean-value function as an AR(p) process where p is constrained to be less than or equal to the order of the autoregressive

process used to prewhiten the separate series. The order constraint guards against removing longer-lag variance that is not related to the multivariate lag artifact. In this case, p=1 and the AR coefficient $\phi_1 = -0.135$. The residual mean-value function was "rewhitened" based on this fit which resulted in the complete removal of the lag-1 autocorrelation. The RACF passed both the portmanteau test (p=.102) and the very sensitive Box-Pierce (1970) significance tests for specific residual autocorrelations.

Although the rewhitening procedure appears to be justified based on the multivariate AR modelling, its effect on the final ARSTND chronology was investigated. Thus, two ARSTND chronologies were created by adding the pooled autoregression into the non-whitened (ARSTND1) and rewhitened (ARSTND2) mean residual series. In each case, the two starting values needed for the autoregression were obtained from the beginning values of the STNDRD chronology. The STNDRD chronology begins in 1766 while the ARSTND1 and ARSTND2 chronologies begin in 1766 and 1767, respectively.

The comparisons of mean sensitivies (m.s.), standard deviations (s.d.) and first-order autocorrelations (r1) from table 6.2 are as follows. For the STNDRD chronology: m.s.= 0.437, s.d.= 0.0368 and r1= 0.096. For the ARSTND1 chronology: m.s.= 0.467, s.d.= 0.370 and r1= -0.083. And for the ARSTND2 chronology: m.s.= 0.428, s.d.= 0.370 and r1= 0.099. The STNDRD and ARSTND2 chronologies agree very closely for all three statistics. The difference in mean sensitivity and standard deviation between the STNDRD and ARSTND1 chronologies reflect

the residual negative autocorrelation in the ARSTND1 mean-value function. The coefficients of skew (g1) and kurtosis (g2) are preserved nicely in both ARSTND chronologies. For the STNDRD chronology: g1= 0.485 and g2= 3.264. For the ARSTND1 chronology: g1= 0.447 and g2= 3.209. And for the ARSTND2 chronology: g1= 0.520 and g2= 3.322. None of these statistics show any appreciable difference between the chronologies.

The spectral analysis was carried out using 53 lags of the autocovariance function. The coherency, gain and phase spectra are shown in Figure 7.5 for the ARSTND1 (solid lines) and ARSTND2 (dashed lines) chronologies versus the STNDRD chronology. The STNDRD-ARSTND1 and STNDRD-ARSTND2 coherency spectra are virtually identical over the entire frequency range indicating that this spectrum is rather insensitive to differences between the competing ARSTND chronologies. Except for a narrow frequency band around a period of four years (harmonics 27-29), the coherencies are all above 0.98. The dip in coherency at about four years occurs near the lag truncation point of the AR(2) prewhitening operator. This effect may arise from variations in the stochastic structure of the individual series that depart from the pooled estimate. The gain and phase spectra reveal the largest differences between the STNDRD and ARSTND chronologies. The STNDRD-ARSTND1 gain spectrum (solid line) shows that the residual lag-1 persistence in the ARSTND1 chronology acts as a high-pass filter. The result is proportionately more high-frequency variance and less low-frequency variance in the ARSTND1 chronology compared to the

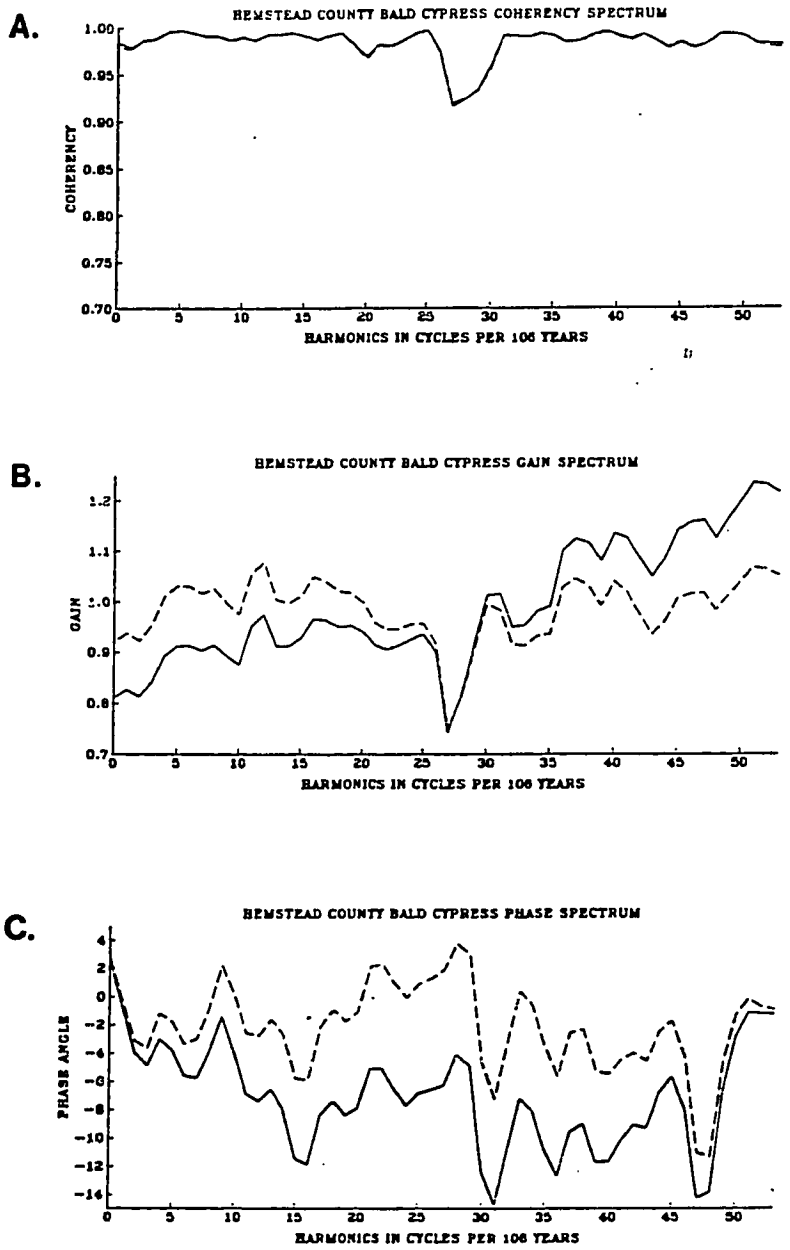

Figure 7.5. The coherency (A), gain (B), and phase (C) spectra for the Hemstead County bald cypress STNDRD chronology versus the ARSTND1 (solid line) and ARSTND2 (dash line) chronologies.

Each spectrum is computed from the auto- and cross-covariance functions of 53 lags. Each spectral estimate has 10 degrees of freedom.

STNDRD chronology. The STNDRD-ARSTND1 phase spectrum (solid lines) reveals a significant phase lag for most frequencies in the ARSTND1 chronology. Again, this is related to the residual persistence.

The STNDRD-ARSTND2 gain and phase spectra (dashed lines) indicate that the rewhitening operation has reduced the effects of the residual persistence. The gain spectrum is flat indicating that the ARSTND2 chronology is now fairly unbiased in its distribution of variance by frequency. The phase spectrum still shows a tendency for phase lag in the ARSTND2 chronology, but most of these values are no longer significant at the 95% level.

Having investigated the frequency domain properties of the STNDRD and ARSTND chronologies, their time domain stochastic structures will now be compared. Due to the loss of one data point due to rewhitening, the common period for all three chronologies is 1767-1980. Each chronology was modelled as an ARMA (p,q) process for all possible models up to p=3 and q=3. The AIC statistic was used to select the best model. As before, an MA(3) model was selected as best for the STNDRD chronology. The estimated MA(3) coefficients are: θ_1= -0.055, θ_2= -0.373 and θ_3= -0.116. The ARSTND1 chronology was also modelled best as an MA(3) process. The estimated MA(3) coefficients are: θ_1= -0.077, θ_2= -0.434 and θ_3= -0.038. The differences between the first coefficients of the STNDRD and ARSTND1 chronologies reflect the negative lag-1 persistence in the ARSTND1 mean residual series. The ARSTND2 chronology was modelled best as an MA(3) process like the others. The estimated MA(3) coefficients are: θ_1= -0.061, θ_2= -0.421

and θ_3= -0.101. The ARSTND2 chronology coefficients are extremely close to those of the STNDRD chronology.

The time and frequency domain comparisons indicate that the ARSTND chronology based on the rewhitened residuals is statistically indistinguishable from the standard chronology. This test case is especially important because it provides evidence that the ARSTND methodology is both unbiased as a chronology development tool and robust with regard to violations of the assumed autoregressive model upon which the method is based.

The STNDRD and rewhitened ARSTND chronologies are plotted together in Figure 7.6 for visual comparison. The two series agree exceptionally well even in the early part of the series where the replication is poor. Unlike the Ditch Canyon case, there is no indication that this ARSTND chronology underestimates extremes.

The SNR and fractional common variance comparisons were made, as before, between the STNDRD and ARSTND chronologies. The common interval covers 1899-1980 and includes 23 of the 29 total series. In table 7.2, the average correlation between trees and SNR of the STNDRD chronology are 0.401 and 12.0, respectively. The corresponding values for the ARSTND chronology are 0.447 and 14.5. In this case, there is a small increase of SNR using the ARSTND methodology. Based on the theoretical SNR derivations in chapter 5, this increase in SNR reflects the presence of autocorrelated noise which is more efficiently minimized through autoregressive modelling.

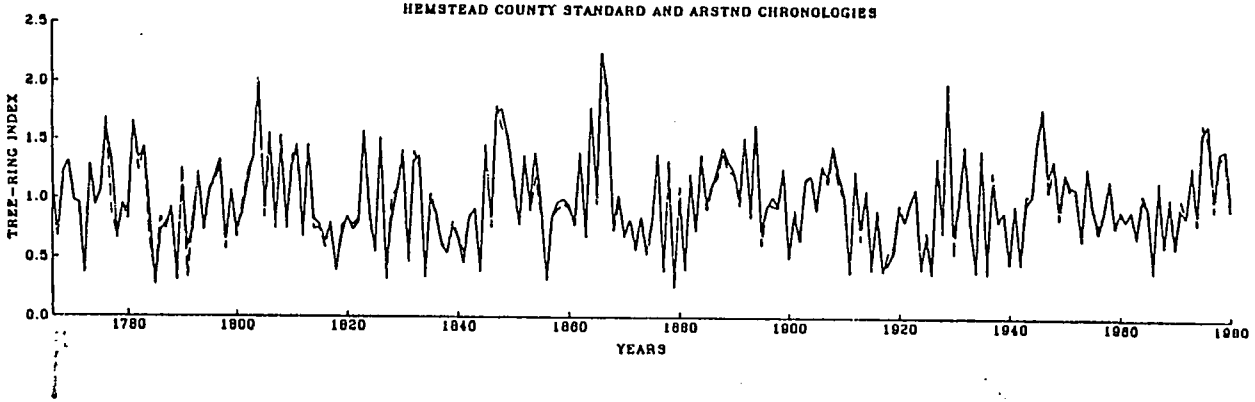

Figure 7.6. The Hemstead County bald cypress standard (STNDRD) and ARSTND chronologies.

The STNDRD chronology is the solid line plot and the ARSTND chronology is the dashed line plot. The ARSTND chronology is the one developed after rewhitening.

Discussion

The Hemstead County bald cyprus comparisons again indicate that the ARSTND approach can produce a site chronology equal in quality to that produced by accepted methods. Important new insights have been gained from this example, however. The autoregressive basis of the ARSTND time series model appears to be robust when that assumed model is incorrect. Thus, the method should work reasonably well within the broader family of ARMA time series models.

The apparent need for "rewhitening" in some cases was a totally unexpected discovery. The removal of this artifact of multivariate lag dependence between series appears to be justified since it is not related to the common signal within each time series. Modelling directly the lagged interactions between series would be a more satisfactory solution were it not for the large number of series in each ensemble and the different number of observations in each time series. Thus, the somewhat ad hoc and pragmatic method utilized here is currently the best solution available.

Conclusions and Synthesis

The test results presented here coupled with the results of Chapter 6 support the contention that the ARSTND methodology is a valuable new tool for dendroclimatic research. Its principal advantages are as follows:

1. The ARSTND methodology has a better defined theoretical basis both biologically and statistically than previous standardization methods. The biological theory is based on the

distinction between exogenous and endogenous disturbances and the way in which endogenous disturbances should create non-synchronous disturbance pulses in an ensemble of tree-ring series. This leads to the concept that only these non-synchronous pulse should be removed using information available within the ensemble of ring-width data.

2. ARSTND can produce a chronology with less error variance than a chronology developed without autoregressive modelling when developed from the same set of detrended indices. This will be true wherever non-synchronous growth fluctuations are present in the data.

3. ARSTND provides insights into the time series properties of tree-ring chronologies on a "real time" basis. These revealed properties should be quite useful in dendroclimatic studies.

The principal disadvantages of ARSTND are as follows:

1. ARSTND is considerably more complex and difficult to understand than previous methods. A familiarity with time series analysis is very desirable in understanding the method.

2. It is a computationally expensive method to use. With the cost of computing power steadily declining, this disadvantage should become less important.

3. The method is much more "black box" in design. This means that it has the potential to be used and accepted blindly. ARSTND is not foolproof, especially in the detrending phase. Any detrending method has the potential for very poor curve fits if the trend component abruptly changes character especially near the beginning or end of a series. If enough very poor curve fits of similar form and

timing occur, then there is the potential for a curve-fitting artifact to remain in the final ARSTND chronology. Such an artifact is most likely in the poorly replicated portion of a chronology where the Law of Large Numbers and the power of robust estimation are weakest. While the trend-in-mean concept is a very useful guide for determining what frequencies of variance to remove prior to autoregressive modelling, the choice of the actual detrending technique may require some judgement and experimentation. The choice of deterministic, stochastic, or hybrid (i.e. double-detrending) methods is still largely up to the research scientist and may, in some cases, be dictated by prior knowledge. However, the use of "prior knowledge" should be minimized as much as possible to be consistent with the underlying philosophy of objectivity in the ARSTND methodology.

The autoregressive modelling phase may also require occasional experimentation by the scientist. The first-minimum AIC criterion will frequently select an adequate AR-order. However, there are times when the AIC trace behaves for most of its length in a sawtooth-like manner which produces multiple minima. Alternately, the AIC trace may be extremely flat for several orders past the first-minimum AIC. In either case, competing models with AR-orders longer than that chosen by the first-minimum AIC criterion may be tried. The autocorrelation function of the residual mean-value function may also indicate the need for a longer model through the presence of "significant" autocorrelation coefficients near to but exceeding the AR-order chosen by the AIC statistic. The decision to use a longer AR-model may be somewhat

subjective. However, there is very little loss incurred by this decision even when it is weakly justified. The longer model will only result in the loss of additional data at the beginning of each series as a consequence of prewhitening the tree-ring indices. This will reduce the replication locally in the mean-value function. Nothing else is lost since the variance explained by the longer AR-model is added back to the ARSTND chronology by the pooled autoregression coefficients.

At this stage in the development of ARSTND, it is not clear how much operational improvement will occur in using ARSTND chronologies in dendroclimatic studies. While it is clear that an increase in signal-to-noise ratio is likely, this increase does not easily translate into a better climatic signal and an improved climatic reconstruction. Insofar as the ARSTND chronology is a more precise estimate of the population common signal among trees, some improvement in climatic reconstructions should be expected. Perhaps the more important consequence of the method is the way in which long-period common variance is conserved through the "trend-in-mean" concept of detrending. Thus, the climatic reconstructions developed from ARSTND chronologies may not have as much low-frequency bias as those developed from older standardization methods.

ARSTND has been developed principally with dendroclimatology in mind. The tree-ring series used in this kind of research are typically 200 or more years long. From a time-series analysis point of view, long series are highly desirable from the initial step in

detrending to the estimation of both the order of the autoregressive process and the resultant AR coefficients. It is not clear how well these procedures will work on short data sets (e.g. less than 100 years long). Sensitivity tests are ARSTND to series length would be desirable at some point.

LIST OF REFERENCES

Akaike, H. 1974. A new look at the statistical model identification. IEEE Transaction on Automatic Control AC19(6):716-723.

Andrews, D. F., P. J. Bickel, F. R. Hampel, P. J. Huber, W. H. Rogers, and J. W. Tukey. 1972. Robust Estimators of Location: Survey and Advances. Princeton, New Jersey: Princeton University Press. 373 p.

Barefoot, A. C., L. B. Woodhouse, W. L. Hafley, E. H. Wilson. 1974. Developing a dendrochronology for Winchester, England. Wood Sci. 6(5):34-40.

Bitvinskas, T. T. 1974. Dendroclimatic Investigations. Gidrometeoizdat, Leningrad.

Blasing, T. J., D. N. Duvick, and E. R. Cook. 1983. Filtering the effects of competition from ring-width series. Tree-Ring Bull. 43:19-30.

Bormann, F. H. and G. E. Likens. 1979. Catastrophic disturbance and the steady state in northern hardwood forests. Amer. Sci. 67:660-669.

Box, G. E. P. and G. M. Jenkins. 1970. Time Series Analysis: Forecasting and Control. Holden-Day, Inc., San Francisco. 553 p.

Box, G. E. P. and D. A. Pierce. 1970. Distribution of residual autocorrelations in autoregressive-integrated moving average time series models. J. Amer. Stat. Assoc. 65:1509-1526.

Box, G. E. P. and G. C. Tiao. 1975. Intervention analysis with applications to economic and environmental problems. J Amer. Stat. Assoc. 70:70-79.

Bray, J. R. 1956. Gap phase replacement in a maple-basswood forest. Ecology 37:598-600.

Briffa, K. R., P. D. Jones, and T. M. L. Wigley. 1983. Climate reconstruction from tree rings: Part 1, Basic methodology and preliminary results for England. J. of Climatology 3:233-242.

Brown, R. G. 1959. Less risk in inventory estimates. Harvard Business Review 37(4):104-116.

Brubaker, L. B. and S. K. Greene. 1979. Differential effects of Douglas-fir tussock moth and western spruce budworm defoliation on radial growth of grand fir and Douglas fir. Can. J. For. Res. 9:95-105.

Bryson, R. A. and A. Dutton. 1961. Some aspects of the variance spectra of tree rings and varves. Annals of New York Academy of Science 95:580-604

Chen, G. G. and G. E. P. Box. 1979a. Implied Assumptions for Some Proposed Robust Estimators. Technical Report No. 568, Department of Statistics, University of Wisconsin, Madison. 60 p.

Chen, G. G. and G. E. P. Box, 1979b. A Study of Real Data. Technical Report No. 568, Department of Statistics, University of Wisconsin, Madison. 68 p.

Cook, E. R. and K. Peters. 1981. The smoothing spline: a new approach to standardizing forest interior tree-ring width series for dendroclimatic studies. Tree-Ring Bull. 41:45-54.

DeWitt, E. and M. Ames, Eds. 1978. Tree Ring Chronologies of Eastern North America. Chronology Series IV, Vol. 1, Laboratory of Tree-Ring Research, University of Arizona, Tucson. 42 p.

Douglass, A. E. 1919. Climatic Cycles and Tree-Growth: A Study of the Annual Rings of Trees in Relation to Climate and Solar Activity. Carnegie Institute of Technology, Washington, D.C. 127 p.

Douglass, A. E. 1928. Climatic Cycles and Tree-Growth, Vol. II: A Study of the Annual Rings of Trees in Relation to Climate and Solar Activity. Publication No. 289, Carnegie Institute of Technology, Washington, D.C., 166 p.

Douglass, A. E. 1936. Climatic Cycles and Tree Growth, Vol. III: A Study of Cycles. Publication No. 289, Carnegie Institute of Technology, Washington, D.C. 171 p.

Drew, L. G., Ed. 1976. Tree-Ring Chronologies for Dendroclimatic Analysis: An Expanded Western North American Grid. Chronology Series II, Laboratory of Tree-Ring Research, University of Arizona, Tucson. 64 p.

Durbin, J. 1960. The fitting of time series models. Review of International Statistical Institute 28:233-289.

Eddy, J. A. 1976. The Maunder minimum. Science 192:1189-1202.

Fowells, H. A., Ed. 1965. Silvics of Forest Trees of the United States. Agriculture Handbook No. 271, Forest Service, U.S. Department of Agriculture, Washington, D.C. 762 p.

Fritts, H. C. 1963. Computer programs for tree-ring research. Tree-Ring Bull. 25(3-4):2-7.

Fritts, H. C. 1976. Tree Rings and Climate. Academic Press, New York, 567 p.

Fritts, H. C., T. J. Blasing, B. P. Hayden, and J. E. Kutzbach. 1971. Multivariate techniques for specifying tree-growth and climate relationships and for reconstructing anomalies in paleoclimate. J. Appl. Meteor. 10(5):845-864.

Fritts, H.C., G. R. Lofgren, and G. A. Gordon. 1979. Variations in climate since 1602 as reconstructed from the rings. Quat. Res. 12:18-46.

Fritts, H. C., J. E. Mosimann, and C.P. Bottorff. 1969. A revised computer orogram for standardizing tree-ring series. Tree-Ring Bull. 29(1-2):15-20.

Fritts, H. C. and D. J. Shatz. 1975. Selecting and characterizing tree-ring chronologies for dendroclimatic analysis. Tree-Ring Bull. 35:31-40.

Fryer, G. J., M. E. Odegard, and G. H. Sutton. 1975. Deconvolution and spectral estimation using final prediction error. Geophysics 40(3):411-425.

Garfinkel, H. L. and L. B. Brubaker. 1980. Modern climate-tree-growth relationships and climatic reconstruction in sub-Arctic Alaska. Nature 286:872-874.

Gilman, D. L., F. J. Fuglister, and J. M. Mitchell, Jr. 1963. On the power spectrum of "red noise". J. Atmos. Sci. 20:182-184.

Granger, C. W. 1966. The typical shape of an econometric variable. Econometrics 34:150-161.

Granger, C. W. J. and M. J. Morris. 1976. Time series modelling and interpretation. J. Roy. Stat. Soc. A 139:246-257.

Graybill, D. A. 1979. Revised computer program for tree-ring research. Tree-Ring Bull. 39:77-82.

Graybill, D. A. 1982. Chronology development and analysis. In: M. K. Hughes, P. M. Kelly, Jr., J. R. Pilcher, and V. C. LaMarche,

Jr., Eds., Climate from Tree Rings. Cambridge University Press, Cambridge. p. 21-28.

Hannan, E. J. and B. G. Quinn. 1979. The determination of the order of autoregression. J. Roy. Stat. Soc. B 41(2): 190-195.

Hett, J. M. and O. L. Loucks 1976. Age structure models of balsam fir and eastern hemlock. J. Ecology p. 1029-1044.

Hipel, K. W., A. I. McLeod and W. C. Lennox. 1977. Advances in Box-Jenkins modeling: I. Model construction. Water Resources Research 13(3):567-575.

Jacoby, G. C. and E. R. Cook. 1981. Past temperature variations inferred from a 400-year tree-ring chronology from Yukon Territory, Canada. Arctic and Alpine Research 13(4):409-418.

Jenkins, G. M. and D. G. Watts. 1968. Spectral Analysis and Its Applications. San Francisco: Holden-Day, 525 p.

Jones, P. D., T. M. L. Wigley, and P. M. Kelly. 1982. Variations in surface air temperatures: Pt. 1, Northern Hemisphere, 1881-1980. Monthly Weather Review 110(2):59-70.

Jones, R. H. 1964. Prediction of multivariate time series. J. Appl. Meteor. 3(3):285-289.

Jones, R. H. 1984. Time series analysis in meteorology, In: A. H. Murphy, and R. W. Katz, Eds., Probability, statistics, and Decision Making in Meteorology. Denver:Westview Press.

Jonsson, B. and B. Matern. 1974. On the computation of annual ring indices. Paper presented at International Workshop on Dendroclimatology, 15-26 April 1974, University of Arizona, Tucson.

Katz, R. W. and R. H. Skaggs. 1981. On the use of autoregressive-moving average processes to model meteorological time series. Monthly Weather Rev. 109:479-484.

Koerber, T. W. and B. E. Wickman. 1970. Use of tree-ring measurements to evaluate impact of insect defoliation, In: J., Smith, G. Harry and J. Worral, Eds., Tree-Ring Analysis with Special Reference to Northwest America. Bulletin No. 7, Faculty of Forestry, University of British Columbia, Vancouver, p. 101-106.

Kutzbach, J. E. and R. A. Bryson, 1975. Variance spectrum of holocene climatic fluctuations in the North Atlantic sector, In: Proceedings of WMO/IAMAP Symposium on Long-Term Climatic Fluctuations, 18-23 August 1975, Norwich, England. Publication No. 421, World Meteorological Organization, Geneva, p. 97-104.

Kuusela, J. and P. Kilkki. 1963. Multiple Regression of Increment Percentage on Other Characteristics in Scotch-Pine Stands. Finnish Society of Forestry, Helsinki, 35 p.

LaMarche, V. C., Jr., and H. C. Fritts. 1972. Tree-rings and sunspot numbers. Tree-Ring Bull., 32:19-33.

Lamb, H. H. 1970. Volcanic dust in the atmosphere; with a chronology and assessment of its meteorological significance. Phil. Trans. Roy. Soc. A,266(1178):425-533.

Levinson, H. 1947. The Wiener RMS (root mean square) error criterion in filter design and prediction. J. Mathematics and Physics 25:261-278.

Ljung, G. M. and G. E. P. Box. 1978. On a measure of lack of fit in time series models. Biometrika 65(2):297-303.

Matalas, N. C., 1962. Statistical properties of tree ring data. International Association of Scientific Hydrology 8(2):39-47.

Meko, D. M. 1981. Applications of Box-Jenkins methods of time series analysis to the reconstruction of drought from tree rings. Ph.D. thesis, University of Arizona, Tucson. 149 p.

Mitchell, J. M., Jr. 1976. An overview of climatic variability and its causal mechanisms. Quat. Res. 6(4):481-493.

Mitchell, J. M., Jr., B. Dzerdzeevskii, H. Flohn, W. J. Hofmeyr, H. H. Lamb, K. N. Rao and C. C. Wallen. 1966. Climatic Change. Technical Note No. 79, World Meteorological Organization, Geneva. 79 p.

Mitchell, J. M., Jr., C. W. Stockton and D. M. Meko. 1979. Evidence of a 22-year rhythm of drought in the western United States related to the Hale solar cycle since the 17th century, In: B.M. McCormac, and T. A. Seliga, Eds., Solar-Terrestrial Influences on Weather and Climate, Proceedings of Symposium/Workshop on Solar-Terrestrial Influences on Weather and Climate, 24-28 July 1978, Columbus, Ohio. D. Reidel Publishing Co., Dordrecht, Holland. p. 125-143.

Mosteller, F. and J. W. Tukey. 1977. Data Analysis and Regression. Reading, Massachusetts:Addison-Wesley. 588 p.

Peacock, K. L. and S. Treital. 1969. Predictive deconvolution: theory and practice. Geophysics 34(2):155-169.

Peters, K., G. C. Jacoby and E. R. Cook. 1981. Principal components analysis of tree-ring sites. Tree-Ring Bull. 41:1-19.

Potter, K. W., 1976. Evidence for nonstationarity as a physical explanation of the Hurst phenomenon. Water Resources Research 12(5):1047-1052.

Rice, J. R. 1969. The Approximation of Functions, Vol. 2. Addison-Wesley, Reading, Mass.

Robinson, E. A. and S. Treital. 1980. Geophysical Signal Analysis. Englewood Cliffs, New Jersey:Prentice-Hall. 466 p.

Romme, W. H. and W. H. Martin. 1982. Natural disturbance by tree-falls in old-growth mixed mesophytic forest: Lilley Cornett Woods, Kentucky, In: R. N. Muller, Ed., Proceedings of Central Hardwood Forest Conference IV, University of Kentucky, Lexington. p. 367-383.

Salas, J. D., J. W. Delleur, V. Yevjevich, and W. L. Lane. 1980. Applied Modeling of Hydrologic Time Series. Littleton, Co.: Water Resources Publications. 484 p.

Schneider, S. H. and C. Mass. 1975. Volcanic dust, sunspots, and temperature trends. Science 190(4216):741-746.

Schwarz, G., 1978. Estimating the dimension of a model. Ann. Statist. 6:461-464.

Shibata, R. 1976. Selection of the order of an autoregressive model by Akaike's information criterion. Ann. Statist. 6:461-464.

Siegel, S. 1956. Nonparametric Statistics for the Behavioral Sciences. New York:McGraw-Hill, 312 p.

Sokol, R. R. and F. J. Rohlf, 1981. Biometry. San Francisco:W.H. Freeman. 859 p.

Spurr, S. H. and B. V. Barnes, 1973. Forest Ecology. New York: Ronald Press. 571 p.

Stahle, D. W., J. G. Hehr and G. G. Hawks, Jr. 1982. The Development of Modern Tree-Ring Chronologies in the Midwest: Arkansas, North Texas, Oklahoma, Kansas, and Missouri. Final Technical Report submitted to NSF for Grant ATM8006964. 153 p.

Steel, R. G. D. and J. H. Torrie, 1960. Principals and Procedures of Statistics. McGraw-Hill, Inc., New York. 481p.

Stockton, C. W. 1971. The feasibility of augmenting hydrologic records using tree-ring data. Ph.D. dissertation, University of Arizona, Tucson. 172 p.

Stockton, C. 1975. Longterm streamflow records reconstructed from tree rings. Research Paper No. 5, Laboratory of Tree-Ring Research, University of Arizona, Tucson,

Ulrych, T. J. and T. N. Bishop 1975. Maximum entropy spectral analysis and autoregressive decomposition. Rev. Geophysics & Space Phys. 13(1):183-200.

Ulrych, T. J. and R. W. Clayton 1976. Time series modelling and maximum entropy. Physics of the Earth and Planetary Interiors 12:188-200.

Warren, W. G. 1980. On removing the growth trend from dendrochronological data. Tree-Ring Bulletin 40:35-44.

White, P. S. 1979. Pattern, process, and natural disturbance in vegetation. Botanical Review 45:229-299.

Wickman, B. E. 1980. Increased growth of white fir after a Doublas-fir tussock moth outbreak. J. Forestry 78(1):31-33.

Wigley, T. M. L., K. R. Briffa, and P. D. Jones. 1984. On the average value of correlated time series, with applications in dendroclimatology and hydrometeorology. J. Clim. and Appl. Meteor. 23(2): 201-213.